

JIMMA UNIVERSITY  
JIMMA INSTITUTE OF TECHNOLOGY  
SCHOOL OF GRADUATE STUDIES  
FACULTY OF CIVIL AND ENVIRONMENTAL ENGINEERING  
GEOTECHNICAL ENGINEERING STREAM

Prediction of Californian Bearing Ratio and Unconfined Compression Strength from Dynamic Cone Penetration for Local Subgrade soil in Jimma Town

A research Thesis submitted to the School of Graduate Studies of Jimma University in Partial Fulfillment of the Requirements for the Degree of Master of Science in Civil Engineering. (Geotechnical Engineering)

By:  
Shelema Amena

November 2018

Jimma, Ethiopia

JIMMA UNIVERSITY  
JIMMA INSTITUTE OF TECHNOLOGY  
SCHOOL OF GRADUATE STUDIES  
FACULTY OF CIVIL AND ENVIRONMENTAL ENGINEERING  
GEOTECHNICAL ENGINEERING STREAM

Prediction of Californian Bearing Ratio and Unconfined compressive strength  
from Dynamic Cone Penetration for Local Subgrade soil in Jimma Town

A research Thesis submitted to the School of Graduate Studies of Jimma University in  
Partial Fulfillment of the Requirements for the Degree of Master of Science in Civil  
Engineering. (Geotechnical Engineering)

By:

Shelema Amena

Main Advisor: Prof. Emer Tucay Quezon, P.Eng

Co-Advisor: Engr. Damtew Tsige (Ph.D Candidate)

November 2018

Jimma, Ethiopia

## DECLARATION

I, the undersigned, declare that this thesis entitled: “Prediction of Californian Bearing Ratio and Unconfined compressive strength from Dynamic Cone Penetration for local subgrade soil in Jimma town.” is my original work, and has not been presented by any other person for an award of a degree in this or any other University, and all sources of material used in this thesis have been duly acknowledged.

Candidate:

**Shelema Amena**

Signature\_\_\_\_\_

As Master’s Research Advisors, we hereby certify that we have read and evaluated this MSc Thesis prepared under our guidance by **Shelema Amena** entitled: “Prediction of Californian and Unconfined compressive strength from Dynamic Cone Penetration for local subgrade soil in Jimma town.”

We recommend that it can be submitted as fulfilling the MSc Thesis requirements.



15/3/2011

Prof. Emer T. Quezon, P.Eng

Advisor

\_\_\_\_\_  
Signature

\_\_\_\_\_  
Date

Damtew Tisge (Ph.D Candidate)

Co- Advisor

\_\_\_\_\_  
Signature

\_\_\_\_\_  
Date

JIMMA UNIVERSITY  
JIMMA INSTITUTE OF TECHNOLOGY  
SCHOOL OF POST GRADUATE STUDIES  
FACULTY OF CIVIL AND ENVIRONMENTAL ENGINEERING  
GEOTECHNICAL ENGINEERING STREAM

Prediction of Californian Bearing Ratio and Unconfined compressive strength  
from Dynamic Cone Penetration for local subgrade soil in Jimma town

By


**Shelema Amena**

**APPROVED BY BOARD OF EXAMINERS**

1. Dr. Eliyas \_\_\_\_\_ /\_\_\_\_\_/\_\_\_\_\_  
External Examiner Signature Date

2. Yada Tesfaye \_\_\_\_\_ /\_\_\_\_\_/\_\_\_\_\_  
Internal Examiner Signature Date

3. \_\_\_\_\_ /\_\_\_\_\_/\_\_\_\_\_  
Chairman of Examiner Signature Date

4. Prof. Emer T. Quezon, P.Eng \_\_\_\_\_ /\_\_\_\_\_/\_\_\_\_\_  
Main Advisor  Signature Date

5. Damtew Tsige (Ph.D Candidate) \_\_\_\_\_ /\_\_\_\_\_/\_\_\_\_\_  
Co- Advisor Signature Date

## ACKNOWLEDGMENT

First of all, I would like to gratefully acknowledge the almighty God to get the chance of this program.

My deepest gratitude goes to my advisor **Prof. Emer Tucay Quezon** and my co-advisor **Mr. Damtew Tsige** for all their limitless efforts in guiding me through my work and for providing me useful reference materials.

Finally, my deepest appreciation goes to Jimma University, School of Graduate Studies, Jimma Institute of Technology, Civil Engineering Department, and Geotechnical Engineering Stream.

Last but not least, I would like to thank Jimma Insitute of technology Soil laboratory technicians Dekebi Chekeri, Haile Tsegay and Hailemariam for their encouragement during my study.

## ABSTRACT

*Determination of subgrade soil strength is a critical step in preliminary investigation of every project. Californian bearing ratio (CBR) and Unconfined compressive strength (UCS) are the widely used subgrade strength parameters used for determination of strength of foundation soil both at in-situ and in laboratory. However, these tests involves sampling, transporting, preparing, compacting, soaking, and penetrating with a plunger of CBR and UCS machine which is difficult and needs much time to have the end result. To avoid such problems, this research introduces the use of Dynamic Cone Penetration (DCP) which is a simple test device that is inexpensive, portable, and easy to operate and understand.*

*The objective of the study to correlate Dynamic Cone Penetration (DCP) with Californian bearing ratio (CBR), and Unconfined compressive strength to derive bearing capacity of typical Jimma clay soil. In this study, field tests and laboratory tests were conducted. Laboratory tests needed to classify the soil and the parameters that affect the result were conducted and the test results are analyzed by statistical software (SPSS) and Microsoft excel to find their correlation functions using regression analysis. The data has been categorized in to two categories, prediction of CBR and UCS with dynamic cone penetration index had been developed.*

*These research work revealed that Californian bearing ratio (CBR) estimated by the developed equation  $\log CBR = 1.9976 - 1.0192 \cdot \ln(DCPI)$  and  $\log CBR = -1.0078 \log DCPI + 2.1001$  while Unconfined compressive strength estimated by  $UCS = 557.06 - 120.8 \cdot \ln(DCPI)$  for black clay soils and  $UCS = 630.82 - 133.2 \cdot \ln(DCPI)$  for red clay soils of Jimma town. The corresponding developed bearing capacity equation of this study based on the bearing capacity theory were  $q_{ult} = 1431.644 - 310.456 \cdot \ln(DCPI) + \gamma h$  for black clay soils of Jimma town while  $q_{ult} = 1621.207 - 342.32 \cdot \ln(DCPI) + \gamma h$  for red clay soils of Jimma town.*

*The results are expected to have wide application in the construction sector.*

**Keywords:** *Black clay, CBR, DCPI, Red clay soils, Unconfined compression strength*

## TABLE OF CONTENTS

DECLARATION .....	i
ACKNOWLEDGMENT.....	ii
ABSTRACT.....	iii
LIST OF TABLES.....	vii
LIST OF FIGURES .....	viii
ACROYNMYS.....	x
1. INTRODUCTION .....	1
1.1 Background .....	1
1.2 Statement of the problem .....	2
1.3 Research Questions .....	3
1.4 Aim and Objective of the study.....	3
1.4.1 General objective.....	3
1.4.2 Specific objectives .....	3
1.5 Scope of the study .....	3
1.6 Significance of the study.....	4
1.7 Thesis Outline .....	4
2. REVIEW OF RELATED LITERATURE .....	5
2.1 General .....	5
2.2 Dynamic Cone Penetrometer .....	5
2.2.1 Factors Affecting DCP Results.....	7
2.3 Undrained Shear Strength of Soil.....	8
2.3.1 General.....	8
2.3.2 Unconfined Compressive Strength (UCS) .....	10
2.4 California Bearing Ratio (CBR).....	12
2.5 Bearing Capacity Theory and Shear Resistance of Penetrometers .....	13
2.5.1 Bearing Capacity Theory.....	13
2.5.2. Shear Resistance of Penetrometers.....	15
2.6 Index properties of the soil.....	16
2.7 Determination of geotechnical parameters using DCP .....	18

2.7.1 Prediction of California Bearing Ratio (CBR) .....	19
2.7.2 Prediction of Undrained Shear Strength.....	21
3. MATERIAL, METHODS AND DATA COLLECTION.....	23
3.1 Study area.....	23
3.2 Data Collection and source of data .....	25
3.2.1 Data collection.....	25
3.2.2 Sample size and sample procedure.....	25
3.2.3 Source of data.....	26
3.2.4 Data analysis.....	26
3.3 Data Analysis .....	27
3.3.1 Normality test.....	27
3.3.2 Significance level .....	27
3.3.3 Inter- variable relationship.....	28
3.4 Test Methods.....	29
3.4.1 Field Test.....	29
3.4.2 Laboratory Tests.....	29
3.5 Field test Results and Discussion.....	30
3.6 Laboratory test Results and Discussion .....	32
3.7 Summary of Test Results .....	37
3.8 Comparison of Index Properties of Current Study with Previous Researches.....	37
4. ANALYSIS AND DISCUSSION.....	40
4.1 General .....	40
4.1.1 Regression .....	40
4.1.2 Normality test and Univariate plots.....	40
4.1.3 Interdependence tests.....	40
4.2 Single Regression.....	41
4.2.1 Scatter Plot for Category-1 (Black clay soils of Jimma Town).....	41
4.2.2 Scatter Plot for Category-2 (Red clay soils of Jimma Town).....	44
4.2.3 Summary of Correlations for Category-1 (Black Clay Soils of Jimma Town).....	46
4.2.4 Summary of Correlations for Category-2 (Red Clay Soils of Jimma Town).....	47



---

4.3 Multiple Regression .....	48
4.3.1 Multiple Regressions for Category-1 (black Clay Soils of Jimma Town) .....	48
4.3.2 Multiple Regression for Category-2 (red clay soils of Jimma town) .....	49
4.4 Discussion .....	49
4.4.1 Category-1 (Black Clayey Soils of Jimma Town).....	49
4.4.2 Category-2 (Red Clayey Soils of Jimma Town) .....	50
4.5 Development of Equation Based On Bearing Capacity Theory .....	51
4.6 Comparison .....	51
4.6.1 Comparison of Measured and Predicted Results .....	52
4.6.2 Comparison with pervious similar studies.....	54
4.6.3 Verification of Developed Bearing Capacity Equation .....	55
5. CONCLUSION AND RECOMMENDATION.....	57
5.1 Conclusion.....	57
5.2 Recommendation.....	58
REFERENCES .....	59
APPENDIX A: DETAIL OF GRAINSIZE ANALYSIS AND ATTERBERG LIMITS.....	63
APPENDIX B: DETAIL OF UNCONFINED COMPRESSION TEST RESULTS .....	79
APPENDIX C: DETAIL OF DYNAMIC CONE PENETRATION DATA.....	88
APPENDIX D: DETAIL OF CBR DATA FOR SELECTED SAMPLES .....	104
APPENDIX E: REGRESSION OUT PUTS.....	119

## LIST OF TABLES

Table 2-1 shows general relationship of consistency and Unconfined Compression Strength. ...	12
Table 3.1 Summary of climate data for Jimma town.....	24
Table 3-2 Summary of laboratory testing procedure standards .....	29
Table 3.3 Sample Field density test result for Kito black 1 soil sample.....	30
Table 3.4 Dynamic cone penetration data for Rift valley 1 soil sample.....	31
Table 3.5 Dynamic cone penetration Index test summary.....	31
Table 3.6 Summary of Atterberg Limits.....	33
Table 3.8 Comparison of index properties and classification of Jimma soils with the previous works.....	37
Table 3.9 Comparison of index properties and classification of Jimma soils with the previous works.....	37
Table 3.10 Summary of the test results.....	38
Table 4.1 Summary of Correlations for Category-1 (Black Clay Soils of Jimma Town) .....	47
Table 4.2 Summary of Correlations for Category-2 (Red Clay Soils of Jimma Town).....	47

## LIST OF FIGURES

Figure 2.1 Dynamic cone penetrometer equipment.....	7
Figure 2.2 Unconfined compression strength.....	11
Figure 2.3 Schematization Prandtl's of strip foundation.....	14
Figure 2.4 Theoretical principles of penetration equipment.....	16
Figure 2.5 Relationships between Penetration Index (PI), California Bearing Ratio (CBR) and Unconfined Compressive Strength (UCS).....	18
Figure 2.6 Relationships between USC and DCPI after Salgado.....	21
Figure 3.1 Map of study area.....	23
Figure 3.2 Average annual rain fall of Jimma town.....	24
Figure 3.3 Graph No. of blows vs depth for Rift valley 1 soil sample.....	31
Figure 3.4 Summary of particle size curve.....	32
Figure 3.5 AASHTO plasticity chart classification for the Jimma fine-grained soils.....	34
Figure 3.6 Classification of the fine-grained Jimma soils using USCS plasticity chart.....	35
Figure 4.1 Scatter plot of UCS with DCPI for black clayey soils of Jimma Town.....	41
Figure 4.2 Scatter plot of UCS with LL for black clayey soils of Jimma Town.....	41
Figure 4.3 Scatter plot of UCS with LI for black clayey soils of Jimma Town.....	42
Figure 4.4 Scatter plot of UCS with NMC for black clayey soils of Jimma Town.....	42
Figure 4-5 Scatter plot of CBR with DCPI for black clayey soils of Jimma Town.....	42
Figure 4.6 Scatter plot of logCBR with logDCPI for black clayey soils of Jimma Town.....	43
Figure 4.7 Scatter plot of CBR with LL for black clayey soils of Jimma Town.....	43
Figure 4.8 Scatter plot of CBR with LI for black clayey soils of Jimma Town.....	43
Figure 4.9 Scatter plot of CBR with NMC for black clayey soils of Jimma Town.....	44
Figure 4.10 Scatter plot of UCS with DCPI for red clayey soils of Jimma Town.....	44
Figure 4.11 Scatter plot of UCS with LL for red clayey soils of Jimma Town.....	44
Figure 4.12 Scatter plot of UCS with NMC for red clayey soils of Jimma Town.....	45
Figure 4.13 Scatter plot of UCS with LI for red clayey soils of Jimma Town.....	45
Figure 4.14 Scatter plot of CBR with LL for red clayey soils of Jimma Town.....	45
Figure 4.15 Scatter plot of CBR with LI for red clayey soils of Jimma Town.....	45
Figure 4.16 Scatter plot of CBR with NMC for red clayey soils of Jimma Town.....	46

---

Figure 4.17 Scatter plot of CBR with DCPI for red clayey soils of Jimma Town .....	46
Figure 4.18 Actual measured versus Current predicted CBR Value of cat -1 Black Soil .....	52
Figure 4.19 Actual measured versus Current predicted UCS Value of cat -1 Black Soil .....	52
Figure 4.20 Actual measured versus Current predicted UCS Value of cat -2 Red soils .....	53
Figure 4.21 Actual measured versus Current predicted CBR Value of cat -2 Red soils .....	53
Figure 4.22 Comparison of previous and current studies for Californian bearing ratio .....	54
Figure 4.24 Comparison of Terzaghi's and current black soils bearing capacity equation .....	55
Figure 4.25 Comparison of Terzaghi's and current red soils bearing capacity equation .....	56

## ACROYNMYS

AASHTO	American Association of State Highway and Transportation Officials
ASTM	American Society for Testing and Materials
CBR	Californian Bearing Ratio
CH	Highly plastic clay soils
CL	Low plasticity clay soils
DCP	Dynamic one penetration
DCPT	Dynamic cone penetration test
ERA	Ethiopian Roads Authority
Gs	Specific gravity
LL	Liquid Limit
Log	Logarithm base 10
KPa	Kilo Pascal
MDD	Maximum Dry density
MH	Highly plastic silty soils
ML	Low plasticity silty soil
NMC	Natural moisture content
OMC	Optimum moisture content
PL	Plastic limit
PI	Penetration index
R <sup>2</sup>	Coefficient of determination
SPSS	Statistical Package for the Social Science
UCS	Unconfined compressive strength

## 1. INTRODUCTION

### 1.1 Background

Subgrade layer plays a vital role in conveying structural strength to the pavement structure as it receives loads enacted upon it by road traffic and other infrastructures. Traffic loads need to be transmitted in effective way that the subgrade-deformation is within elastic limits, and the shear forces developed is within safe limits under adverse climatic and loading conditions [23].

The subgrade comprises unbound earth materials such as gravel, sand, silt and, clay that influence the design and construction of foundation and roads. The assessment of properties of soil subgrades, in terms of density, soil stiffness, strength, and other in-situ parameters is vital in the design of foundation and roads, and their performance. There are various tests including Californian bearing ratio (CBR) and Unconfined compressive strength (UCS) which are mandatory parameters for subgrade strength evaluation. The laboratory determination of CBR and UCS tests requiring considerable effort and time in strength of subgrade determination [1].

The CBR is a measure of shearing resistance of material under controlled density & moisture condition. It is a ratio of the force per unit area required to penetrate a soil mass with a standard circular plunger of 50 mm diameter at the rate of 1.25 mm/min to that required for the corresponding penetration of a standard material. The CBR value obtained is an integral part of several flexible pavement design method.

The unconfined compression strength of subgrade soil is a load per unit area at which an unconfined cylindrical specimen of soil will fail in simple compression test. UCS test gives the shear strength of the soil that is useful parameters for computing safe bearing capacity of soil as well as strength of soil. These tests are lengthy, precise and need experienced engineer to conduct [1].

The dynamic cone penetration test (DCPT) has been widely used for field exploration and quality assessment of subsoil layers. DCP testing can be used in the characterization of soil properties in many ways. Perhaps the most important advantage of the dynamic cone penetrometer (DCP) device is related to its ability to provide a continuous record of relative soil strength with depth. DCP device is distinguished by its economy and simplicity to operate and its

superiority to provide repeatable results and rapid property assessment. DCPT has the main features that are similar to those of CPT. It can also be used for the assessment of compaction quality for sand backfilling [3].

## 1.2 Statement of the problem

In civil engineering the investigation of subgrade materials for pavement design works become necessary to optimize structural safety and economy aspects of the road and other infrastructures such as buildings foundation, earthen dam, slope etc. One of the activities during the site investigation is determination of subgrade material strength with different in-situ and laboratory tests such as the Dynamic Cone Penetrometer (DCP) test, unconfined compressive strength and California Bearing Ratio (CBR) test. California Bearing Ratio is a parameter that measures the strength of road soil layers and used as an integral part of pavement design. And the UCS is also a parameter used as key in bearing capacity. These tests involves sampling, transporting, preparing, compacting, soaking, and penetrating with a plunger of CBR and UCS machine to measure the soil resistance. As it needs much time to have the end result and it cannot be easily determined in the field, civil engineers always encounter difficulties in obtaining representative CBR and UCS values for design of pavements. Whereas conducting DCP test including its analysis and interpretation takes a very short time. Many researchers concluded that DCP is also multi-advantageous equipment used to evaluate the in-situ strength of subgrade soil materials for road pavement works at shallow depths [4][3].

In our country only few researches was done concerning to correlation of Dynamic cone penetration with Californian bearing ratio and unconfined compressive strength. These researches were limited to the study area.

Therefore, predicting CBR value from DCP test and exploiting it during performance evaluation of pavement layers makes better option than using costly and time intensive procedures. The aim of this study is to establish a relationship between CBR, and UCS with DCP which helps to predict CBR and UCS value for Jimma town subgrade materials from DCP test results that suits for these soils.

### **1.3 Research Questions**

1. What are the types and index properties of locally used subgrade soil materials in the study area?
2. Is there any strong relationship between CBR (California bearing ratio) and DCPT (Dynamic cone penetration test) in predicting the CBR value?
3. Is there any strong relationship between UCS (unconfined compressive strength), DCPT (Dynamic cone penetration test) in establishing the bearing capacity equation?
4. How can the equations developed for prediction are validated?

### **1.4 Aim and Objective of the study**

#### **1.4.1 General objective**

The aim of this study is to develop a correlation of Californian Bearing Ratio and Unconfined compressive strength with DCP for locally used subgrade soil material in Jimma town.

#### **1.4.2 Specific objectives**

- To determine the index properties of the soil found in Jimma town.
- To develop correlation between CBR (California bearing ratio) and DCPT (Dynamic cone penetration test)
- To develop correlation between UCS (unconfined compressive strength) and DCPT (Dynamic cone penetration test) and deriving bearing capacity equation for Jimma town soil
- Validating the equations developed for prediction

### **1.5 Scope of the study**

The study was carried out in Jimma town. The sample collection for this study limited to some area around the town by taking the representative samples from these selected areas. The field tests such as DCP, moisture content and field dry density was conducted at field. Disturbed and undisturbed samples for laboratory tests was taken for the testing of physical and engineering properties such as grain size analysis, atterberg limits, compaction parameters, CBR, and UCS of soils obtained from site. Then the correlation was done on CBR and UCS depending on the



values of DCP, liquid index, liquid limit, and natural moisture content using single linear and multiple linear regressions. Finally the equation was derived for the dependent variables.

### **1.6 Significance of the study**

These correlations are very important to estimate engineering property of soils, especially for preliminary investigation of projects. Correlations may be also used for projects where there is financial limitation, lack of test equipment and limited time to conduct CBR and UCS tests for the study area.

The finding of this study may also contribute important role in science of using dynamic cone penetration. The study will benefit consultants, contractors, researchers and the public at large.

### **1.7 Thesis Outline**

The structure of this thesis divided in to five separated but integrated chapters. The first Chapter presents the general statement, objective and scope of this thesis with limitation and application of the study result. In chapter two, the previous works concerning applications, principles, factors, and relationships of Dynamic Cone Penetrometer (DCP), Californian Bearing Ratio (CBR), and unconfined compressive strength (UCS) are reviewed and discussed. The third Chapter presents the study area description, the data collection methods, and testing analyses of all fields and laboratory tests results for different studied parameters of soil samples. The fourth Chapter presents the single and multiple correlation procedures, results, analysis and discussion. Finally, conclusion and recommendation of the thesis are presented in chapter five. All field and laboratory test results, and software outputs are presented in the Appendixes parts.

## 2. REVIEW OF RELATED LITERATURE

### 2.1 General

The quality of the road or runways and other infrastructures depends to a large extent on the strength and shear characteristics of subgrade material. To perform optimistic foundation and pavement design, an accurate and representative material characterization technique is essential; such technique would be more acceptable if it is simple, rapid and economic. So that, the evaluation of subgrade strength plays a great role for the foundation and road pavement during design, construction and service stages [1].

Laboratory determination of California Bearing Ratio useful for flexible pavement design, and unconfined compressive strength (UCS) is required for determination of shear strength parameter of subgrade are time consuming and demand significant effort but mandatory. Dynamic Cone Penetration test can be a faster and easier way to evaluate subgrade strength [1].

### 2.2 Dynamic Cone Penetrometer

During the preliminary exploratory phase, penetration tests are employed to determine the soil conditions, such as soil type, the depth, thickness and lateral extent of the soil strata. During the detailed exploration phase, penetration tests are also important. The shear strength and stiffness of the soil can be estimated from penetration testing data, so that the ultimate bearing capacity of the soil can be assessed [14].

The Dynamic Cone Penetrometer (DCP), also known as the Scala penetrometer, was developed in 1956 in South Africa as an in situ pavement evaluation technique consists of about 9kg hammer with a dropping vertical distance of 510mm with a 15.875mm diameter rod. The hammer impact energy is ultimately applied on to a 30 degree angle cone fitted at bottom end of the 762mm guide rod [6][7].

Since 1991, the DCP has undergone significant changes at the connection of the upper and lower rods, a threaded simple slip plug change to bolt connection. Other notable modifications make to increase device life and to make a hand safety guard on the anvil [8].

The approach of determining the strength of the soil property involves the determination of property of the medium from known penetration energy and penetration depth. Blow counts with

penetration depth can generally be used to identify material strength. The soil strength is measured by the penetration (usually in millimeters or inches) per hammer blow, which is called Dynamic Cone Penetration Index (DCPI) [2].

The DCP consists of a steel rod with a steel cone attached to one end of lower shaft driven into the soil using a sliding hammer on the upper shaft with a diameter of 16 mm. The hammer weighs 8 or 4kg and the cone has an angle of 30 or 60 degrees and a drop height of 575mm. As a reading device, additional measured flat steel is used as an attachment to the lower shaft. The diameter of the cone is slightly larger than that of the rod to ensure the resistance to penetration exerted on the cone [6]. Tests can be performed continuously to the desired depth with an expendable cone, which is left in the ground upon drill rod withdrawal, or they can be performed at specified intervals by using a retractable cone and advancing the hole by auger or other means between tests [9].

Data from a DCP test processed to produce a Dynamic Cone Penetration Index (DCPI), the average penetration of the cone per blow is reported in as an index value and it may be represented in many forms, viz. Dynamic Cone Penetration Index (DCPI), Penetration Rate (PR), Penetration Index (PI), Number of blows required to penetrate a given thickness of layer as Dynamic Cone Penetration Number (DCPN /NDCP/), Blow Rate (BR) and DCP Structural Number (DSN).

In this thesis, the cone's average penetration per blow (mm/blow) is denoted as Dynamic Cone Penetration Index (DCPI). The Dynamic Cone Penetration Index (DCPI) can be plotted on a layer strength diagram, or can be correlated directly and indirectly with a number of common subsoil strength parameters. UK DCP software is used to analyze the result obtained from field by plotting a diagram of penetration depth versus number of blow required. Then after the data is analyzed the dynamic cone penetration index is obtained from the slope of the of curve at the depth of which the sample for laboratory tests are taken. [10]

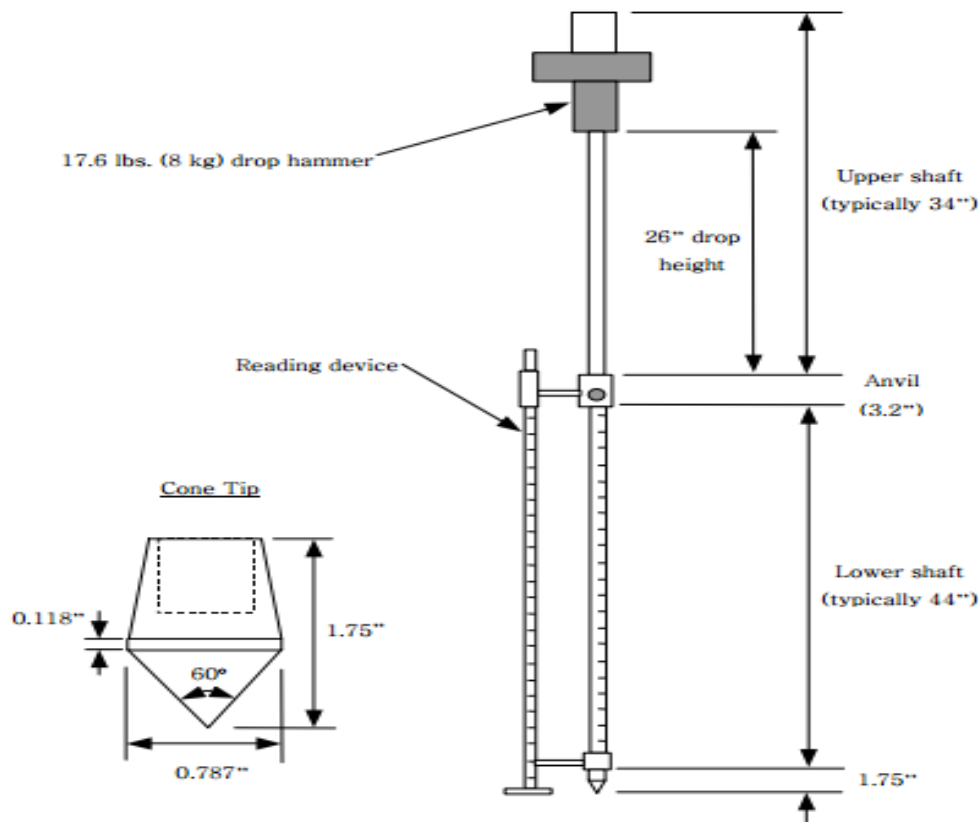


Figure 2.1 Dynamic cone penetrometer equipment [9].

### 2.2.1 Factors Affecting DCP Results

A study on the effects of several variables on the determination of DCPI and operation of DCP was performed by Hassan. He concluded that for fine-grained soils, moisture contents, soil classification, soil density and confining pressures influence the value of DCPI. For coarse-grained soils, coefficient of uniformity and confining pressures were affecting DCPI result [11].

#### *I. Soil Material Properties (Soil Type) and Depth*

DCP tests in highly plastic clays are generally accurate for shallow depths. At deeper depths, clay sticking to the lower rod may indicate higher Strength values than the actual values by adding skin friction on cone tip resistance. Many sands occur in a loose state at shallow depths. Such sands when relatively dry will show no DCP index values for the top few inches and then may show increasing DCP index values with depth. Several investigators indicated that moisture content, gradation, density, and plasticity were important material properties influencing the DCPI [9].

## ***II. Moisture Content and Density***

Salgado et al. and Tuncer et al., conclude that Penetration Index affected by Unit Weight and Water Content. They indicate the value of strength index in term of DCPI is more dependent on dry Unit Weight than the Water Content. Studies show the penetration index decreases as the dry density increases and slightly increases as moisture content increases; however, both studies recommended need of additional studies for better understand of the relationships [3].

Furthermore, another study concluded that moisture content and dry density do not affect the relationship or correlation of CBR and DCPI. Because, moisture content and dry density are affect both parameters (CBR and DCPI), but they affect in similar ways.

## **III. Vertical Confinement and Side Friction**

Livneh et al. indicated that there is no vertical confinement effect by rigid pavement structure or by upper cohesive layers on the DCP values of lower subgrade layers. Vertical confinement effect may occur at the upper layers in the DCP values of the granular pavement layers. These confinement effects usually result a decrease in the DCP values [14].

Because of the DCP device is not completely vertical while penetrating through the soil, DCPI value would be apparently very lower due to side friction. This apparent higher resistance may also be caused when penetrating in a collapsible granular material. This effect is usually small in cohesive soils [9].

## **IV. Damaged DCP Apparatus**

The cone should be replaced when its diameter is reduced, when its surface is badly gouged or the tip very blunt. The cone should be examined for wear before any test. A visual comparison to a new cone is a quick way to decide if the test should proceed. Additionally, the rod leave its vertical alignment, no attempt should be made to correct this, as contact between the bottom rod and the sides of the hole lead to erroneous results and may the rod bend [14].

## **2.3 Undrained Shear Strength of Soil**

### **2.3.1 General**

Shearing strength of soil is the most important of its engineering properties. This is because all stability analysis in the field of geotechnical engineering, either they relate to foundation, slope

of cuts or earth dam, involve a basic knowledge of this engineering property of the soil. Shear strength may be defined as the resistance to shearing stresses and a consequent tendency for shear deformation [14].

Basically, a soil derives its shearing strength from resistance due to the interlocking of particles, frictional resistance between the individual soil grains which may be sliding friction, rolling friction or both friction and cohesion between soil particles.

Granular soils of sands may derive their strength from the first two sources, while cohesive soils may derive their shear strength from the second and third source. Highly plastic clays, however, may exhibit the third source alone for their shearing strength. Most natural soil deposits are partially cohesive and partially granular and as such, may fall in to the second of the three categories just mentioned, from the point of view of shearing strength [16].

The shear strength is measured in terms of two soil parameters; inter-particle attraction or cohesion and resistance to inter-particle slip called the angle of internal friction .Grain crushing resistance to rolling, and other factors are implicitly include in these two parameters.

In equation form the shear strength in terms of total stress is

$$s = c + \sigma \tan \phi \quad (2.1)$$

A complication arises when the normal stresses within a soil are carried partly by the soil skeleton itself and partly by water within the soil voids. Considering only the stresses within the soil skeleton the above equation is modified to: [15]

$$s = c' + (\sigma - u) \tan \phi = s = c' + \sigma' \tan \phi \quad (2.2)$$

Where:  $s$  is the shear stress at failure along any plane

$\sigma$  is the normal stress on that plane and

$c$  and  $\phi$  are the shear strength parameters; cohesion and angle of shearing resistance.

$\sigma' = (\sigma - u)$  , the effective normal stress (on the soil skeleton) and

$u$  is pore water pressure developed

$c'$  and  $\phi'$  are the shear strength parameters related to effective stresses.

The choice between total and effective stress analysis depends on the application. In case of foundation design, because it imposes both shear stresses and compressive stresses (confining pressures) on the underlying soil; the shear stresses must be carried by the soil skeleton but the compressive stresses are initially carried largely by the resulting increase in pore water pressures. This leaves the effective stresses little changed, which implies that the foundation loading is not accompanied by any increase in shear strength. As the excess pore pressures dissipate, the soil consolidates, and effective stresses increase, leading to an increase in shear strength. For foundations, it is the short term condition, the immediate response of the soil, which is most critical. This is the justification for the use of quick undrained shear strength tests rather than effective stress analysis for foundation design. Effective stress analysis must be used where long-term stability is important. Based on the AASHTO the soil in the research area is categorized as A-7-5 and A-7-6. Most of the discussions in this thesis consider fine grained soils. The undrained shear strength of soil can be determined from the laboratory test and beside that there are other methods of determining the shear strength of fine-grained soil.

### **2.3.2 Unconfined Compressive Strength (UCS)**

The maximum load that can be transmitted to the subsoil depends upon the resistance of the underlying soil. The unconfined compression strength of soil is a load per unit area at which an unconfined cylindrical specimen of soil will fail in simple compression test. It used to calculate the unconsolidated undrained shear strength of the soil under unconfined conditions.

The choice between total and effective stress analysis depends on the load application, which is by considering and comparing the soil response during and after construction, after construction effective stresses or shear strength increased due to excess pore pressures dissipated as of the soil consolidated. Thus, the immediate total stress response of the soil during construction is most critical. This is the justification for the use of quick undrained shear strength tests rather than effective stress analysis for foundation design.

To measure the resistance of the soil by compressibility or shearing deformation, UCS test gives the shear strength of the soil that is useful parameters for computing safe bearing capacity of soil as well as strength of soil. The undrained shear strength is necessary for the determination of the bearing capacity of foundations, dams, etc.

The Unconfined Compressive Strength is a measure of the cohesive strength of a soil, but it is lengthy and need experienced engineer to conduct. The test can be conducted only on intact (non- fissured) soil specimen, which can stand without confinement [14].

Determine the Unconfined Compressive Strength (UCS) of undisturbed soil specimen and the test is a special case of a triaxial compression test, especially for cohesive soils only which can stand alone without confinement. A simple compression axial load is applied quickly in the soil specimen in which the all-round pressure (confined pressure) is equal to zero. The test is an undrained test and is based on the assumption that there is no moisture loss during the test. The soil specimen is sheared by applying an axial load of major principal stress ( $\sigma_1$ ) and failure is reached. The Deviator stress ( $\sigma_1 - \sigma_3$ ) is equal to the major principal stress and minor principal stress ( $\sigma_3$ ) is equal to zero [15].

The unconfined compression test is a special case of the unconsolidated undrained triaxial test. In this case no confining pressure to the specimen is applied (i.e.,  $\sigma_3 = 0$ ). For such conditions, for saturated clays, the pore water pressure in the specimen at the beginning of the test is negative (capillary pressure). Axial stress on the specimen is gradually increased until the specimen fails (Figure 2.2). At failure,  $\sigma_3 = 0$  and so, [15]

$$\sigma_1 = \Delta\sigma_f = q_u \tag{2.3}$$

Where,  $q_u$  is the unconfined compression strength.

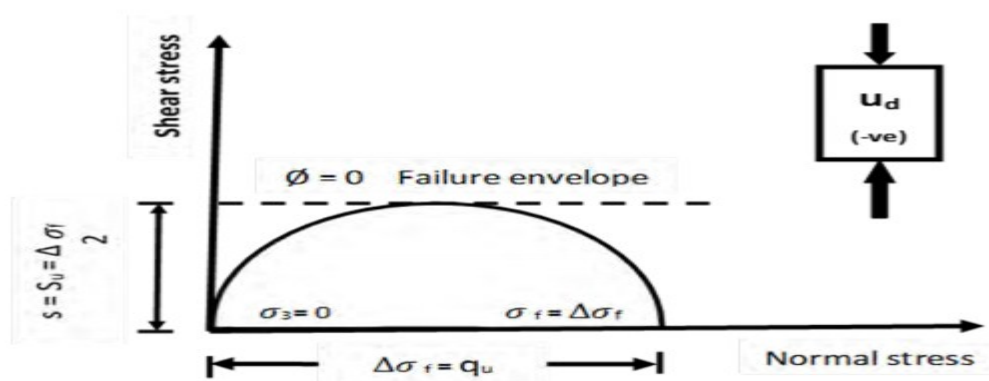


Figure 2.2 Unconfined compression strength [15]



The bearing capacity of the soil can be determined from the UCS result depending on theoretical basis by the theory of plasticity. Terzaghi and Brinch Hansen with various terms, including one for the unit weight of the soil. The complete formula is written in the form

$$p = cN_c + qN_q + 0.5B\gamma N_\gamma \quad (2.4)$$

Where the coefficients  $N_c$  and  $N_q$  are dimensionless constants,  $B$  is the total width of the loaded strip,  $q$  is the ultimate bearing capacity,  $c$  is undrained shear strength ( $c_u$ ),  $h$  depth to cone tip and  $\gamma$  is average unit weight of the soil

Table 2-1 shows general relationship of consistency and Unconfined Compression Strength. [16]

Consistency	$q_u$ (kN/m <sup>2</sup> )	Remarks
Very Soft	0-25	Squishes between finger when squeezed
Soft	25-50	Very easily deformed by squeezing
Medium stiff (firm)	50-100	Thumb makes impression to deform
Stiff	100-200	Hard to deform by hand squeezing
Very stiff	200-400	Very hard to deform by hand
Hard	>400	Nearly impossible to deform by hand

## 2.4 California Bearing Ratio (CBR)

In road constructions, the most widely used laboratory test for evaluating the potential strength of subgrade, sub base, and base course materials is the California Bearing Ratio test. This test method is a simple strength test that compares the bearing capacity of a material with that of a well graded standard crushed stone base kept in California Division of Highways Laboratory. Another penetration test which can replace CBR test is Dynamic Cone Penetrometer (DCP) test. The Dynamic Cone Penetrometer has been increasingly used for road constructions in many parts of the world due to its simplicity, and cheapness. Furthermore, a lot of empirical equations have been established to correlate the CBR values with DCPI values, which made DCP tests preferable. [5]

The California Bearing Ratio (CBR) is a very commonly used laboratory test for predicting the strength of a subgrade layer. This test method was first introduced into the California State Highway Department in the 1920's. The US Army Corps of Engineers then adapted the method in the 1940's for military airfields. After the Second World War, the CBR was also used in the UK and its use spread to European countries. CBR test was standardized by American Society Of Testing Materials (ASTM) as D1883-05 for laboratory prepared samples or re-molded samples and D4429 for on field soils; and by American Association of State Highway and Transportation officials (AASHTO) T193; and by British Standard as BS 1377 part 4 [17][18].

Soaked CBR test is used to simulate the worst scenario that would likely happen to the sample due to wet weathers. Hence, before performing the tests, soaking the remolded samples for four days is mandatory.

## 2.5 Bearing Capacity Theory and Shear Resistance of Penetrometers

### 2.5.1 Bearing Capacity Theory

An important problem of foundation engineering is the computation of the maximum load (the bearing capacity) and Coulomb's method for the analysis of soil pressures in which the soil is on the verge of failure. This type of analysis can be given a firm theoretical basis by the theory of plasticity [30].

Based on this theory, Prandtl (1920) as cited by [30] described the punching resistance of an ideal plastic medium. In this theory, the material is considered to be weightless ( $\gamma = 0$ ), and frictionless ( $\phi = 0$ ), so that its only relevant property that is considered is the cohesive strength  $c$ .

$$p_c = (\pi + 2)c = 5.14c \dots \dots \dots (2.5)$$

After this finding, many others incorporated the influence of the depth of the foundation and other parameters in to the equation. Influence of depth of the foundation was accounted for by considering a surcharge at the foundation level, to the left and the right of the applied load. The foundation pressure is denoted by  $p$ . The surcharge  $q$ , next to the foundation, is supposed to be given (refer to Figure 2.3). It can be used to represent the effect of the depth of the foundation ( $d$ ) below the soil surface. In that case  $q = \gamma d$ , where  $\gamma$  is the unit weight of the soil.

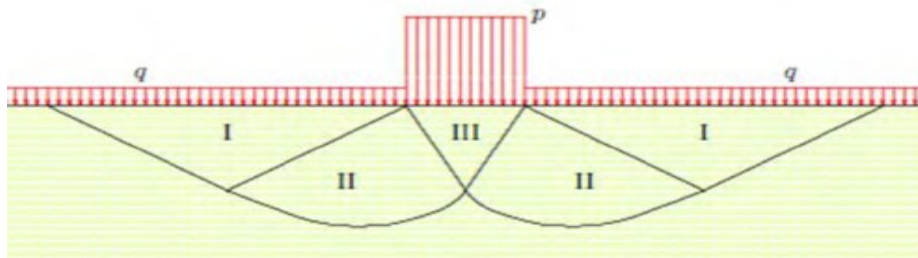


Figure 2.3 Schematization Prandtl's of strip foundation as cited by [30]

The results of the analysis of the three zones can be written as

$$p = cN_c + qN_q \quad (2.6)$$

Where the coefficients  $N_c$  and  $N_q$  are dimensionless constants, for which Prandtl (1920) as cited by obtained the following expressions, [30]

$$N_q = \frac{1 + \sin \phi'}{1 - \sin \phi'} \exp(\pi \tan \phi') \quad (2.7)$$

$$N_c = (N_q - 1) \cot \phi \quad (2.8)$$

The above formula has been extended by Keverling Buisman, Caquot, Terzaghi and Brinch Hansen with various terms, including one for the unit weight of the soil. The complete formula is written in the form [19]

$$p = cN_c + qN_q + 0.5B\gamma N_\gamma \quad (2.9)$$

$B$  is the total width of the loaded strip. For the coefficient  $N_\gamma$ , various suggestions have been made on the basis of theoretical analysis or experimental evidence or depending on the safety needed, for instance [30]

$$N_\gamma = 2(N_q - 1) \tan \phi \quad (2.10)$$

or

$$N_\gamma = 1.5(N_q - 1) \tan \phi \quad (2.11)$$

Even though the values of  $N_c$ ,  $N_q$  and  $N_\gamma$  are given, as a function of the friction angle  $\phi$ , since we are considering the limiting case  $\phi = 0$ , the value of  $N_c = 2 + \pi = 5.142$ ,  $N_q = 1$  and  $N_\gamma = 0$ .

The following ultimate bearing capacity equation is used for the current thesis:

$$q_{ult} = 5.142c + \gamma h \quad (2.12)$$

Where,  $q_{ult}$  = the ultimate bearing capacity,  $c$  = undrained shear strength ( $c_u$ )

$h$  = depth to cone tip

$\gamma$  = average unit weight of the soil

### 2.5.2. Shear Resistance of Penetrometers

This topic states about the theoretical principles that exist on shear resistance of penetrometers. As a cone penetration device, the DCP provides some measurement of the shear strength of a soil. Research has been conducted looking at both the forces imparted by a DCP cone tip, and the behavior of the soil caused by the application of these forces. DCP tip to soil interaction behavior models are various and these models are developed to analyze soil failure caused by air-dropped projectiles. While projectiles begin with velocities of several hundred meters per second, DCP tip penetrations are considered "slow" penetrations [31].

Chua formulated his modeling by considering the penetration of an axis-symmetric soil disc with a thickness equal to the height of the cone. Using stresses and strains from the model, Chua developed a correlation of Penetration Index (PI) versus elastic modulus for various types of soils [29].

Before the cone point is forced into the level of the soil to be tested, the soil is in a state of elastic equilibrium. When the cone point is forced to the test level the soil passes into a state of plastic equilibrium with the cone point becoming the element forming part or all of Zone I (Figure 2.4). Assuming an ideal soil and a smooth cone point, the zone of plastic equilibrium is subdivided into a cone-shaped zone (later displaced by the penetrometer point), an annular zone of radial shear emanating from the outer edges of the cone, and an annular passive Rankine zone. The dashed lines on the right-hand side of the same indicate the boundaries of Zones I to III at the failure stage or Penetrometer movement, and the solid lines represent the same boundaries after the cone point has moved into the level being tested [29].

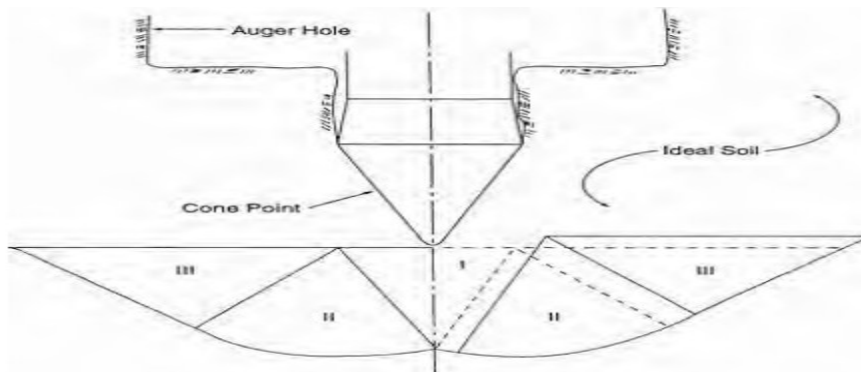


Figure 2.4 Theoretical principles of penetration equipment [29]

## 2.6 Index properties of the soil

Consistency is a term used to indicate the degree of firmness of cohesive soils. The consistency of natural cohesive soil deposits is expressed qualitatively by such terms as very soft, soft, stiff, very stiff and hard. The physical properties of clays greatly differ at different water contents. A soil which is very soft at a higher percentage of water content becomes very hard with a decrease in water content. However, it has been found that at the same water content, two samples of clay of different origins may possess different consistency [14].

### 2.6.1 Grain Size Distribution

Based on the ASTM D1140-97 wash method or wet sieve analysis is conducted to determine the percentage material finer than  $75\mu\text{m}$  more efficiently and accurately. The material retained on the  $75\mu\text{m}$  (No.200) sieve is collected and dried in oven for 24 hours. The dried soil sample is weighed accurately to determine the grain size distributions of coarser than  $75\mu\text{m}$  materials by using the dry sieve technique. The distribution of particle sizes in soil samples determined after plotting the distribution curve by combining above three test result [20].

### 2.6.2 Atterberg Limits

The objective of the Atterberg Limits test is to obtain basic index information about plasticity of the soil. Fine-grained soils are tested to determine the liquid and plastic limits, and plastic index which are moisture contents that define boundaries between material consistency states as per ASTM D 4318-98, which used for soil identification, classification and correlations to other properties [20].

### **2.6.2.1 Liquid Limit**

The liquid limit (LL) is the water content, expressed in percent, at which the soil changes from a liquid state to a plastic state and principally it is defined as the water content at which the soil pat cut using standard groove closes for about a distance of 13cm (1/2 in.) at 25 blows of the liquid limit machine (Casagrande Apparatus). The liquid limit of a soil highly depends upon the clay mineral present. The conventional liquid limit test is carried out in accordance of test procedures of AASHTO T 89 or ASTM D 4318. A soil containing high water content is in the liquid state and it offers no shearing resistance [20].

### **2.6.2.2 Plastic Limit**

The moisture at which soil has the smallest plasticity is known as the plastic limit. Which the soil stops behaving as a plastic material Just after plastic limit the soil displays the properties of a semi-solid. For determination purpose, the plastic limit is defined as the water content at which soil will just begin to crumble when rolled into a thread of 3mm in diameter.

### **2.6.2.3 Plastic Index**

The amount of water which must be added to change a soil from its plastic limit to liquid limit is an indication of the plasticity of the soil. The degree of plasticity is measured by the plasticity index (PI), which is the numerical difference between liquid limit and plastic limit ( $PI=LL - PL$ ). The greater the plasticity index means that the soil is more plastic, compressible and the greater volume change characteristic of the soil.

### **2.6.3 Specific Gravity (Gs) and Natural Moisture Content (NMC)**

The term specific gravity is defined as the ratio of the weight of a given volume of material to the weight of an equal volume of water. It used to determine the unit weights or density of the soil grain. The specific gravity value can be used in calculations of the hydrometer portion and used to in the determination of soil identification, classification and correlation to other properties [15].

The subgrade strength is very much dependent on moisture content. As the subgrade is intended to variation of moisture due to flood, precipitations or all other climatic changes, so it is

necessary to enable or understand the subgrade according to the variation of moisture. The Specific Gravity and the Natural Moisture Content (NMC) of soil samples presented in this research are determined according to ASTM D 854-98 and ASTM D 2216-98 a standard respectively [20].

### 2.6.4 Compaction tests

Compaction of a soil improves the engineering properties, i.e. it increases the shear strength of the soil and hence, the bearing capacity. It increases the stiffness and thus, reduces future settlement, void ratio and permeability. At lower water content than the optimum the soil is rather stiff and has a lot of void spaces and hence, the dry density is low. The laboratory standard proctor and modified proctor tests performed normally as per (AASHTO T 99 or ASTM D 698) and (AASHTO T 180 or ASTM D 1557) respectively [20][21].

### 2.7 Determination of geotechnical parameters using DCP

The correlation that is used for prediction is that of DCPI versus unconfined compressive strength (UCS), and Californian Bearing Ratio was done by Kleyn and the following graph was plotted.

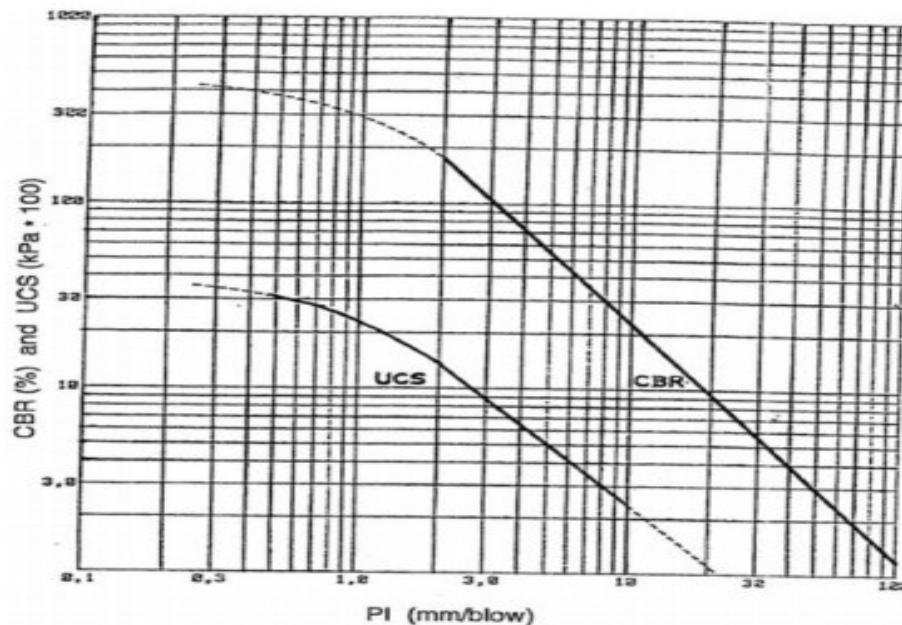


Figure 2.5 Relationships between Penetration Index (PI), California Bearing Ratio (CBR) and Unconfined Compressive Strength (UCS) [28]

### 2.7.1 Prediction of California Bearing Ratio (CBR)

The most common correlation of the Dynamic Cone Penetration Index (DCPI) is with California Bearing Ratio (CBR). The CBR is defined as the ratio of the resistance to penetration developed by a subgrade soil to that developed by a standard material. By plotting a graph of cumulative Dynamic Cone Penetration Index (DCPI) versus cumulative depth below the testing surface, a user can also observe a profile showing layer, thicknesses, and strength conditions. The soil layer of DCP value is converted to CBR by projecting the corresponding soil layer DCP slope value from its location on the X-axis vertically up to slope deflection and then horizontally over to the Y-axis. This time taking slow process may be eliminated by using a spreadsheet and different developed computer programs [2].

Several authors have investigated relationships between the DCP penetration index PI and California Bearing Ratio (CBR). CBR values are often used in road and pavement design. Two types of equations have been considered for the correlation between the PI and CBR [23].

$$\text{log - log equation: } \log CBR = A - B * (\log PI)^c \quad (2.13)$$

$$\text{inverse equation: } CBR = D(PI)^E + F \quad (2.14)$$

Where A, B, E and F are regression constants for the relationship

Harrison (1987) concluded that the log-log equation produces more reliable results while the inverse equation contains more errors and is not suitable to use. Livneh (1987) Livneh, M. (1989) and Livneh et al. (1994) proposed the following relationships based on field and laboratory tests respectively [13].

$$\log CBR = 2.20 - 0.71 * (\log PI)^{1.5} \quad (2.15)$$

$$\log CBR = 2.14 - 0.69 * (\log PI)^{1.5} \quad (2.16)$$

$$\log CBR = 2.46 - 1.12 * (\log PI) \quad (2.17)$$

Correlations are very important to estimate engineering property of soils, especially for preliminary investigation of projects. Correlations may be also used for projects where there is financial limitation, lack of test equipment and limited time.



A relation between CBR of subgrade, DCP, Modified Liquid Limit and Moisture Content is determined from regression analysis of results obtained from Experimental Investigation is expressed as: [1]

$$CBR = 0.26235 * DCP - 0.29716 * W_{LM} - 0.34399 * MC + 18.59709 \quad (R^2 = 0.83) \quad (2.18)$$

Regression analysis was performed by Munir to correlate the laboratory CBR and the DCPPR. The following non-linear regression model was obtained [28].

$$CBR = \frac{2559.44}{(-7.35 + PR^{1.84})} + 1.04 \quad R^2 = 0.93 \quad (2.19)$$

In our country, Feleke G. investigated the relationship between field DCP and Laboratory CBR around Mekele City and the following correlation were established. The first two equations are stands for fine grained soils and the last two equations for coarse grained soils.

$$\log_{10} SCBR = 2.015 - 0.906 \log_{10} DCPI \quad R^2 = 0.93 \quad (2.20)$$

$$\log_{10} UCBR = 1.6677 - 0.895 \log_{10} DCPI \quad R^2 = 0.902 \quad (2.21)$$

$$\log_{10} SCBR = 2.197 - 0.852 \log_{10} DCPI \quad R^2 = 0.836 \quad (2.22)$$

$$\log_{10} UCBR = 1.953 - 1.167 \log_{10} DCPI \quad R^2 = 0.898 \quad (2.23)$$

Yitagesu developed empirical equation is based on laboratory unsoaked CBR with in-situ conditions and field DCP tests conducted for soil samples obtained from Jima – Mizan road section [37].

$$\text{Log (CBR)} = 2.954 - 1.496 \log (\text{DCPI})$$

The Ethiopian Roads Authority in its Pavement design manual presented a DCP correlation which is drafted from TRL. Although this correlation was not developed for local soils, it has been used as the only means to estimate CBR values from the in-situ DCP tests [38].

$$\text{Log (CBR)} = 2.48 - 1.057 \text{ Log (DCPI)}$$

### 2.7.2 Prediction of Undrained Shear Strength

Based on laboratory studies, McElvaney and Djatnika (1991) have concluded that DCPI values can be correlated to the unconfined compressive strength (UCS). They considered both individual soil material and combined soil- lime mixtures types in their analysis. The developed relationship with 99 percent confidence is presented below [9].

$$\log UCS = 3.21 - 0.809 \log * (DCPI) \quad (2.24)$$

Where; UCS (unconfined compressive strength) in kPa

DCPI (Dynamic Cone Penetration Index) in inches/blow

Salgado, et al., proposed correlation of the Unconfined Compressive Strength (UCS) with Dynamic Cone Penetration Index (DCPI) that were conducted for clayey sand and well graded sand with in deferent Study area. The result shows that Unconfined Compressive Strength (UCS) decreases as the Dynamic Cone Penetration Index (DCPI) increases [3].

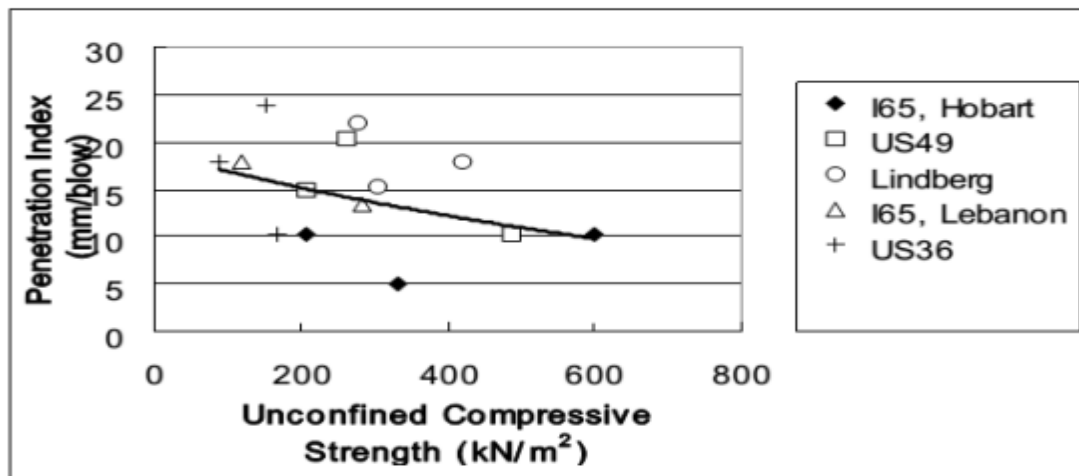


Figure 2.6 Relationships between USC and DCPI after Salgado, et al., [3]

A relation between UCS of subgrade, DCP, Modified Liquid Limit and Moisture Content is determined from regression analysis of results obtained from Experimental Investigation is expressed as: [1]

$$UCS = 0.07904 * DCP - 0.05686 * W_{LM} - 0.07359 * MC + 3.223091 \quad (R^2 = 0.70) \quad (2.25)$$

According to Alemayehu D. the research was investigated on relationship between field DCP and UCS around Alemgena town and the following correlation were established for red and black soils respectively [10].

$$UCS = -24.56*\ln(DCPI) + 223.05, R^2 = 0.805 \quad (2.26)$$

$$UCS = -58.59*\ln(DCPI)+308.04 \text{ with } R^2 = 0.831 \quad (2.27)$$

The other research was done by Anteneh G. on Addis Abeba fine grained soils and the following correlations were obtained [26].

$$UCS=-197\ln (DCPI) + 735.5 \quad R^2 = 0.711 \text{ for red clay soils of Addis Ababa and by} \quad (2.28)$$

$$UCS=895.8*DCPI^{-0.56} \text{ with } R^2=0.52.4 \quad (2.29)$$

Temnit indicated that DCPI values can be correlated to the unconfined compressive strength (UCS) of Addis Ababa Red clay soil. She took undisturbed sample and performed the unconfined compressive strength test in the laboratory and made the DCP tests on the field. She had concluded that the unconfined compression strength (UCS) is highly influenced by DCPI, bulk unit weight and natural moisture content (NMC) and liquidity Index (LI) [33].

This observation was valid only for red clay soil of Addis Ababa and have the following form:

$$UCS (kPa) = -115.59*\ln(DCPI) +456.41 LI + 645.70, \text{ with } R2=0.676 [N=30] \quad (2.30)$$

Another research done in our country revealed that UCS is significantly influenced by DCP and Liquidity index. UCS, for this category, can be estimated from DCPI by:[34]

$$UCS=-209.5*\ln(DCPI) + 800.5, R2=80.19\% \text{ for red soils in Debre Markos town and} \quad (2.31)$$

$$UCS=-7.1661*(DCPI) +416.82, R2=82.15\% \text{ for black soils in the same town} \quad (2.32)$$

### 3. MATERIAL, METHODS AND DATA COLLECTION

#### 3.1 Study area

The study carried out in Jimma town which located within latitude  $7^{\circ}40'0''N$  and longitude  $36^{\circ}50'00''E$  and elevation 1780 m asl. This study will be conducted in Jimma town by considering representative areas for sample collection process. Jimma town is found in Oromia regional state and it is located at a distance of 346 km from capital city of the country, Addis Abeba.

The excavation was done for a depth of 1 up to 2.5 m for all soils as per their existing level of natural soil considering depth of shallow foundation and effective road pavement.



Figure 3.1 Map of study area (from Google map)

#### 3.1.1 Climate

The project area is characterized by temperate humid climate that has high precipitation, warm temperature and long wet period. The mean annual rainfall in the area is around 1500mm and annual potential evaporation is about 1465mm.

The rainfall pattern shows major seasonal variation ranging from mean monthly rainfall of about 40mm in January to 215 mm in August. The main rainy season extends from April to September [32].

Table 3.1 Summary of climate data for Jimma town [32]

Month	Jan	Feb	Mar	Apr	May	Jun	Jul	Aug	Sep	Oct	Nov	Dec	Year
Av. Max temp (0C)	28	29	28	27	26	24	24	25	27	27	28	28	27
Daily mean (0C)	23	24	24	24	23	22	22	22	23	23	23	23	23
Average Low (0C)	18	19	20	20	20	19	19	19	19	19	18	17	19
Average rainfall mm	40	55	95	140	160	215	215	215	185	90	55	35	1,500
Average rainy days	5	10	14	15	18	24	25	25	22	18	10	5	191

According to the data from Jimma Town Water Supply and Sanitation Project ESIA published in 2011 the annual rainfall data was analyzed as below:

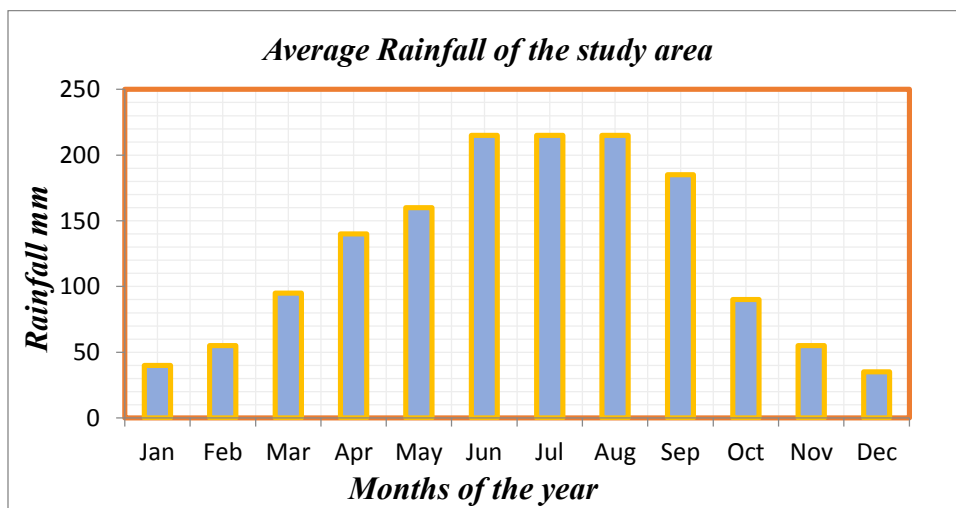


Figure 3.2 Average annual rain fall of Jimma town [32]

### 3.1.2 Topography

The major part of Jimma town, including the central, southern and western parts, is characterized by flat to gently sloping/undulating topography, while the northern and eastern parts of the town

and its peripheries are characterized by hilly/ sloping landscape. Most of the major sub-project components, including the Clear Water Rising Main, the Main Reservoir, the New Distribution Sub-mains, and Aba-Jifar Reservoir, are situated in the latter part of the City. The elevation within the town boundary and its peripheries ranges from around 1700 masl in the south/along Gilgel Gibe river to over 2000 masl in the northern periphery of the town, i.e. in the Jiren area [32].

### **3.1.3 Geology and Soils**

On the basis of information provided in the Jimma City Profile of 2008/2009, the geological formation of the Jimma area consists of various Tertiary Volcanic and younger Quaternary Sediments. Due to mostly thick soil formation and good vegetation cover, outcrops of the volcanic rocks are not common in the area. Two major soil types are observed in Jimma area. These are reddish brown residual soils and alluvial soils of brownish gray and grayish white clay soils. The reddish brown soils are well-drained soils which are found in the hilly and rolling/sloping areas. Whereas the alluvial soils are found in the low-lying flatter or gently sloping plains and these soils are poorly drained [32].

## **3.2 Data Collection and source of data**

### **3.2.1 Data collection**

The data collection stage consists of gathering relevant information from Jimma Town Municipality and collection of soil samples and in situ field test during site visits. Sampling locations were selected within Jimma Town using descriptive sampling technique in each kebeles. After completing the DCP test, the cone-rod is removed and soil samples are collected. The collected soil samples from the field are further analyzed in the laboratory to classify and categorize the soil type and determine UCS strength.

### **3.2.2 Sample size and sample procedure**

Fourteen test pits are excavated using local labor and samples were collected from each test pits at different depth in different parts of Jimma Town. The number of samples taken from one pit mainly depends on the penetration resistance or strength dictated by the DCP test and observed changes in color and moisture conditions of the soil. Up to two soil samples are taken from one

test pit, in total thirty disturbed and undisturbed samples collected for further laboratory investigations. Disturbed and undisturbed soil samples were collected from test pits to determine index properties, soil classification, Unconfined Compression Strength (UCS), etc. Tube sampling techniques used to extract undisturbed soil as per ASTM D1587-94 specification in different area of Jimma Town. Plastic bag, due to its very minimum degree of disturbance, is used for sampling and transporting representative disturbed soil samples at different layers of test pits to keep the moisture of the sample according to ASTM D 4220-95.

Representative disturbed soil samples were collected using plastic bag from the different layers of test pits, individually, for classification tests (refer to ASTM D 4220). Undisturbed samples were collected for unconfined compressive strength, bulk density and in situ moisture content tests (refer to ASTM D 1587)

### **3.2.3 Source of data**

In this study primary data which is obtained from laboratory tests and field tests was used. Samples were taken from test pits at desired depth through disturbed and undisturbed sampling methods. For comparison of index properties secondary data were used.

### **3.2.4 Data analysis**

In this study the data obtained from laboratory tests was analyzed. Method of analysis includes tabulation and graphical to discuss the result obtained from laboratory tests. The regression or correlations of the data were analyzed using single linear and multiple linear regressions and the validation of the equation using graphs.

The results were analyzed accordingly and whenever the site is found to lie within the scope of the study it is incorporated into the study. Therefore, for analysis and correlation development purpose the two categories will be:

Category-1) clayey soils including both grey and black cotton soils of Jimma town

Category-2) Red clay soils of Jimma Town

### 3.3 Data Analysis

In this study the data obtained from laboratory tests was analyzed. Method of analysis includes tabulation and graphical to discuss the result obtained from laboratory tests.

The data variables are classified in to two: independent and dependent variables. CBR and UCS are considered as dependent variables while DCPI, atterberg limits and moisture contents are independent variables. To analyze the data linear regression method was used by considering single variable relationship and multiple variable relationships.

#### 3.3.1 Normality test

An assessment of the normality of data is a prerequisite for many statistical tests because normal data is an underlying assumption in parametric testing. There are two main methods of assessing normality: graphically and numerically.

There are formal ways to perform normality tests such as Shapiro-Wilk and Shapiro-Francia tests. The Shapiro-Wilk Test is more appropriate for small sample sizes ( $< 50$  samples), but can also handle sample sizes as large as 2000. For this reason, we will use the Shapiro-Wilk test as our numerical means of assessing normality. If the significance value of the Shapiro-Wilk Test is greater than 0.05, we can reject the alternative hypothesis and conclude that the data comes from a normal distribution or the data is normal. If it is below 0.05, the data significantly deviate from a normal distribution. In order to determine normality graphically, we can use the output of a normal Q-Q Plot. If the data are normally distributed, the data points will be close to the diagonal line. If the data points stray from the line in an obvious non-linear fashion, the data are not normally distributed [39].

#### 3.3.2 Significance level

**Correlation coefficient (R):** correlation coefficient is the act of the linear correlation between two variable  $x$  and  $y$ , between +1 and -1 for sale inclusive.  $R = 1$  indicates a perfect linear correlation and linear regression perfect,  $R = 0$  is no correlation, and  $R = -1$  total negative correlation.



***P-value:*** P-values do not simply provide you with a Yes or No answer; they provide a sense of the strength of the evidence against the null hypothesis. The lower the p-value, the stronger the evidence is. *P-value* is simply the ratio of the model mean square error to the mean square. The confidence level for the statistical analysis is 95% which indicate that the p-value of the analysed data should be less than 0.05 [39]

***Standard error:*** The average error of each measurement sample points on the line of best fit. Out of all the curves, the best-fit curve through the standard error smaller and it is important because it is used to calculate other measures, such as confidence intervals and margin of error.

### **3.3.3 Inter- variable relationship**

**Chi square test:** The research hypothesis states that the two variables are dependent or related. This will be true if the observed counts for the categories of the variables in the sample are different from the expected counts. The null hypothesis is that the two variables are independent. This will be true if the observed counts in the sample are similar to the expected counts [39].

If the probability of the test statistic is less than or equal to the probability of the alpha error rate (0.05), we reject the null hypothesis and conclude that our data supports the research hypothesis. We conclude that there is a relationship between the variables. If the probability of the test statistic is greater than the probability of the alpha error rate, we fail to reject the null hypothesis. We conclude that there is no relationship between the variables, i.e. they are independent [39].

### **3.3.4 Univariate/scatter plot analysis**

In developing correlations, the first step is creating a scatter plot of the data, to visually assess the strength and form of some type of relationship.

If the points are very close to each other, a fairly good amount of correlation can be expected between the two variables. On the other hand if they are widely scattered a poor correlation can be expected between them. If the points are scattered and they reveal no upward or downward trend then we say the variables are uncorrelated [39]

### 3.4 Test Methods

#### 3.4.1 Field Test

Sand cone replacement method was used to determine the in-place density and unit weight of soils using ASTM D1556-07.

The sample for Unconfined Compressive Strength test was taken from the site with a good care and laboratory test conducted using ASTM D2166-98a

#### 3.4.2 Laboratory Tests

The entire laboratory tests are performed in Jimma Institute of Technology Geotechnical Laboratory using the following standard testing procedures, (Table 3-1).

Table 3-2 Summary of laboratory testing procedure standards

Test Description	Standard Testing Procedure
Natural Moisture Content	ASTM D 2216-98a
Atterberg Limits	ASTM D 4318-98
Specific Gravity	ASTM D 854-98
Unconfined Compressive Strength	ASTM D2166-98a
California Bearing Ratio	AASHTO T-193
Grain Size Distribution Analysis	ASTM D 1140-97 and D 422-98
Compaction	AAHTO T-180

The CBR test is performed by measuring the pressure required to penetrate a soil sample with a plunger of standard area. The measured pressure is then divided by the pressure required to achieve an equal penetration on a standard crushed rock material. This test method is primarily intended for but not limited to, evaluating the strength of cohesive materials having maximum particle sizes less than 19mm. If materials having maximum particle sizes greater than 19mm are to be tested, modifying the gradation of the material is applicable so that the material used for tests all passes the 19mm sieve while the total gravel between 4.75mm and 75mm fraction remains the same [19].

While performing laboratory CBR test, the force or load required to cause the penetration will be recorded with respect to the standard penetration depths at each 0.5mm penetration, including the load value at 2.54 mm and 5.08 mm until the total penetration is 12.7mm. The penetration resistance load is then plotted against the penetration depth. From the curve, the bearing ratio is calculated by dividing the loads obtained at 2.54 mm and 5.08mm penetrations by their corresponding standard loads, 13.24KN and 19.96KN respectively. If the bearing ratio of 2.54 mm is greater than that of 5.08 mm, the bearing ratio that should be reported for the soil is normally the one at 2.54 mm penetration. [19]

Laboratory CBR tests can be performed for optimum water content or for the range of water contents. The CBR is determined at optimum water content when and where the effect of compaction water content on CBR is small, such as cohesion less, coarse grained materials, or where an allowance is made for the effect of differing compaction water contents in the design procedure.

### **3.5 Field test Results and Discussion**

#### **3.5.1 Field dry density**

The dry density and the natural moisture content of the soil are conducted at field. Field dry density is conducted using sand cone replacement method and the range of dry density obtained is between 9.12 kN/m<sup>3</sup> to 12.98 kN/m<sup>3</sup>. Hence the relationship of natural moisture content and field dry density is inversely proportional.

#### **3.5.2 Dynamic Cone Penetrometer**

The DCP index or reading is defined as the penetration depth (D) in mm for a single drop of hammer. The cone is driven in to the ground up to the desired depth and average DCP index is calculated for a single blow. Depth of penetration considered in the study was 800 to 850 mm depending upon the resistance offered by the soil [2].

The dynamic cone penetration index (DCPI) obtained from field was varies from 12.2 to 58.8 which differ from place to place.

Table 3.4 Dynamic cone penetration data for Rift valley 1 soil sample

No. of blows	Cumulative no. of blows	depth of penetration (mm)	DCPI	Penetration rate
0	0	160		
1	1	278	118	118
1	2	362	84	84
1	3	431	69	69
1	4	498	67	67
1	5	529	31	31
1	6	561	32	32
1	7	589	28	28
1	8	618	29	29
1	9	653	35	35
1	10	693	40	40
1	11	732	39	39
1	12	769	37	37
1	13	815	46	46
1	14	870	55	55
1	15	933	63	63

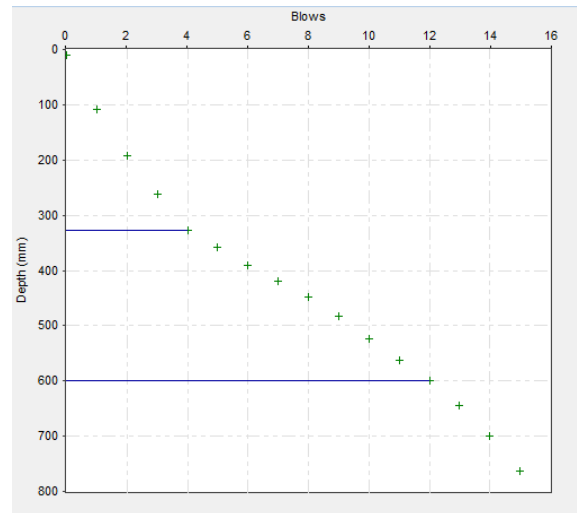


Figure 3.3 Graph No. of blows vs depth for Rift valley 1 soil sample

Table 3.5 Dynamic cone penetration Index test summary

Sample designation	Depth (m)	DCPI (mm/blow)	Sample designation	Depth (m)	DCPI (mm/blow)
Riftvalley	1	58.8	Agri campus	2.5	29.2
	2	51.9	Frustale	1.5	12.2
Kochi	1	21		2.5	13.9
	2.5	16.1	Teknik sefer	1.5	19.5
Mercato	1.2	30		2.5	19.7
	2.5	24.4	B/Bore	1	23.2
H/Mercato	1.5	23.1		2	29.6
	2.5	26.2	Ajip	1	22.8
Kito Red	1.5	13.5		2	28.9
	2.5	15.6	Ifabula	1.5	31.8
Kito Black	1	48.5		2.5	33.9
	2	46.2	Bore	1	28.3
Bosa Kito	1.5	14		2	31
	2.5	20.8	Jiren	1.5	15.3
Agri campus	1.5	25.3		2.5	23.2

### 3.6 Laboratory test Results and Discussion

#### 3.6.1 Grain size Analysis

The objective of grain size analysis is to determine the percentage of soils passing different sieve opening sizes. In this study, this determination is used for classification purpose and for overall engineering characteristics indication. Wet sieve was conducted for cohesive soils to disintegrate sticky soil particles into their original particle size by soaking and washing in water and sieving the retained portion mechanically as per AASHTO T88.

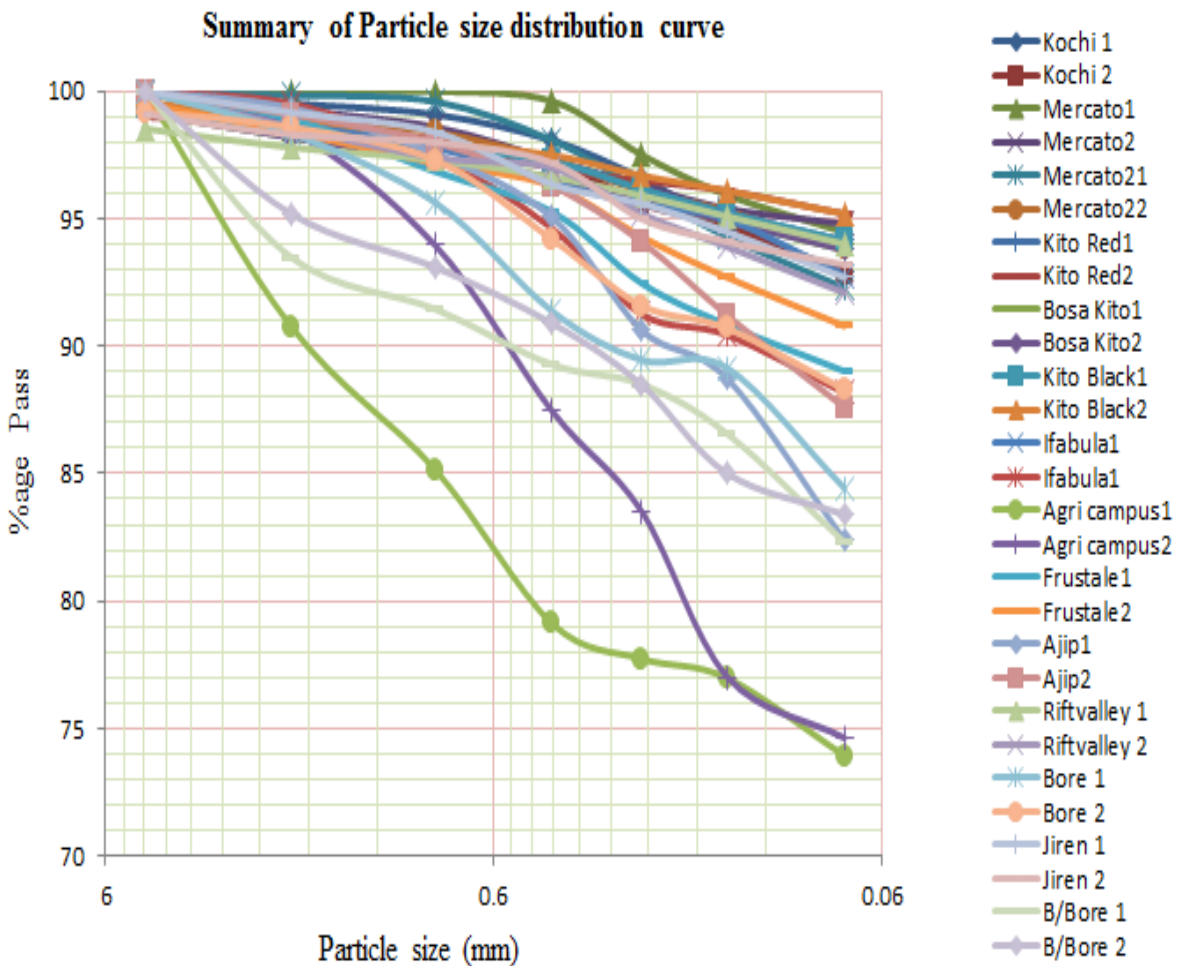


Figure 3.4 Summary of particle size curve

This graph shows that above 50 % of the entire soil samples pass sieve 0.075 mm. This indicated that these all soils are categorized under fine grained soils according to Unified Soil Classification System.

### 3.6.2 Atterberg Limits

The purpose of conducting Atterberg limit test is to know the plasticity property of a soil passing the No. 40 (425  $\mu$ m) sieve with varying degrees of moisture content as these are helpful as input index parameters to make the soil classification together with the particle size distribution results. The basic limits needed for this research are the liquid limit and the plastic limit. In this research, casagrande method was used to carry out liquid limit. The liquid limit (LL) is the water content, expressed in percent, at which the soil changes from a liquid state to a plastic state, a liquid limit value ranging from 93.5 up to 56, The moisture at which soil has the smallest plasticity is known as the plastic limit, plasticity limit value of 24 up to 51 and the degree of plasticity is measured by the plasticity index (PI), which is the numerical difference between liquid limit and plastic limit ( $PI=LL - PL$ ). Plasticity index values of 24% up to 58.5% were obtained. (Refer to Table 3.6)

Table 3.6 Summary of Atterberg Limits

Sample designation	Depth (m)	LL (%)	PI (%)	PL (%)	Sample designation	Depth (m)	LL (%)	PI (%)	PL (%)
Riftvalley	1	93.5	58.5	35	Agri campus	2.5	57	27	30
	2	90	50.4	39.6	Frustale	1.5	82	24	58
Kochi	1	86.5	46.5	40		2.5	79	43	36
	2.5	72	43	29	Teknik sefer	1.5	65	40	25
Mercato	1.2	81	49.2	31.8		2.5	62	34	28
	2.5	83	48.9	34.1	B/Bore	1	61	31	30
H/Mercato	1.5	69	44	25		2	59	30	29
	Kito Red	1.5	80	45	35	Ajip	1	69	35.4
2.5		84	44	40	2		72	42	30
Kito Black	1	88	53	35	Ifabula	1.5	59	35	24
	2	79	44	35		2.5	56	31	25
Bosa Kito	1.5	81	41	40	Bore	1	71	41	30
	2.5	79	44	35		2	69	39	30
Agri campus	1.5	71	41	30	Jiren	1.5	65	31.1	33.9
						2.5	68	33	35

### 3.6.3 Soil Classification

From visual observations and field tests, the soils of the area are classified as clay with high plasticity. According to AASHTO classification system the soil are classified as A-7-5 and A-7-6 which are clayey soils. This implies that the soils of the study area are fine grained soils which are highly clayey soils.

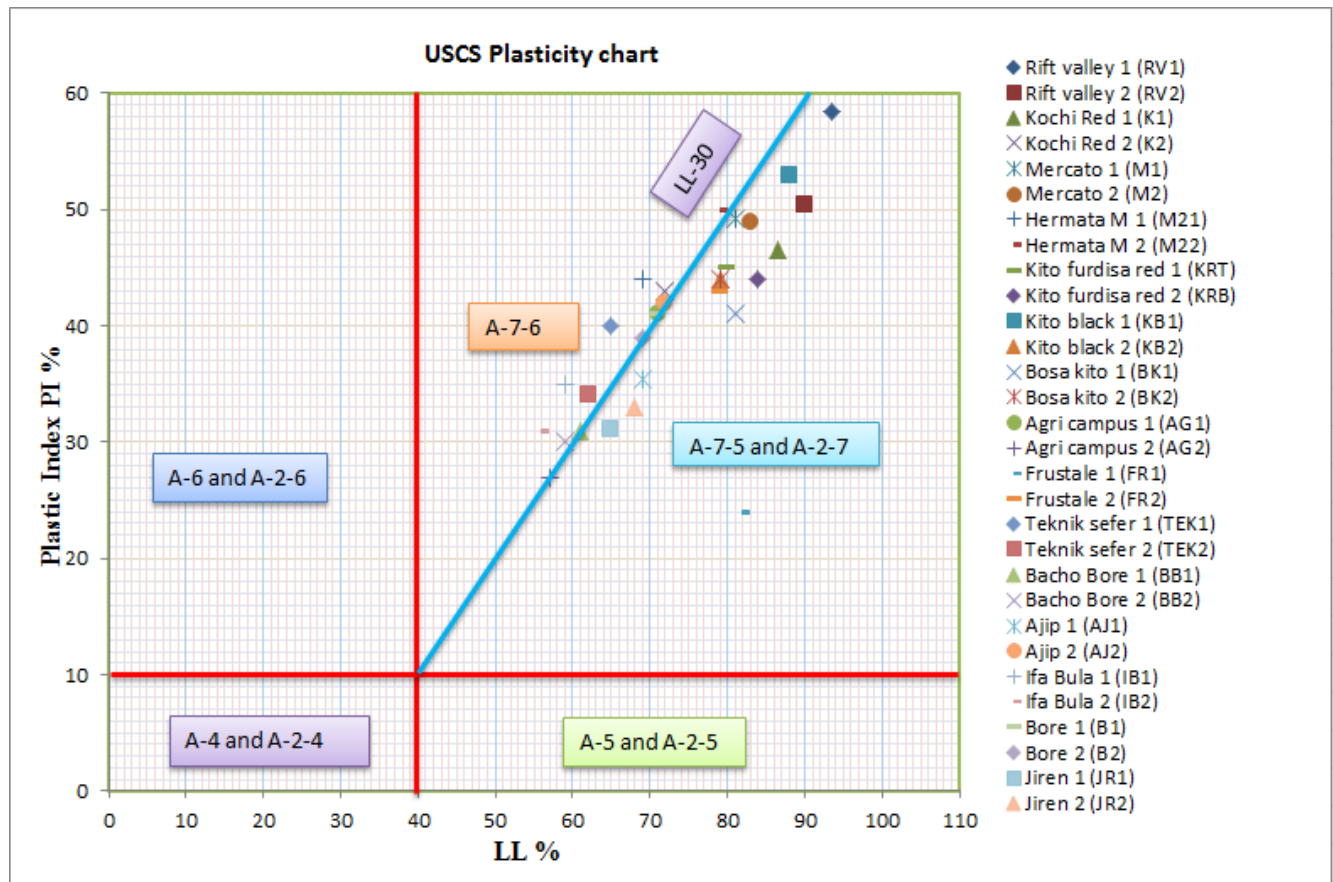


Figure 3.5 AASHTO plasticity chart classification for the Jimma fine-grained soils

From figure 3.5 it concluded that the most of the soil samples taken in this study fall in A-2-5 by AASHTO plasticity chart classification and some of the samples are A-7-6.

According to USCS plasticity chart classification most of the soils fall in to CH while some of the soils are in MH. This shows that most of soil at study site are highly plastic clayey soils where as some of the soils are highly plastic silty soils.

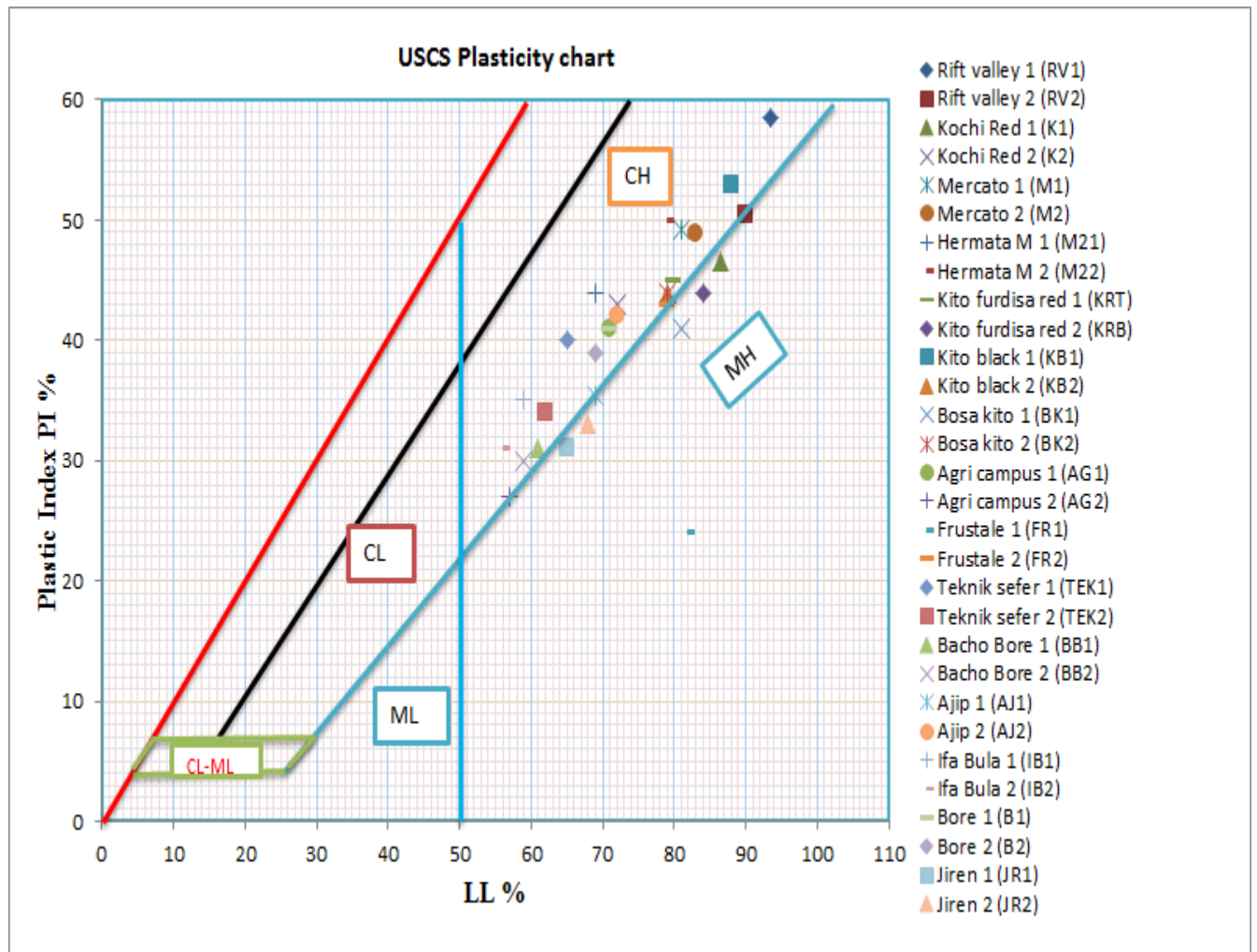


Figure 3.6 Classification of the fine-grained Jimma soils using USCS plasticity chart

### 3.6.4 Modified Proctor Test

A modified proctor test conducted as per AASHTO T 180 A, through which samples compacted at five layers each compacted by 25 uniform blows using 4.54 kg weight of hammer. From the modified proctor test, after plotting moisture-density curve, a range of maximum dry density along with the optimum moisture content were obtained.

From data obtained in laboratory tests compaction curves was drawn to show the peak of the curve of moisture-density relationship and to extract MDD and OMC values from it.

The result obtained from laboratory varies from 1.36 to 1.48 g/cm<sup>3</sup> for maximum dry density and from 23.6 % to 30.6 % for optimum moisture content. (Refer to table 3.7)



Table 3.7 Detail of the compaction characteristics of the study samples

Sample designation	Depth (m)	MDD (g/cm <sup>3</sup> )	OMC %	Sample designation	Depth (m)	MDD (g/cm <sup>3</sup> )	OMC %
Riftvalley	1	1.39	29.4	Agri campus	2.5	1.4	27
	2	1.4	30.6	Frustale	1.5	1.42	24.8
Kochi	1	1.37	32		2.5	1.44	25.5
	2.5	1.41	30.2	Teknik sefer	1.5	1.45	24.9
Mercato	1.2	1.38	29		2.5	1.42	26
	2.5	1.36	29.4	B/Bore	1	1.46	28.5
H/Mercato	1.5	1.38	29.2		2	1.43	28
	Kito Red	2.5	1.39	28.6	Ajip	1	1.41
1.5		1.39	25.7	2		1.38	25.2
Kito Black	2.5	1.42	26.3	Ifabula	1.5	1.48	26.8
	1	1.4	29		2.5	1.47	25.3
Bosa Kito	2	1.43	27	Bore	1	1.4	28.2
	1.5	1.42	27		2	1.41	27
Agri campus	2.5	1.42	26.5	Jiren	1.5	1.46	23.6
	1.5	1.39	26.2		2.5	1.48	24.5

### 3.6.5 California Bearing Ratio

The CBR data is important variable to make relationship with the DCP data. Three-point CBR Test was conducted according to AASHTO T 193. From CBR data analysis, it has been observed that the ranges of CBR values for these soils are from 1.25 % to 10.5% obtained at 95% MDD of standard AASHTO proctor density. The sample remolded with OMC which is obtained from compaction test and soaked for four days to check for the worst condition of the pavement. The detail of this test is attached on Appendix D.

### 3.6.6 Unconfined Compressive Strength

The Unconfined compressive strength test was conducted according to ASTM D2166-98a. The result obtained was indicated that the UCS value varies from 62 kPa to 300 Kpa. Depending on these values the consistency of these soils is ranged from stiff to very stiff. Refer to table 3.10 and the detail of this test is found in Appendix B.

### 3.7 Summary of Test Results

All the properties of soil are expressed by field density, water content, specific gravity, atterberg's limit unconfined compression test, Californian Bearing Ratio and Dynamic cone penetration test. These have been done both in the field and laboratory. (Refer to table 3.10)

### 3.8 Comparison of Index Properties of Current Study with Previous Researches

The index properties of Jimma clay soils from current research and previous researches are presented in Table 3.8 and 3.9. Specific gravity, liquid limit, plastic limit, NMC, percentage of finer and classification are presented.

Table 3.8 Comparison of index properties and classification of Jimma soils with the previous works [35][36].

Research work	Liquid limit, LL (%)	Plastic limit, PL (%)	Plastic index, PI (%)	USCS Classification	Colors
Jemal J. [35]	53 - 108	27 - 41	22 - 68	CH , MH	Black, Gray, Red
Gifti H. [36]	44 - 77	18 - 45	17 - 50	-----	Black, Gray, Red
Current	56 - 93.5	24 - 51	24 - 58.5	CH , MH	Black, Gray, Red

Table 3.9 Comparison of index properties and classification of Jimma soils with the previous works [35][36].

Research work	Specific gravity	Natural moisture content	Percentage of fine	AASHTO classification
Jemal J. [35]	2.58 - 2.81	40.88 - 70	61 - 99	A-7-6 & A-7-5
Gifti H. [36]	2.61 - 2.78	-----	56.6 - 98.9	A-7-6 & A-7-5
Current	2.57 - 2.74	35 - 59	73 - 98.1	A-7-6 & A-7-5

Table 3.10 Summary of the test results

Sample site		Depth (mm)	DCPI	NMC %	Gs	Atterberg limits			Compaction parameters		Subgrade strength		AASHTO Classification
			(mm/blow)			LL (%)	PL (%)	PI (%)	MDD (g/cc)	OMC (%)	UCS (kPa)	CBR (%)	
Rift valley	RV1	1	58.8	59	2.65	93.5	41.3	52.2	1.39	29.4	77.8	1.25	A-7-5
	RV2	2	51.9	58	2.63	90	39.6	50.4	1.4	30.6	90	1.6	A-7-5
Kochi Red	K1	1	21	36	2.68	86.5	30.2	56.3	1.37	32	270	6.8	A-7-5
	K2	2.5	16.1	35	2.66	72	29	43	1.41	30.2	284	7.1	A-7-6
Mercato	M1	1.2	30	58	2.67	81	31.8	49.2	1.38	29	130	3.9	A-7-5
	M2	2.5	24.4	51	2.7	83	34.1	48.9	1.36	29.4	174	4.8	A-7-5
Hermata	M21	1.5	23.1	57	2.69	69	33	36	1.38	29.2	127	3.7	A-7-6
	M22	2.5	26.2	54	2.64	79	29	50	1.39	28.6	139	3.25	A-7-6
Kito furdisa red	KRT	1.5	13.5	44	2.67	80	41.7	38.3	1.39	25.7	281	10.5	A-7-5
	KRB	2.5	15.6	44	2.64	84	44	40	1.42	26.3	253	9.4	A-7-5
Kito black	KB1	1	48.5	50	2.63	88	43.6	44.4	1.4	29	79	2.25	A-7-5
	KB2	2	46.2	50.5	2.59	79	46	33	1.43	27	62	1.85	A-7-5
Bosa kito	BK1	2.5	14	35	2.69	81	43.3	37.7	1.42	27	271	6.9	A-7-5
	BK2	1.5	20.8	41	2.64	79	40	39	1.42	26.5	219	6.5	A-7-5
Agri campus	AG1	2.5	25.3	52	2.73	71	30	41	1.39	26.2	215	5.5	A-7-5
	AG2	1.5	29.2	53	2.69	57	27	30	1.4	27	189	3.5	A-7-5
Frustale	FR1	2.5	12.2	42	2.61	82	58	24	1.42	24.8	296.9	8.7	A-7-5
	FR2	1.5	13.9	43	2.64	79	46	33	1.44	25.5	273	8.3	A-7-5
Teknik sefer	TEK1	1.5	19.5	56	2.68	65	32.9	32.1	1.45	24.9	199.6	4.3	A-7-6
	TEK2	2.5	19.7	58	2.63	62	28	34	1.42	26	235	3.8	A-7-6

Sample site		Depth (mm)	DCPI	NMC %	Gs	Atterberg limits			Compaction parameters		Subgrade strength		AASHTO Classification
			(mm/blow)			LL (%)	PL (%)	PI (%)	MDD (g/cc)	OMC (%)	UCS (kPa)	CBR (%)	
Bacho Bore	BB1	1	23.2	52	2.57	61	34.2	26.8	1.46	28.5	159.8	4.25	A-7-5
	BB2	2	29.6	54	2.62	59	29	30	1.43	28	169	4	A-7-6
Ajip	AJ1	2	22.8	52	2.69	69	33.6	35.4	1.41	23.9	177.6	4.8	A-7-5
	AJ2	1	28.9	54	2.7	72	51	21	1.38	25.2	156	4.2	A-7-5
Ifa Bula	IB1	1.5	31.8	54	2.67	59	24	35	1.48	26.8	135	3.7	A-7-6
	IB2	2.5	33.9	56	2.64	56	25	31	1.47	25.3	116.8	3.1	A-7-6
Bore	B1	1	28.3	52	2.62	71	16.8	54.2	1.4	28.2	184	3.4	A-7-5
	B2	2	31	53	2.58	69	35	34	1.41	27	171	3.1	A-7-5
Jiren	JR1	1.5	15.3	37	2.71	65	33.9	31.1	1.46	23.6	249	7.6	A-7-5
	JR2	2.5	23.2	42.5	2.74	68	32	36	1.48	24.5	256	7.3	A-7-5

## 4. ANALYSIS AND DISCUSSION

### 4.1 General

#### 4.1.1 Regression

Regression analysis is concerned with the procedure how the values of Y depend on the corresponding values of X. Y, whose value is to be predicted, is known as dependent variable and X, which is used in predicting the value of dependent variable, is called independent variable. A regression model that contains more than one independent variable is called multiple regression models. Alternatively, regression model containing one independent variable is termed as simple regression model.

$$y = a + bx$$

Where  $y$  = the response variable,  $x$  = the predictor variable,  $a$ , and  $b$  are coefficient letters,  $a$  stands for the  $y$ -intercept and  $b$  stands for the slope

In this study two sets of investigations have been conducted. The first set considers UCS as the dependent variable where as DCPI and other parameters are independent variables. The second set considers CBR as the dependent variable and the independent parameters employed for the investigation of UCS are used.

#### 4.1.2 Normality test and Univariate plots

The normality of the data obtained from laboratory and field was analyzed using SPSS software for normality to check the normality of the data. Depending on the significance value of Shapiro-Wilk the datas with significance greater than 0.05 are taken as normal data. The univariate plots are checked using normal Q-Q plots. For both categories the normality test was conducted and the result of analysis shows that all datas are normally distributed. (Refer to appendix E1)

#### 4.1.3 Interdependence tests

The data was analyzed using chi square test by assuming the research hypothesis and null hypothesis to check whether the variables are dependent or independent of each other. Depending on the value of Asymptotic Significance (2-sided) the interdependence condition of

research parameters was decided. The value of Asymptotic Significance (2-sided) obtained from the analysis shows that there is no inter-dependence between DCPI and NMC, LL, LI, MDD; PL and MDD, LL, FDD; LL and LI, MDD for both category because the Asyptotic Significance value is greater than 0.05. (Refer to Appendix E2.1 and E2.2)

## 4.2 Single Regression

### 4.2.1 Scatter Plot for Category-1 (Black clay soils of Jimma Town)

In developing correlations, the first step is creating a scatter plot of the data, to visually assess the strength and form of the relationship. In the figures below (Figure 4-1 to 4-9) the scatter plot of UCS and CBR with DCPI, LI, LL and NMC are presented.

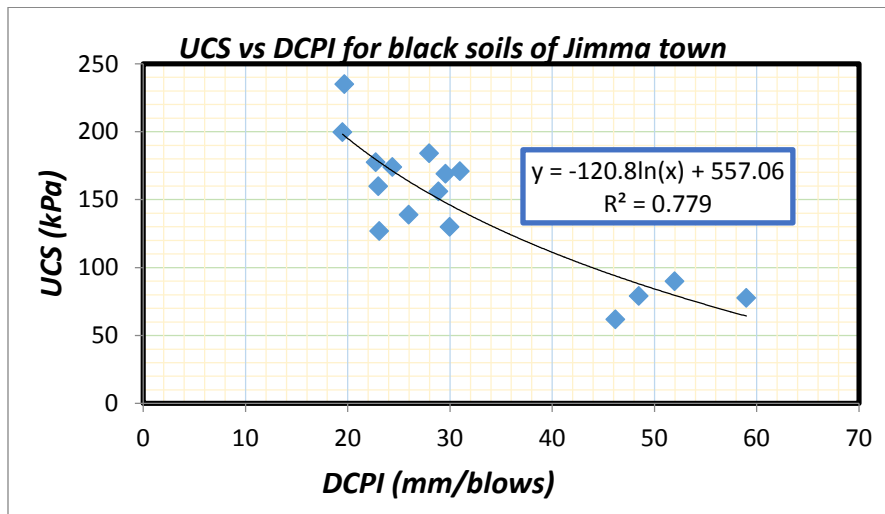


Figure 4.1 Scatter plot of UCS with DCPI for black clayey soils of Jimma Town

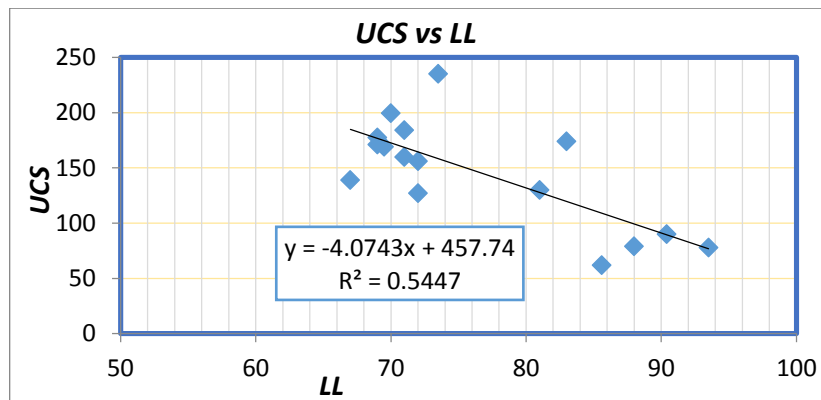


Figure 4.2 Scatter plot of UCS with LL for black clayey soils of Jimma Town

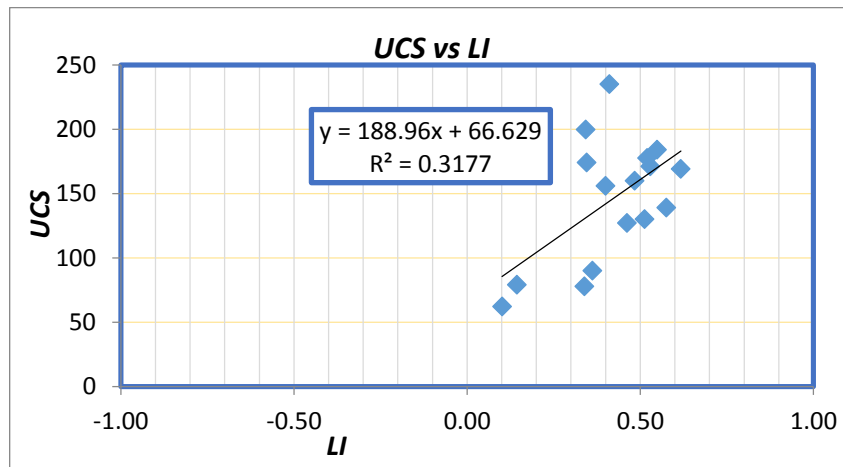


Figure 4.3 Scatter plot of UCS with LI for black clayey soils of Jimma Town

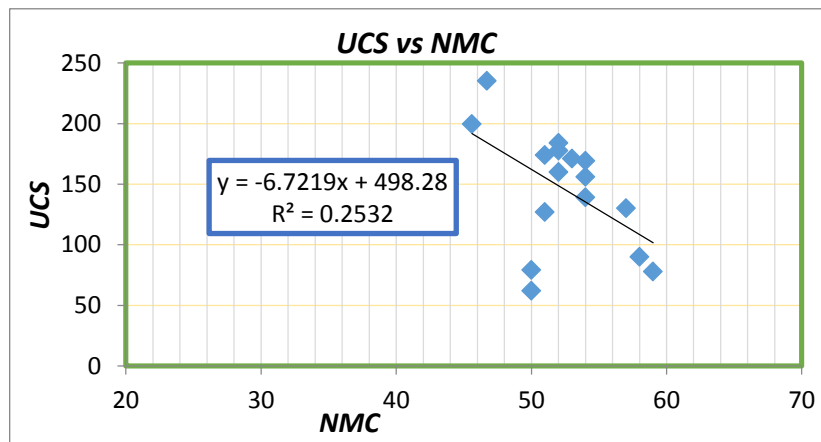


Figure 4.4 Scatter plot of UCS with NMC for black clayey soils of Jimma Town

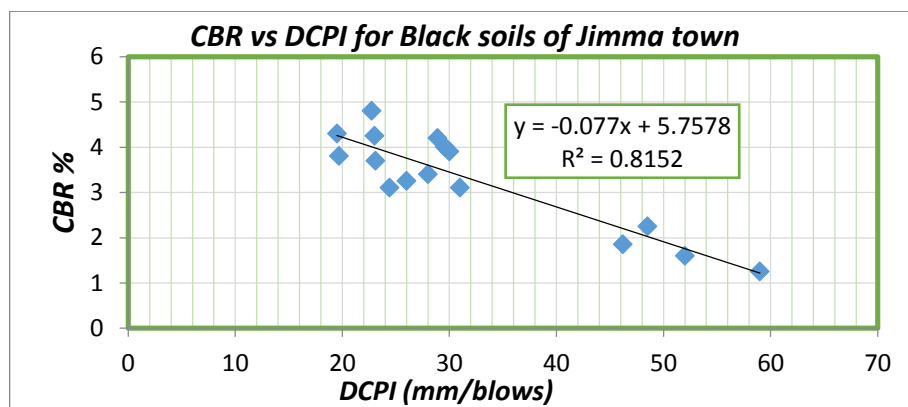


Figure 4-5 Scatter plot of CBR with DCPI for black clayey soils of Jimma Town

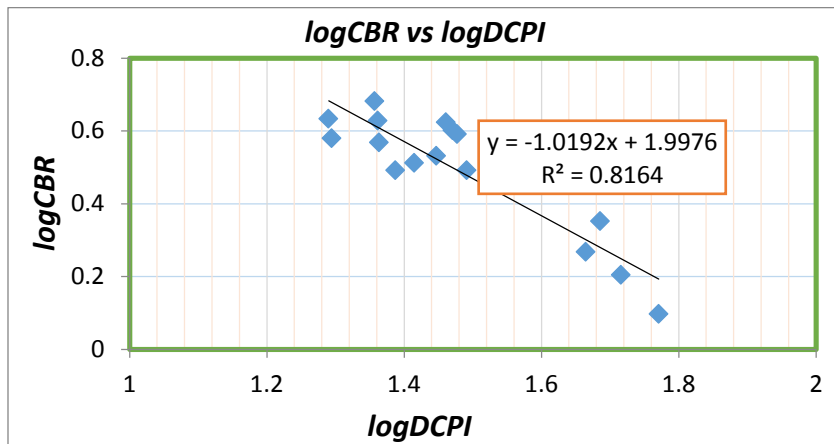


Figure 4.6 Scatter plot of logCBR with logDCPI for black clayey soils of Jimma Town

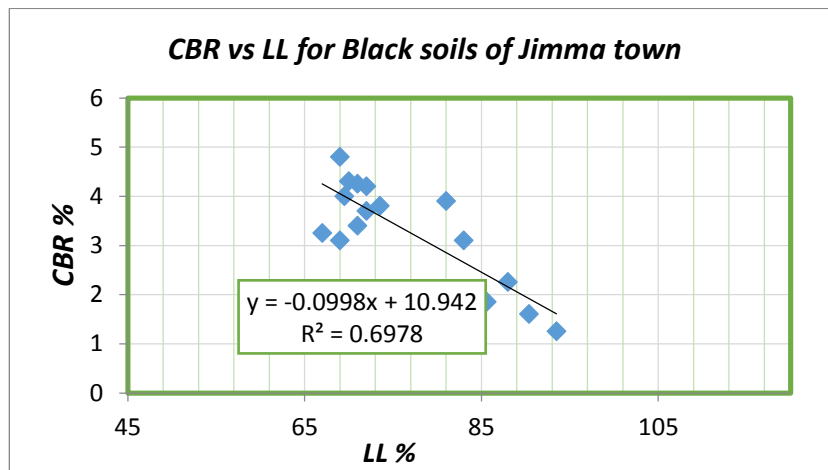


Figure 4.7 Scatter plot of CBR with LL for black clayey soils of Jimma Town

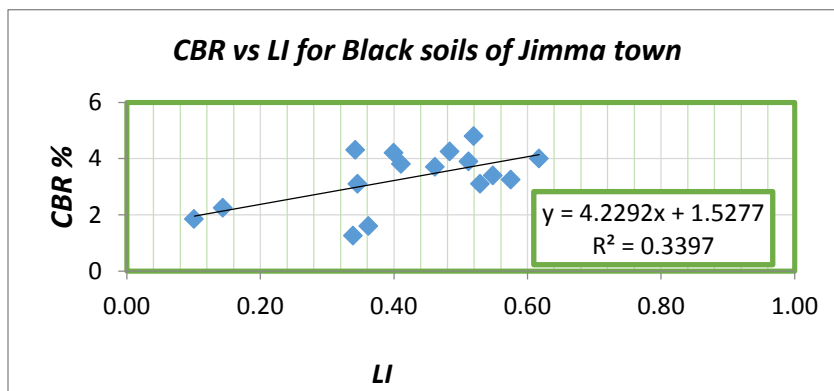


Figure 4.8 Scatter plot of CBR with LI for black clayey soils of Jimma Town



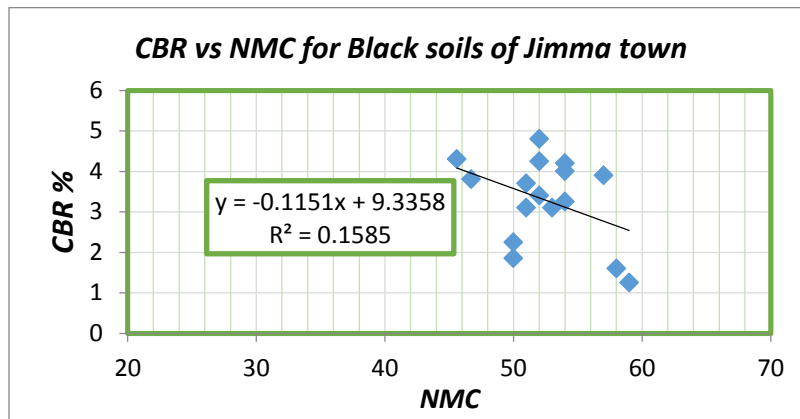


Figure 4.9 Scatter plot of CBR with NMC for black clayey soils of Jimma Town

#### 4.2.2 Scatter Plot for Category-2 (Red clay soils of Jimma Town)

Similar to 5.2.1 the scatter plots of UCS and CBR with DCPI and LL and NMC are presented for black clay soils of Jimma Town (Figure 4-10 – 4-17).

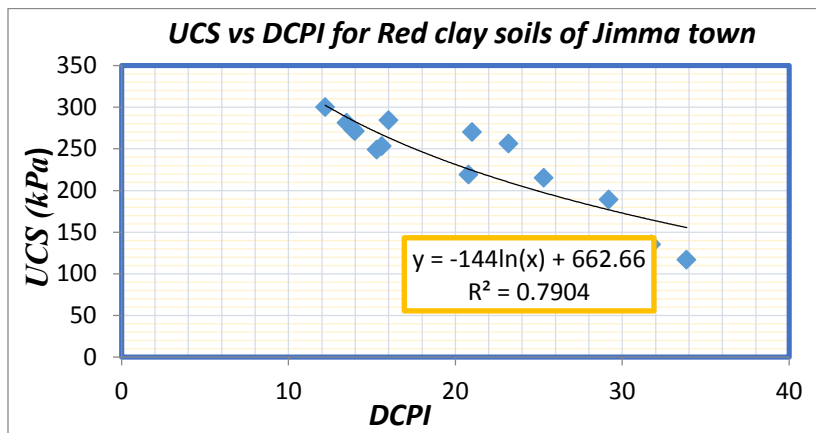


Figure 4.10 Scatter plot of UCS with DCPI for red clayey soils of Jimma Town

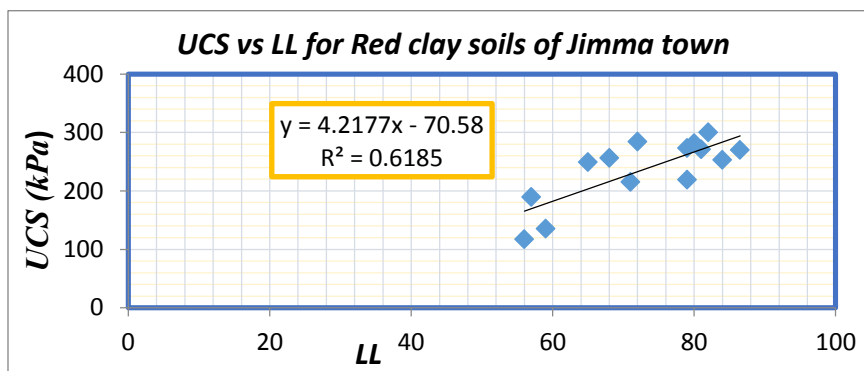


Figure 4.11 Scatter plot of UCS with LL for red clayey soils of Jimma Town

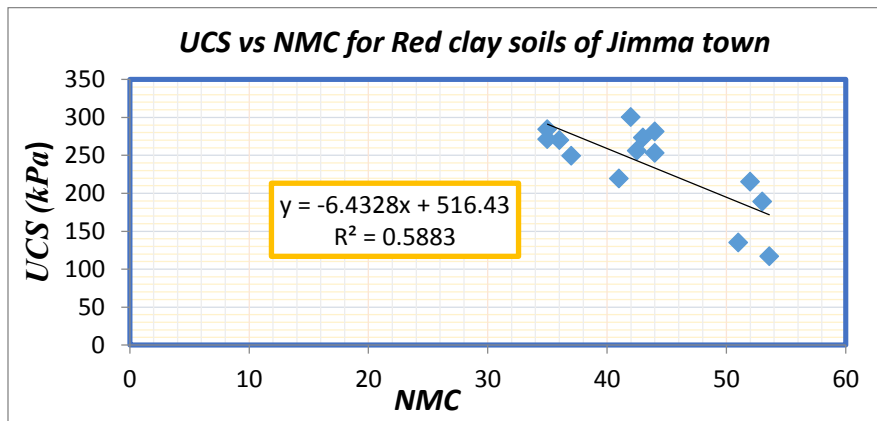


Figure 4.12 Scatter plot of UCS with NMC for red clayey soils of Jimma Town

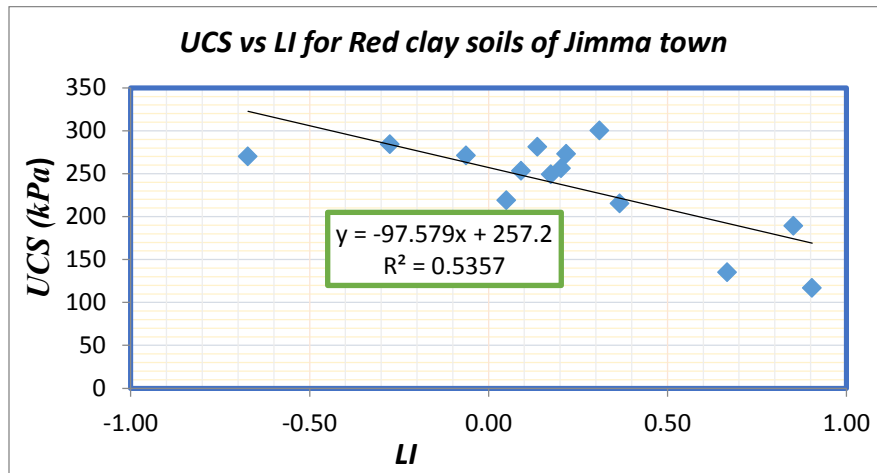


Figure 4.13 Scatter plot of UCS with LI for red clayey soils of Jimma Town

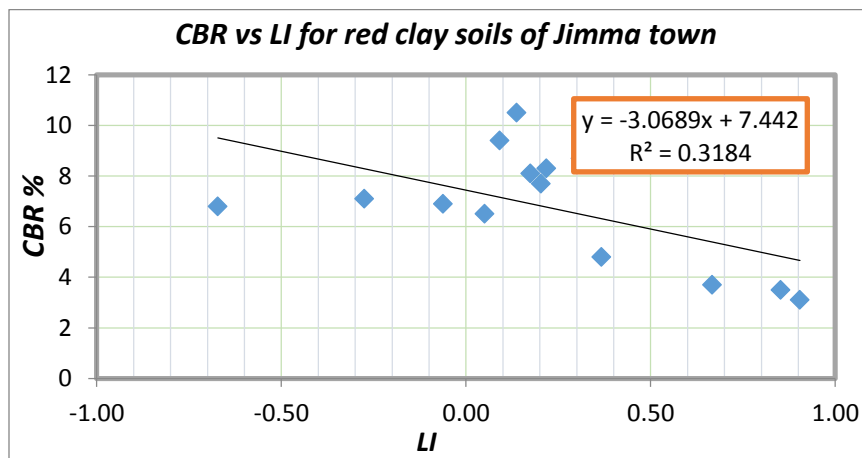


Figure 4.15 Scatter plot of CBR with LI for red clayey soils of Jimma Town

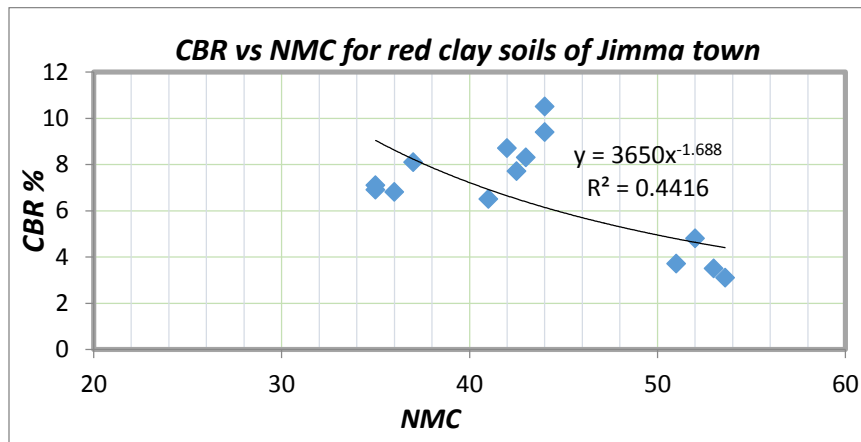


Figure 4.16 Scatter plot of CBR with NMC for red clayey soils of Jimma Town

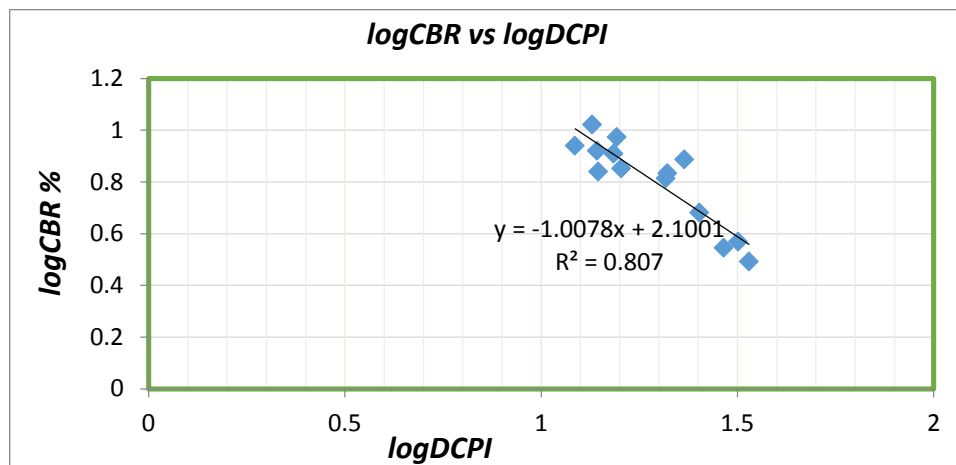


Figure 4.17 Scatter plot of CBR with DCPI for red clayey soils of Jimma Town

#### 4.2.3 Summary of Correlations for Category-1 (Black Clay Soils of Jimma Town)

After carefully studying the data trend, correlations were developed for this category. The correlation was done for CBR, with Dynamic cone penetration, liquid limit, liquid index, optimum moisture content, and maximum dry density. UCS with Dynamic cone penetration index, liquid limit, liquid index, natural moisture content, and field dry density. For DCPI the field condition such as natural moisture content and field density parameters are considered. The summary of the correlations is presented in Tables 4-1.

Table 4.1 Summary of Correlations for Category-1 (Black Clay Soils of Jimma Town)

Dependent variable	Independent variable	Equation	R2	Sample size	P value
CBR	DCPI	$\log\text{CBR}=1.9976-1.0192\log\text{DCPI}$	0.8164	16	1.61E-06
	PL	$\text{CBR} = 7.71 - 0.124 \text{ PL}$	37.1	16	7.29E-03
	LI	$\text{CBR} = 1.5227 + 4.23 \text{ LI}$	0.339	16	0.0178
	OMC	$\text{CBR} = 12.7 - 0.337 \text{ OMC}$	0.325	16	0.1720
	MDD	$\text{CBR} = -9.3 + 9.0 \text{ MDD}$	0.053	16	0.0340
UCS	DCPI	$\text{UCS}=557.06-120.8\ln\text{DCPI}$	0.779	16	6.28E-05
	LL	$\text{UCS} = 457.74 - 4.0743 \text{ LL}$	0.5447	16	4.69E-03
	LI	$\text{UCS} = 66.629 + 188.96 \text{ LI}$	0.3177	16	3.18E-02
	NMC	$\text{UCS} = 498 - 6.72 \text{ NMC}$	0.2	16	1.41E-01
	$\gamma_d$	$\text{UCS} = 19 + 12.4 \gamma_d$	0.017	16	7.32E-01
DCPI	NMC	$\text{DCPI} = -67.1 + 1.89 \text{ NMC}$	0.261	16	1.52E-01
	LI	$\text{DCPI} = 51.6 - 46.9 \text{ LI}$	0.254	16	2.34E-02
	$\gamma_d$	$\text{DCPI} = 134 - 10.0 \gamma_d$	0.112	16	6.30E-01

#### 4.2.4 Summary of Correlations for Category-2 (Red Clay Soils of Jimma Town)

After carefully studying the data trend, correlations were developed for this category. The correlation was done for CBR, with Dynamic cone penetration, liquid limit, liquid index, optimum moisture content, and maximum dry density. UCS with Dynamic cone penetration index, liquid limit, liquid index, natural moisture content, and field dry density.

Table 4.2 Summary of Correlations for Category-2 (Red Clay Soils of Jimma Town)

Dependent variable	Independent variable	Equation	R2	Sample size	P value
CBR	DCPI	$\text{LogCBR}=-1.0078\text{LogDCPI}+2.1001$	0.807	14	2.12E-05
	NMC	$\text{CBR} = 16.0 - 0.213 \text{ NMC}$	0.312	14	0.023928
	PL	$\text{CBR} = 0.72 + 0.168 \text{ PL}$	0.516	14	0.002832
	LI	$\text{CBR} = 7.442 - 3.069 \text{ LI}$	0.3184	14	0.005818
	OMC	$\text{CBR} = 10.2 - 0.129 \text{ OMC}$	0.017	14	0.000946
	MDD	$\text{CBR} = 32.4 - 18.0 \text{ MDD}$	0.005	14	0.002979
UCS	DCPI	$\text{UCS}=630.82-133.2\ln(\text{DCPI})$	0.7904	14	9.98E-06
	NMC	$\text{UCS} = 516.43 - 6.4328 \text{ NMC}$	0.536	14	0.002406
	LL	$\text{UCS} = -70.58 + 4.2118 \text{ LL}$	0.6185	14	0.001283
	LI	$\text{UCS} = 257.2 - 97.579 \text{ LI}$	0.5357	14	0.000976
	$\gamma_d$	$\text{UCS} = 41 + 15.9 \gamma_d$	0.017	14	0.405299
DCPI	NMC	$\text{DCPI} = -15.4 + 0.823 \text{ NMC}$	0.531	14	0.000909
	$\gamma_d$	$\text{DCP} = 61.7 - 3.39 \gamma_d$	0.07	14	0.206108
	LI	$\text{DCPI} = 18.1 + 10.8 \text{ LI}$	0.337	14	0.000941

### 4.3 Multiple Regression

Multiple regression attempts to model the relationship between two or more explanatory variables and a response variable by fitting an equation to observed data. Every value of the independent variable  $x$  is associated with a value of the dependent variable  $y$ .

Before analyzing multiple regressions the interdependence of the variables was assessed. If there is no significant dependence between two variables the variables are considered as independent variables. If not the variables are dependent on each other and no need of using such variables. So that the multiple linear regressions were done using the variables that are independent of each other.

#### 4.3.1 Multiple Regressions for Category-1 (black Clay Soils of Jimma Town)

When developing this equation using linear regression models, the significance of the parameter and the Adjusted R Square is analyzed. The interdependence of the variables to be used as independent variables was analyzed and those variables which have statistics probability greater or equal to alpha probability value are taken as independent variables. After Analysis those variables that have significant contribution to Unconfined Compression Strength (UCS) are Liquid index, field dry unit weight ( $\gamma_d$ ) and Natural moisture content (NMC), while in case of Californian bearing Ratio (CBR) it is dynamic cone penetration index (DCPI), maximum dry density (MDD), and Optimum moisture content as presented in Eq. 4-1 and 4.2.

The following significant model indicator emerged in the developed correlation equation depending on p-value and significance of the variables is: (all variables with p-value less than 0.05) is;

$$\text{CBR} = 12.9 - 4.65 \text{ MDD} - 0.0735 \text{ DCPI} - 0.0342 \text{ OMC with } R^2=80.12\% \quad (4.1)$$

$$\text{UCS} = 957 - 11.8 \text{ NMC} - 29.4 \gamma_d + 258 \text{ LI with } R^2 = 71.8\% \quad (4.2)$$

Developed equation for multiple regressions of DCPI (mm/blow) with NMC (%) and LI (%) for black clayey soils of Jimma Town, with  $N=16$  and adjusted  $R^2=0.81$  depending on p-value and significance of the variables is: (all variables with p-value less than 0.05) is:

$$\text{DCPI} = - 75.9 + 2.57 \text{ NMC} - 64.0 \text{ LI} \quad (4.3)$$

### 4.3.2 Multiple Regression for Category-2 (red clay soils of Jimma town)

When developing this equation using linear regression models, the significance of the parameter and the Adjusted R Square is analyzed. The interdependence of the variables to be used as independent variables is analysed and those variables which have statistics probability greater or equal to alpha probability value are taken as independent. After Analysis those variables that have significant contribution to Unconfined Compression Strength (UCS) are Dynamic Cone Penetration Index (DCPI), liquid index, and field dry density while in case of Californian bearing Ratio (CBR) it is OMC, MDD and PL as presented in Eq. 4-4 and 4.5.

Developed equation for multiple regression of  $q_u$  (kPa) and CBR(%) for red clay soils of Jimma, with  $N=14$  depending on p-value and significance of the variables is: (all variables with p-value less than 0.05)

$$UCS = 506 - 6.20 DCPI - 11.1 \gamma_d - 37.3 LI, \text{ with } R^2 = 69.1 \% \quad (4.4)$$

$$CBR = - 43.2 + 0.442 OMC + 23.1 MDD + 0.122 PL, \text{ with } R^2 = 69.8\% \quad (4.5)$$

Developed equation for multiple regressions of DCPI (mm/blow) with NMC (%), and PL (%) for red clayey soils of Jimma Town, with  $N=14$  and adjusted  $R^2 = 0.85$  is:

$$DCP = 11.4 + 0.575 NMC - 0.446 PL \quad (4.6)$$

## 4.4 Discussion

### 4.4.1 Category-1 (Black Clayey Soils of Jimma Town)

#### Simple regression

This category revealed that unconfined compression strength is significantly influenced by dynamic cone penetration index, liquid limit, and liquid index by achieving coefficient of determination of 77.9, 54.47 and 31.77% respectively depending on p-value. Those variables which have p-value less than 0.05 are taken. Californian bearing ratio is significantly influenced by dynamic cone penetration index, liquid Index, plastic limit and OMC by achieving coefficient of determination of 81.64%, 33.9, 37.1% and 32.5% respectively with p-value greater than 0.05. The summary of the correlations is presented in Tables 4-1.

### **Multiple regressions**

The multiple regression of UCS with NMC,  $\gamma_d$ , and LI indicated that UCS has good correlation with the NMC, LI and  $\gamma_d$  by achieving adjusted coefficient of determination of 71.8% with 16 samples while CBR has some what good correlation with DCPI, MDD and OMC by achieving adjusted coefficient of determination of 80.1%. (Refer to Equation 4.1 and 4.2).

#### **4.4.2 Category-2 (Red Clayey Soils of Jimma Town)**

##### **Single Regression**

This category revealed that unconfined compression strength is significantly influenced by dynamic cone penetration index, natural moisture content, liquid index and liquid limit by achieving coefficient of determination of 79.04%, 53.6%, 53.57% and 61.85% respectively. Californian bearing ratio is significantly influenced by dynamic cone penetration index, plastic limit and Liquid index by achieving coefficient of determination of 80.07 %, 51.6% and 31.84 respectively with p-values greater than 0.05. The summary of the correlations is presented in Tables 5-2.

The dynamic cone penetration index is also influenced by natural moisture content and liquid index by achieving coefficient of determination of 53.1 and 33.2% respectively.

##### **Multiple regressions**

The multiple regression of UCS with DCPI, LI and  $\gamma_d$  indicate that UCS has good correlation with the parameters by achieving adjusted coefficient of determination of 69.1% while multiple regression of CBR with OMC, MDD and PL has a good correlation with these parameters by achieving adjusted coefficient of determination of 69.8% with 14 samples.

Finally depending on coefficient of determination the equation with high value of coefficient of determination is selected.

#### 4.5 Development of Equation Based On Bearing Capacity Theory

Some good correlations between undrained shear strength, and the DCP penetration index and other parameters for the two categories are obtained (refer to Table 4-1 and Table 4-2 respectively). It is tempting to develop a bearing capacity equation from the correlations developed.

Converting unconfined compression strength into cohesion (i.e.,  $c=qu/2$ ) is applicable for saturated soils. Since the soil in the current research is unsaturated, the reader should understand that this equation can only give an approximate estimate of the cohesion for this type of soils.

Using the observed a correlation between UCS (kPa) and DCPI (mm/blow) using multiple regressions:

$$UCS = 630.82-133.2*\ln(DCPI), R^2 = 79.04\% \text{ and } N=14, \text{ for red clay soils} \quad (4.7)$$

$$UCS = 557.06-120.8*\ln(DCPI) \text{ with } R^2=77.9\% \text{ and } N=16, \text{ for black clay soils} \quad (4.8)$$

Inserting equations 4.5 and 4.6 into equation of cohesion, the corresponding relation will be:

$$C = 315.41 - 66.6*\ln(DCPI), \text{ for red clay soils of Jimma} \quad (4.9)$$

$$C = 278.53 - 60.4*\ln(DCPI), \text{ for black clay soils of Jimma} \quad (4.10)$$

After inserting equations 4.9 and 4.10 into equation 2.12, the corresponding relation of bearing capacity equation for initial loading condition it will be:

$$q_{ult} = 1621.207 - 342.32\ln(DCPI) + \gamma h \text{ for red clay soils} \quad (4.11)$$

$$q_{ult} = 1431.644 - 310.456\ln(DCPI) + \gamma h, \text{ for black clay soils} \quad (5.12)$$

#### 4.6 Comparison

To evaluate the capabilities of the proposed correlations in this research, predicted Unconfined Compression Strength (UCS) and Californian Bearing Ratio (CBR) values were plotted against measured Actual values.



#### 4.6.1 Comparison of Measured and Predicted Results

The predicted Californian Bearing Ratio (CBR) and Unconfined Compression Strength (UCS) results using the proposed equations are compared with the actual measured in laboratory for validation.

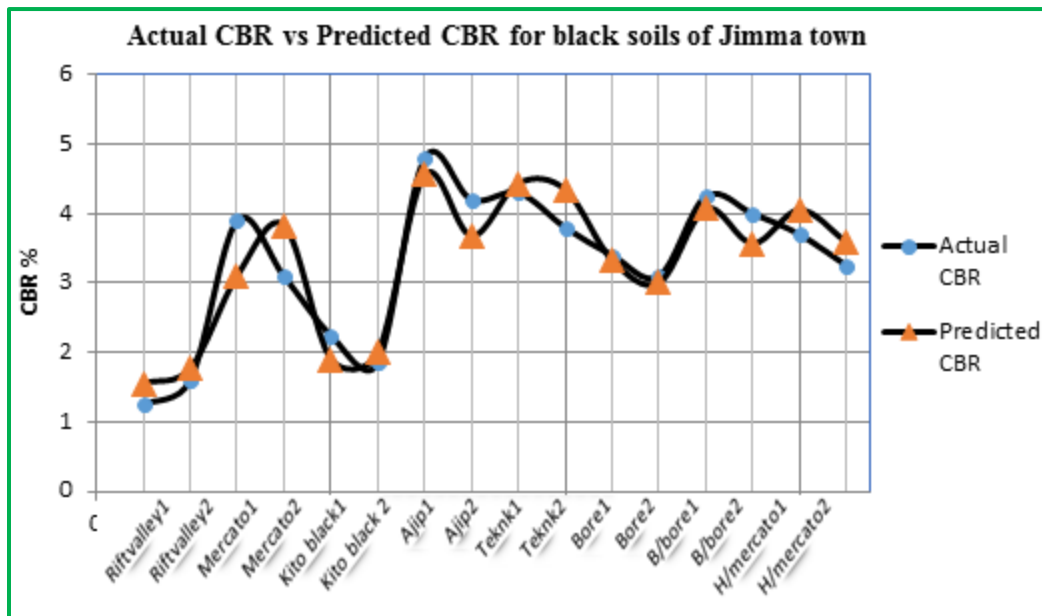


Figure 4.18 Actual measured versus Current predicted CBR Value of cat -1 Black Soil

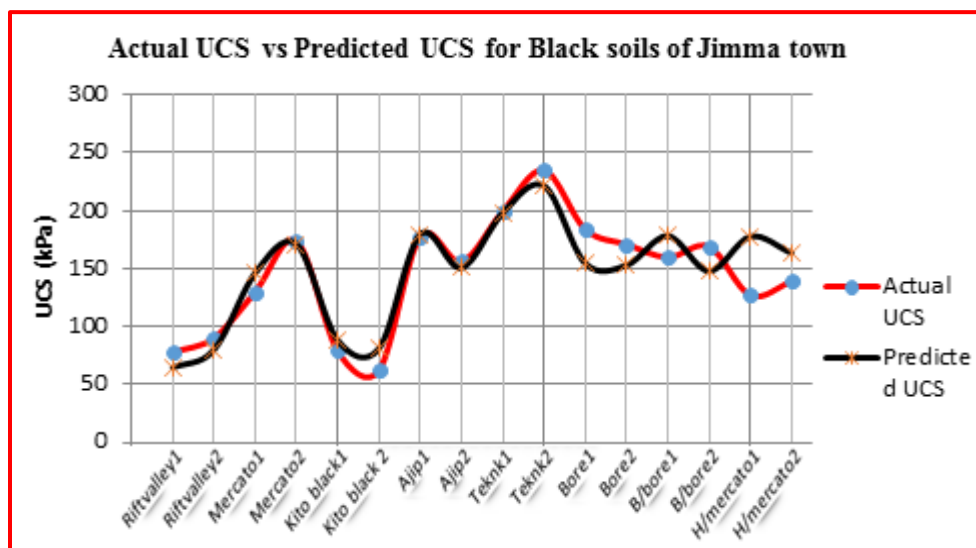


Figure 4.19 Actual measured versus Current predicted UCS Value of cat -1 Black Soil

Graph 4.18 and 4.19 shows that there is a strong relationship between the predicted values of CBR and UCS and actual values obtained in laboratory for black soils of Jimma town with variation up to 9.7% for UCS and 16.3% for CBR. This indicates that the developed equations for these soils validated for the study area.

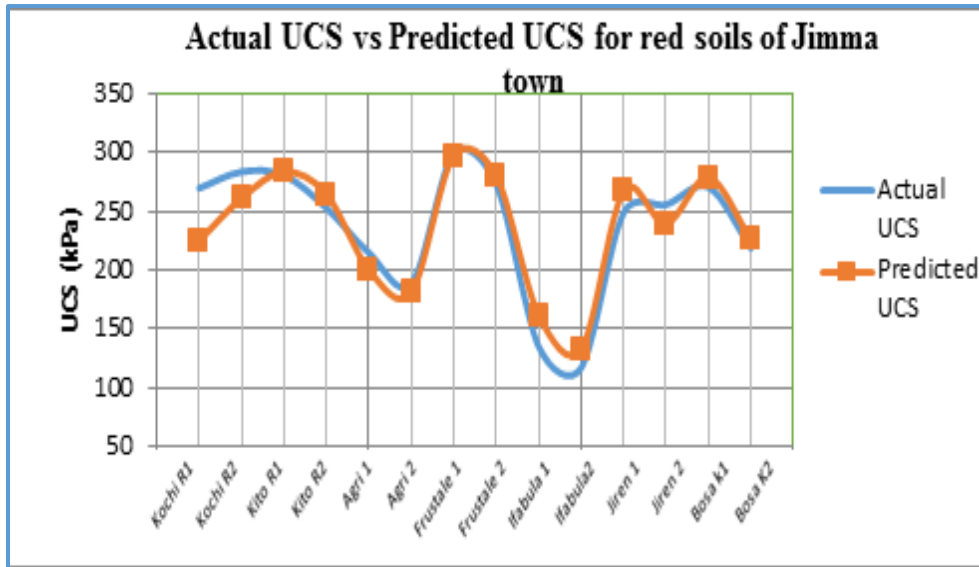


Figure 4.20 Actual measured versus Current predicted UCS Value of cat -2 Red soils

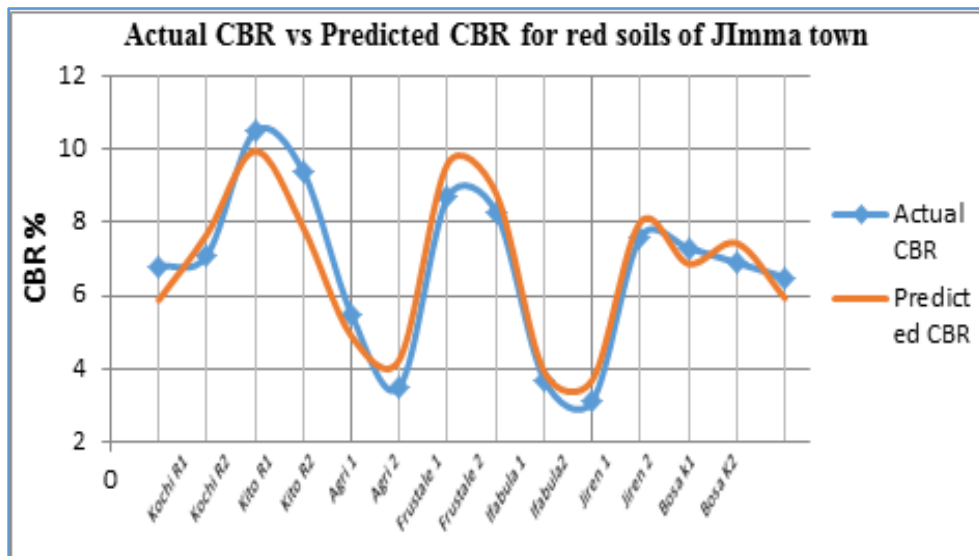


Figure 4.21 Actual measured versus Current predicted CBR Value of cat -2 Red soils

Figure 4.20 and 4.21 shows the current predicted Californian Bearing Ratio and Unconfined Compression Strength (UCS) values of red soils of Jimma town has a good relation with actual values obtained from laboratory. The variation of the predicted and actual CBR values ranges from 2.3% to 14.8% and for UCS it varies from 0.9% to 7.13%.

#### 4.6.2 Comparison with pervious similar studies

Correlations developed by Patel, et al., Temnit [33], Anteneh [26], Gedion [34], and Alemayehu [10], were selected for comparison of present proposed single correlation relationships for Unconfined compressive strength of both categories. Figure 4.23 compares the suggested correlations by above stated studies to the proposed correlations in this study between the Unconfined Compression Strength (UCS) and Dynamic Cone Penetration Index (DCPI)

Correlation equation developed by Feleke, [25] is selected for comparison of present proposed single correlation relationships for Californian bearing ratio. Figure 4.22 compares the suggested correlations by above stated studies to the proposed correlations in this study between the Californian bearing ratio (CBR) and Dynamic Cone Penetration Index (DCPI)

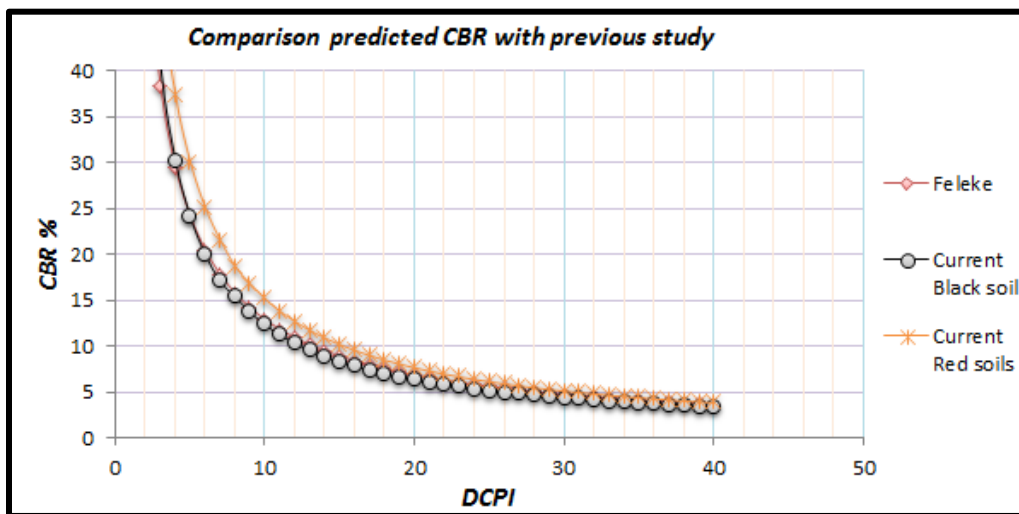


Figure 4.22 Comparison of previous and current studies for Californian bearing ratio

As shown in figure 4.22 the curve drawn using the equation developed for current studies follow the same trend but not in equal position with the previous studies. There is a little variation which may be due to difference in geographical and type of soils of the study area

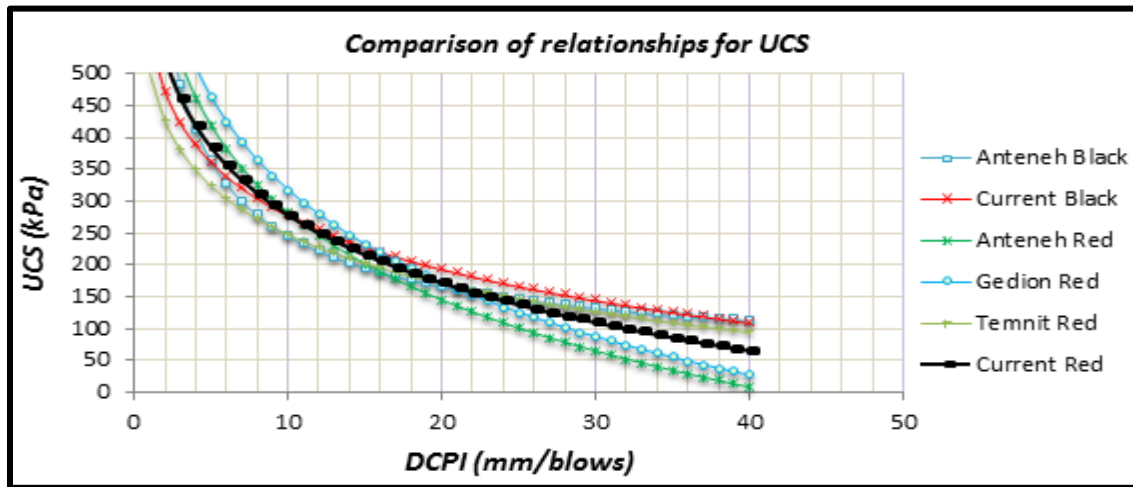


Figure 4.23 Comparison of previous and current studies for unconfined compression strength

As shown in figure 4.22 the curve drawn using the equation developed for current studies follows the same trend but not in equal position with the previous studies. There is a little variation which may be due to difference in geographical and type of soils of the study area.

#### 4.6.3 Verification of Developed Bearing Capacity Equation

The equation of bearing capacity in this study was derived using Terzaghi's bearing capacity equation considering the initial condition of foundation soil. So that the comparison of bearing capacity equation developed for in this study with that of Terzaghi's bearing capacity equation was done.

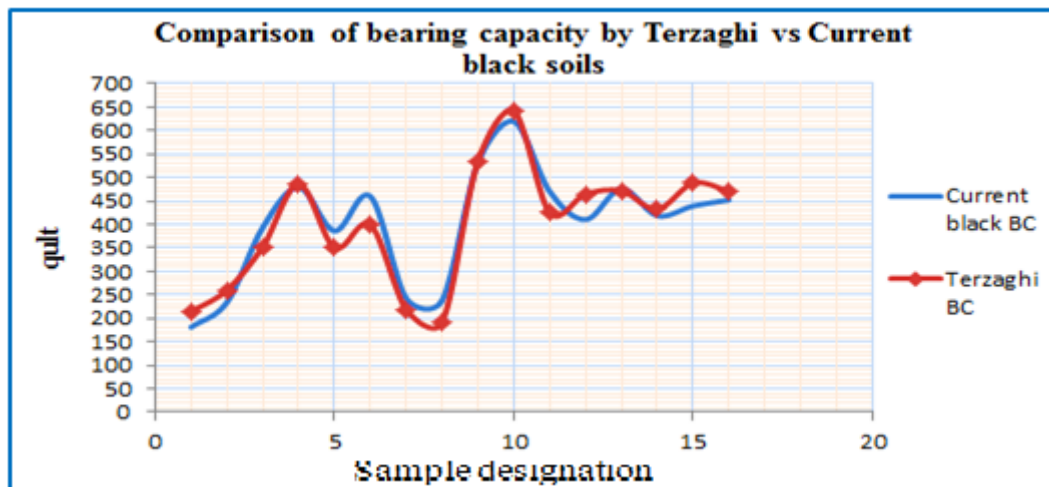


Figure 4.24 Comparison of Terzaghi's and current black soils bearing capacity equation

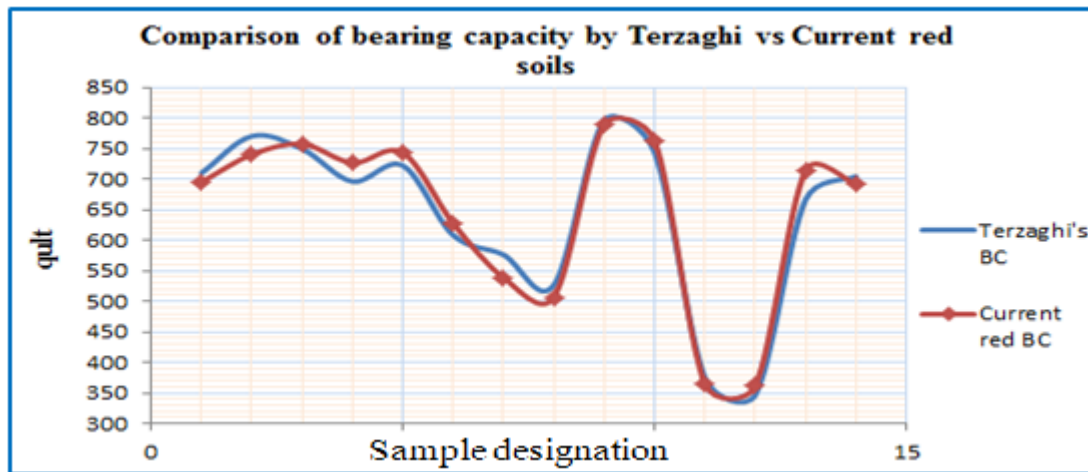


Figure 4.25 Comparison of Terzaghi's and current red soils bearing capacity equation

From figure 4.24 and figure 4.25 the bearing capacity of red soils and black soils in Jimma town have a good approach with Terzaghi's bearing capacity with variation from 0.764% to 7.12% and from 0.65% to 13.25% respectively. Terzaghi's equation derived from cohesion or UCS which is obtained directly in the laboratory while the current equation derived from correlation of the UCS with DCPI values. This may be a reason for a little variation between curves of these two equations.

## 5. CONCLUSION AND RECOMMENDATION

### 5.1 Conclusion

Generally, Californian bearing Ratio influenced by Dynamic Cone Penetration Index, Plastic Limit and liquid index for both categories. Unconfined Compression Strength affected by Dynamic Cone Penetration Index, natural Moisture Content and Liquidity Index. But both parameters are highly affected by DCPI.

The subgrade CBR and UCS values determined from DCP using the established relationships can be used for local soils since the result obtained from local soils shows substantial and strong relationships. So that CBR and UCS tests can be replaced by DCP test.

The following single regression equations have been developed to estimate the CBR and Unconfined Compression Strength from field test of Dynamic Cone Penetration Index for both categories.

✚ **Category-1(Black Clay Soils of Jimma Town)** revealed that UCS is highly influenced by DCPI and parameters like liquid index also have some influence. In addition CBR is influenced by DCPI, PL, and LI. For this category, UCS and CBR can be estimated from DCPI by:

$$\log\text{CBR} = 1.9976 - 1.0192\log(\text{DCPI}) \text{ with } R^2 = 81.64\%$$

$$\text{UCS} = 557.06 - 120.8 \cdot \ln(\text{DCPI}) \text{ with } R^2 = 77.9\%, \text{ with corresponding bearing capacity } q_{ult} = 1431.644 - 310.456 \ln(\text{DCPI}) + \gamma h$$

✚ **Category-2 (Red Clay Soils of Jimma Town)** revealed that UCS is highly influenced by DCPI and parameters like natural moisture content, and liquidity index have influence. In addition CBR is influenced by DCPI, LI and plastic limit. For this category, CBR and UCS can be estimated from DCPI by:

$$\log\text{CBR} = 2.1001 - 1.0078 \log\text{DCPI}, \text{ with } R^2 = 80.07\%$$

$$\text{UCS} = 630.82 - 133.2 \ln^*(\text{DCPI}), \text{ with } R^2 = 79.04\% \text{ with corresponding bearing capacity } q_{ult} = 1621.207 - 342.32 \ln(\text{DCPI}) + \gamma h$$

## 5.2 Recommendation

In this research it is observed that there is a correlation between of fine grained soils of Jimma town. To get reliable correlation in the future:

- ✚ It is recommended to collect more data in order to get a better correlation between unconfined compressive strength, and Californian bearing ratio with dynamic cone penetration since the size of sample did not cover the whole area of the town. Hence detail investigation should be done by increasing the size of samples.
- ✚ Thus, from practical point of view it is easier and feasible to use DCP to evaluate the subgrade strength.
- ✚ From the Comparison made one can see that the newly developed equations are acceptable. But applicability of the result will be limited to the study area. Therefore the results should only be applied to the study area.
- ✚ Even though, a good prediction of Californian bearing ratio and Unconfined Compression Strength (UCS) from Dynamic Cone Penetration Index (DCPI) has been developed, they should be used with caution since these are dependent on material properties.

## REFERENCES

- [1]. Mukesh A. (2013), Prediction of Subgrade Strength Parameters from Dynamic Cone Penetrometer Index, Modified Liquid Limit and Moisture Content. CRTG, India
- [2]. ASTM-D6951-3 ASTM, "ASTM D6951/D6951M –09, (2009). Standard Test Method for Use of the Dynamic Cone Penetrometer in Shallow Pavement Applications," West Conshohocken, Pennsylvania, American Society for Testing and Materials,
- [3]. Salgado, R. et al, (2003). Dynamic Cone Penetration Test for Subgrade Assessment. Publication FHWA/IN/JTRP-2002/30. Joint Transportation Research Program, Indiana
- [4]. Paige-Green, P., and Plessis, L. D. (2009). The use and interpretation of the Dynamic Cone Penetrometer (DCP) test. CSIR Built Environment Pretoria
- [6]. Srinivasa Kumar, (2010), "Comparative study of subgrade soil strength estimation models developed based on CBR, DCP and FWD test results," vol. II, no. 4, pp. 111-122,.
- [7]. Solomon A., (2012), "Correlation between Dynamic Cone Penetrometer and California Bearing," Arba Minch university, Arba Minch.
- [8]. Tom B et al, (1993), "In Situ Foundation Characterization Using the Dynamic Cone Penetrometer," Minnesota Department of Transportation Office of Materials Research and Engineering, Minnesota,.
- [9]. Amini F., (2003), "Potential Applications of the Static and Dynamic Cone Penetrometers in MDOT," Jackson State University, Mississippi,.
- [10]. Alemayehu D., (2017) Developing Correlation between Dynamic Cone Penetration Index (DCPI) and Unconfined Compression Strength (UCS) of the Soils in Alemgena Town.
- [11]. Hassan A., (1996) "The Effect of Material Parameters on Dynamic Cone Penetrometer Results for Fine-Grained Soils and Granular Materials," Oklahoma State University, Stillwater, Oklahoma.
- [12]. Tuncer et al., (2005) "Investigation of the DCP and SSG as Alternative Methods to Determine Subgrade Stability," Department of Civil and Environmental Engineering University of Wisconsin-Madison, Madison.



- [13]. Livneh et al., (1995) "Effect of Vertical Confinement on Dynamic Cone Penetrometer Strength Values in Pavement and Subgrade Evaluations," *Transport Research Rec.*, no. 1473, pp. 1-9,.
- [14]. Arora R. K., (2004) Soil mechanics and foundation engineering, Nai Sarak, Delhi: Standard Publishers distributors.
- [15]. Braja M., (2010) Principles of Geotechnical Engineering, 7th, Ed., Stamford: Cengage Learning.
- [16]. Bowels J., (1988) "*Foundation Analysis and Design*," McGraw-Hill (5th ed), Peoria, Illinois
- [17]. Ashworth, R. (1972) 'Highway Engineering', London, Heinemann Educational Book
- [18]. Croney, D. & Croney, P. (1991) 'The Design & Performance of road pavements', London, Mc-Graw Hill Book Company.
- [19]. American Association of State Highway & Transportation Officials (2001), 'Standard specification for transportation materials & methods of sampling & testing', 444 North Capitol street
- [20] ASTM Vol. 0408, (1998) "Standard test methods for soil and rock," *American Standard for Testing and Materials*, New York
- [21] AASHTO (2001), 'Standard specification for transportation materials & methods of sampling & testing', 444 North Capitol street N.W., Suite 249, Washington, D.C.
- [22]. Piouslin Samuel and Simon Done, (2006) "Measuring Road Pavement Strength and Designing Low Volume Sealed Roads using the Dynamic Cone Penetrometer,"
- [23] Harison J. A., (1987) "Correlation between California bearing ratio and dynamic cone penetrometer strength measurement of soils," vol. Part 2, pp. 833-844,.
- [24]. Munir D. (2003) Field Evaluation Of In-Situ Test Technology For Qc/Qa During Construction Of Pavement Layers And Embankments. Beirzet University West Bank
- [25]. Feleke G. (2016) Prediction Of CBR Using DCP For Local Subgrade Materials Mekelle University, EiT-M, Ethiopia
- [26]. Anteneh G. (2012) Correlating Dynamic Cone Penetration Index with Undrained Shear Strength for Clayey Soils. Addis Ababa institute of Technology, Ethiopia.

- [27]. Kofi A., (2015) The influence of water content on the Dynamic Cone Penetration Index of a lateritic soil stabilized with various percentages of a quarry by-product. Kwame Nkrumah University of Science and Technology, College of Engineering, Kumasi, Ghana
- [28]. Kleyn, E. etal, (1983) "Using DCP Soundings to Optimize Pavement Rehabilitation, " Paper presented at the annual Transportation Convention, Milner Park Showground, Johannesburg, S. Africa.
- [29] Chua, K., (1988) "*Determination of CBR and Elastic Modulus of Soils Using a Portable Pavement Dynamic Cone Penetrometer,*" Penetration Testing, ISOFT-1, De Ruiter (ed.), Balkema, Rotterdam.
- [30] Verruijt, A., (2001) "Soil Mechanics", Delft University of Technology, Netherland,
- [31] Bumharn, T. etal, (May 1993) "In Situ Foundation Characterization Using the Dynamic Cone penetrometer," Office of Research Administration, Minnesota Department of Transportation.
- [32] Jimma Town Water Supply and Sanitation Project, (2011), Environmental and Social Impact Assessment Study.
- [33] Temnit F., (2014) "Determination of unconfined compressive strength (UCS) from dynamic cone penetrometer index (DCPI) for red clay soil of Addis Ababa, Ethiopia," a Thesis presented to School of Graduate Studies, Addis Ababa University.
- [34] Gedeyon A, (2015) Developing correlation between dynamic cone penetration index and undrained shear strength of soils that are found in Debre Markos town.
- [35] Jemal, J.,( 2014), '*In-depth Investigation into Engineering Characteristics of Jimma Soils*', a Master thesis presented to School of Graduate Studies, Addis Ababa University, Addis Ababa.
- [36] Gifti H., (2017), '*Correlation of California Bearing Ratio with Soil Index Properties for Subgrade Soil in Jimma Town,*' a Master thesis presented to School of Graduate Studies, Jimma institute of technology
- [37] ERA (2002), 'Pavement Design Manual, vol-1' Ethiopian Roads Authority
- [38] Yitagesu D., (2012) 'Developing correlation between DCP & CBR for locally used subgrade material' A Thesis presented to School of Graduate Studies, Addis Ababa University
- [39] Park HM. (2008), '*Univariate analysis and normality test using SAS, Stata, and SPSS.*' Indiana University

## **APPENDIXES**

## **APPENDIX A: DETAIL OF GRAINSIZE ANALYSIS AND ATTERBERG LIMITS**

Table A-1-1 Grain size analysis for Rift valley 1

Depth: 1.2 m

Opening (mm)	Mass of Retained Soil (g)	Percentage Retained (%)	Cumulative % Retained	%age Passing
4.75	14.7	1.47	1.47	98.53
2	7.3	0.73	2.2	97.8
0.85	4.9	0.49	2.69	97.31
0.425	6.7	0.67	3.36	96.64
0.25	7.3	0.73	4.09	95.91
0.15	8.2	0.82	4.91	95.09
0.075	10.8	1.08	5.99	94.01
pan	940.1	94.01		

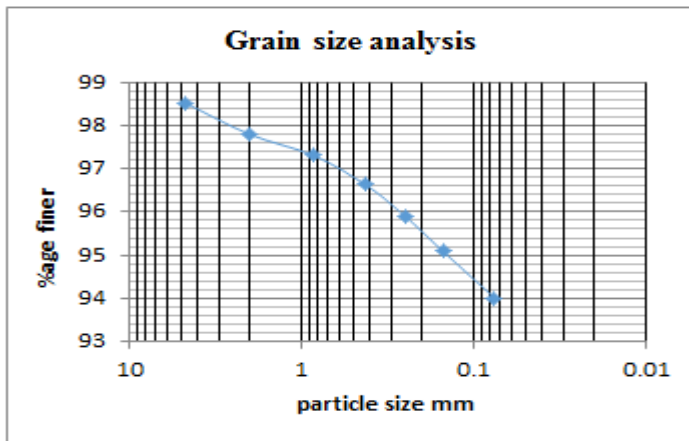


Figure A.1.1 Particle distribution curve for Riftvalley 1

Table A-2-1 Atterberg limit test for Rift valley 1

Trial No	Liquid Limit			Plastic Limit	
	1	2	3	4	1
Container No	T2C1	NB	P6	2	13
Mass of container, g	17.50	17.40	17.00	5.7	5.7
Mass of container + Wet soil, g	31.40	31.00	27.00	13.1	13
Mass of container + Dry soil, g	24.90	24.30	22.01	10.95	10.85
Mass of water, g	6.50	6.70	4.99	2.15	2.15
Mass of dry soil, g	7.40	6.90	5.01	5.25	5.15
Water content, %	87.84	97.10	99.60	40.95	41.75
No of blows	35	22	15	41.35	
				LL=93.5	PL=41.3

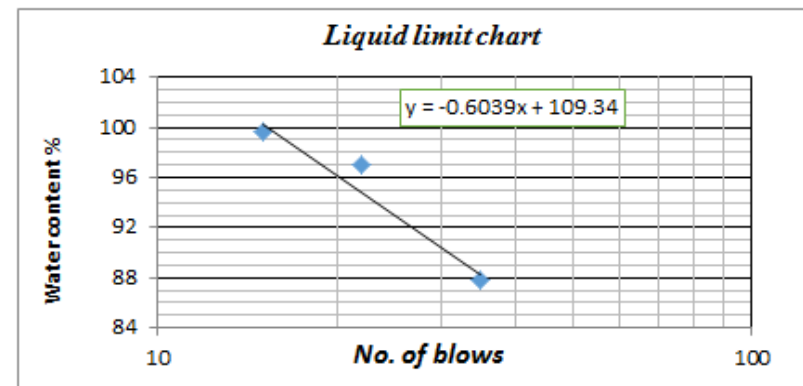


Figure A.2.1 Liquid limit chart for Riftvalley 1

Table A-1-2 Grain size analysis for Kochi 1

Depth: 1m

Opening (mm)	Mass of Retained Soil (g)	Percentage Retained (%)	Cumulative % Retained	%age Passing
4.75	1.6	0.16	0.16	99.84
2	3	0.3	0.46	99.54
0.85	4.5	0.45	0.91	99.09
0.425	10.1	1.01	1.92	98.08
0.25	14.9	1.49	3.41	96.59
0.15	18.2	1.82	5.23	94.77
0.075	18.4	1.84	7.07	92.93
pan	929.3	92.93		

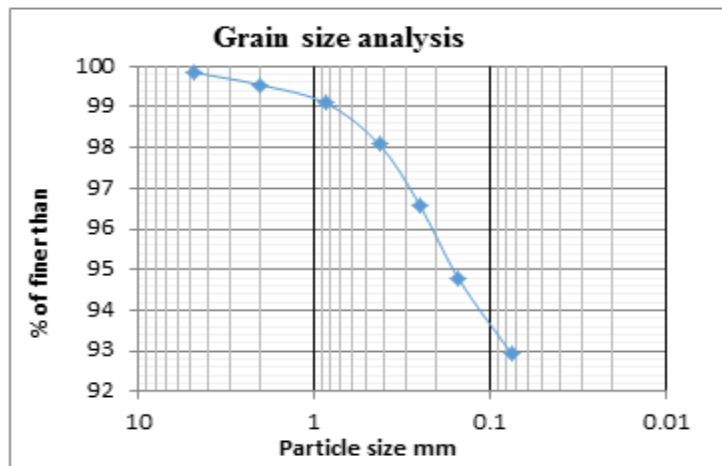


Figure A.1.2 Particle distribution curve for Kochi 1

Table A-2-2 Atterberg limit test for Kochi 1

Trial No	Liquid Limit			Plastic Limit	
	1	2	3	1	2
Container No	I23	A2	T65	A	B
Mass of container, g	17.50	17.40	18.10	6.50	6.30
Mass of container + Wet soil, g	34.40	29.70	27.10	13.00	14.10
Mass of container + Dry soil, g	26.42	24.22	22.53	11.38	12.43
Mass of water, g	7.98	5.48	4.57	1.62	1.67
Mass of dry soil, g	8.92	6.82	4.43	4.88	6.13
Water content, %	89.46	80.35	103.2	33.20	27.24
No of blows	24	29	15	30.22	
	LL=86.5			PL=30.22	

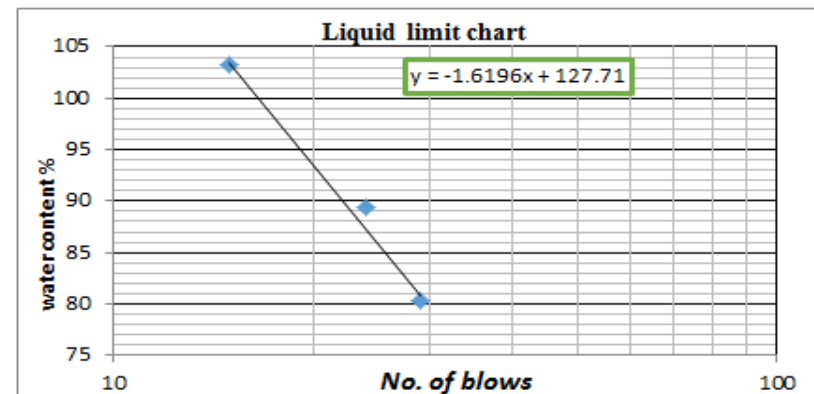


Figure A.2.2 Liquid limit chart for Kochi 1

Table A-1-3 Grain size analysis for mercato 22

Depth: 2.5m

Opening (mm)	Mass of Retained Soil (g)	Percentage Retained (%)	Cumulative % Retained	%age Passing
4.75	0.5	0.05	0.05	99.95
2	1	0.1	0.15	99.85
0.85	2.5	0.25	0.4	99.6
0.425	15.2	1.52	1.92	98.08
0.25	19.5	1.95	3.87	96.13
0.15	18.4	1.84	5.71	94.29
0.075	19.9	1.99	7.7	92.3
pan	923	92.3		

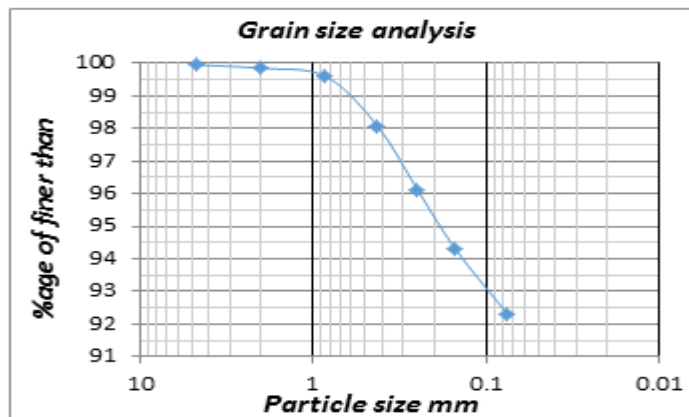


Figure A.1.2 Particle distribution curve for Mercato 22

Table A-2-3 Atterberg limit test for mercato 22

Trial No	Liquid Limit			Plastic Limit	
	1	2	3	1	2
Container No	13	2	K	R2	2
Mass of container, g	5.70	5.70	5.60	5.40	5.50
Mass of container + Wet soil, g	28.30	28.70	27.10	12.80	14.20
Mass of container + Dry soil, g	19.16	17.88	16.38	10.93	11.97
Mass of water, g	9.14	10.82	10.72	1.87	2.23
Mass of dry soil, g	13.46	12.18	10.78	5.53	6.47
Water content, %	67.90	88.83	99.44	33.82	34.47
No of blows	34	24	16	34.14	
			LL=83		PL=34.1

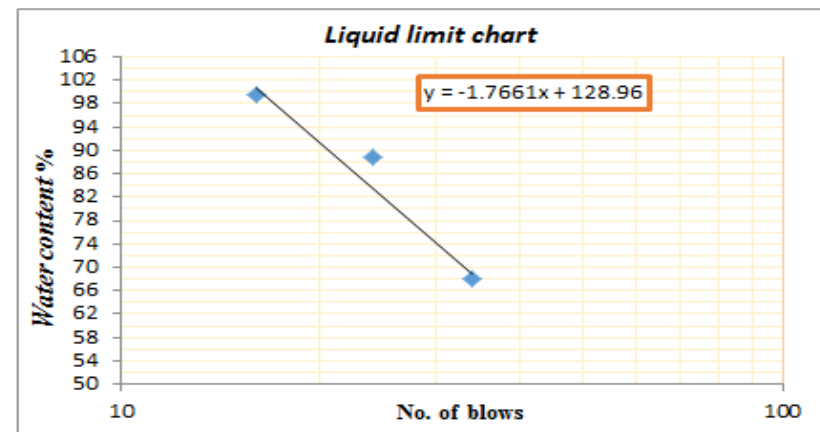


Figure A.2.3 Liquid limit chart for Mercato 22

Table A-1-4 Grain size analysis for Kito red 1

Depth: 1.5 m

Opening (mm)	Mass of Retained Soil (g)	Percentage Retained (%)	Cumulative % Retained	%age Passing
4.75	6.8	0.68	0.68	99.32
2	8.3	0.83	1.51	98.49
0.85	6.7	0.67	2.18	97.82
0.425	5.8	0.58	2.76	97.24
0.25	10.6	1.06	3.82	96.18
0.15	9.5	0.95	4.77	95.23
0.075	10.9	1.09	5.86	94.14
pan	941.4	94.14		

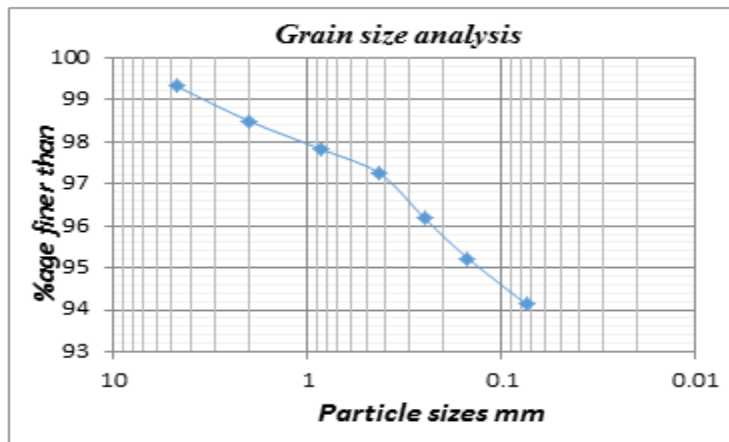


Figure A.1.4 Particle distribution curve for Kito red 1

Table A-2-4 Atterberg limit test for Kito red 1

Trial No	Liquid limit			Plastic limit	
	1	2	3	1	2
Container No	T3	D	H	12	B
Mass of container, g	5.20	5.80	6.00	6.50	6.40
Mass of container + Wet soil, g	21.20	25.20	21.70	15.80	14.80
Mass of container + Dry soil, g	14.48	16.67	13.49	13.10	12.30
Mass of water, g	6.72	8.53	8.21	2.70	2.50
Mass of dry soil, g	9.28	10.87	7.49	6.60	5.90
Water content, %	72.41	78.47	109.6	40.91	42.37
No of blows	34	27	13	41.64	
	LL=80			PL=41.7	

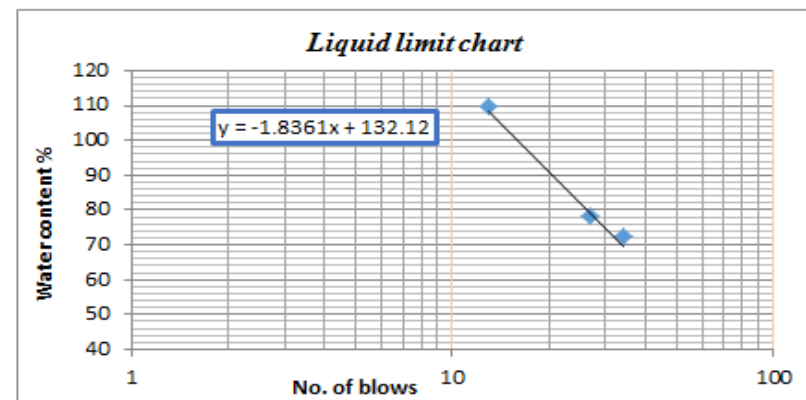


Figure A.2.4 Liquid limit chart for Kito red 1



Table A-1-5 Grain size analysis for Bosa Kito 1

Depth: 2.5 m

Opening (mm)	Mass of Retained Soil (g)	Percentage Retained (%)	Cumulative % Retained	%age Passing
4.75	8.4	0.84	0.84	99.16
2	9.6	0.96	1.8	98.2
0.85	8.8	0.88	2.68	97.32
0.425	7.1	0.71	3.39	96.61
0.25	8.4	0.84	4.23	95.77
0.15	8.6	0.86	5.09	94.91
0.075	11.2	1.12	6.21	93.79
pan	940.1	94.01		

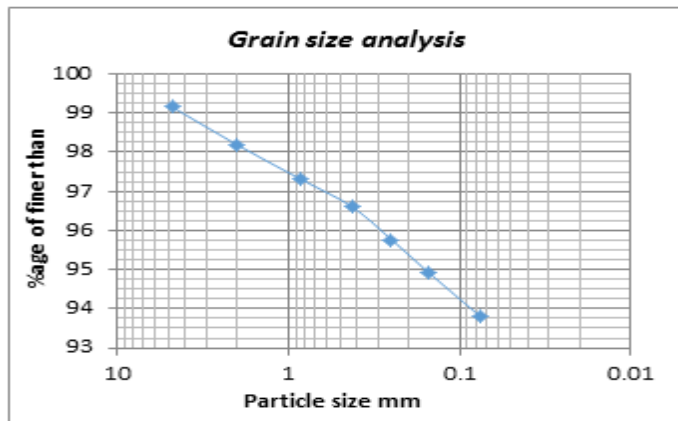


Figure A.1.5 Particle distribution curve for Bosa Kito 1

Table A-2-5 Atterberg limit test for Bosa Kito 1

Trial No	Liquid Limit			Plastic Limit	
	1	2	3	1	2
Container No	DB	T8	A2	13	N4
Mass of container, g	6.50	5.90	6.00	6.40	6.00
Mass of container + Wet soil, g	18.80	20.10	20.90	12.60	14.50
Mass of container + Dry soil, g	13.65	13.62	13.88	10.75	11.90
Mass of water, g	5.15	6.48	7.02	1.85	2.60
Mass of dry soil, g	7.15	7.72	7.88	4.35	5.90
Water content, %	72.03	83.94	89.09	42.53	44.07
No of blows	33	23	18	43.30	
	LL=81			PL=43.3	

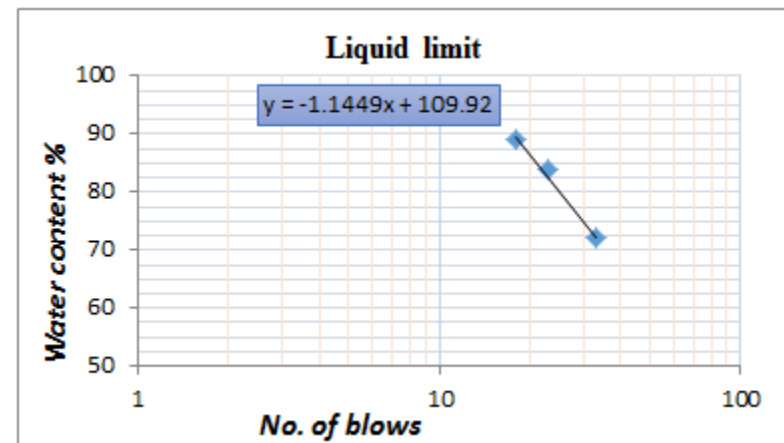


Figure A.2.5 Liquid limit chart for Bosa Kito 1

Table A-1-5 Grain size analysis for Kito black 1

Depth: 1

Opening (mm)	Mass of Retained Soil (g)	Percentage Retained (%)	Cumulative % Retained	%age Passing
4.75	6.8	0.68	0.68	99.32
2	8.3	0.83	1.51	98.49
0.85	6.7	0.67	2.18	97.82
0.425	5.8	0.58	2.76	97.24
0.25	10.6	1.06	3.82	96.18
0.15	9.5	0.95	4.77	95.23
0.075	10.9	1.09	5.86	94.14
pan	941.4	94.14		

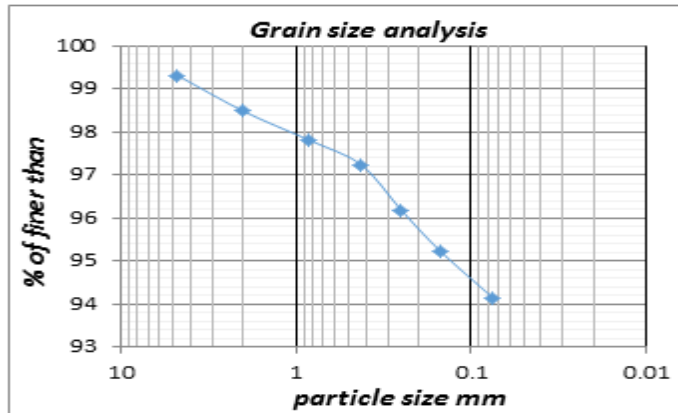


Figure A.1.5 Particle distribution curve for Kito black 1

Table A-2-5 Atterberg limit test for Kito black 1

Trial No	Liquid limit			Plastic limit	
	1	2	3	1	2
Container No	T6	3M	13	A	T65
Mass of container, g	7.80	6.00	6.10	6.50	6.30
Mass of container + Wet soil, g	22.20	21.00	17.60	13.30	12.50
Mass of container + Dry soil, g	15.83	13.64	11.63	11.17	10.68
Mass of water, g	6.37	7.36	5.97	2.13	1.82
Mass of dry soil, g	8.03	7.64	5.53	4.67	4.38
Water content, %	79.33	96.34	107.96	45.61	41.55
No of blows	32	21	17	43.58	
	LL=88			PL=43.6	

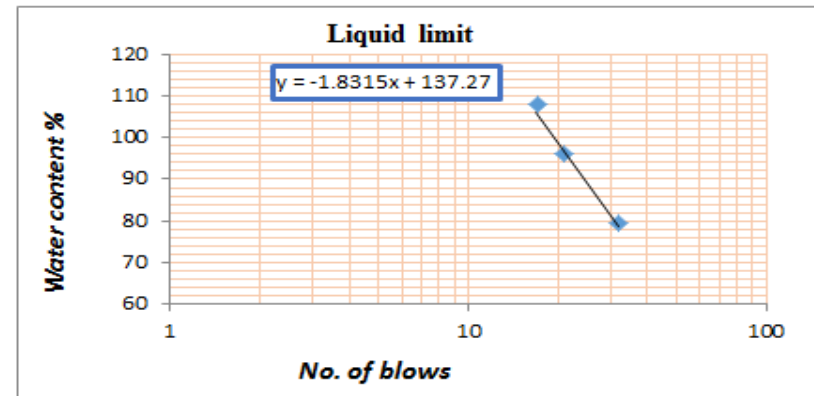


Figure A.2.5 Liquid limit chart for Kito black 1

Table A-1-5 Grain size analysis for Ifabula 1

Depth: 1.5m

Sieve opening	Weight retained (gm)	Percent retained (%)	Cumulative retained %	%age passing
4.75	8.3	1.66	0	100.0
2	6.2	1.24	1.24	98.8
0.85	4.8	0.96	2.2	97.8
0.425	6.9	1.38	3.58	96.4
0.25	4.2	0.84	4.42	95.6
0.15	3	0.6	5.02	95.0
0.075	11	2.2	7.22	92.8
pan	0	0	7.22	92.8

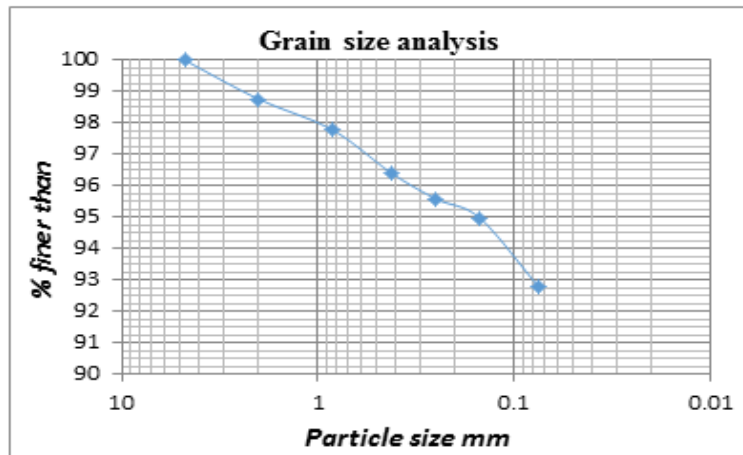


Figure A.1.5 Particle distribution curve for Ifabula 1

Table A-2-5 Atterberg limit test for Ifabula 1

Trial No	Liquid limit			Plastic limit	
	1	2	3	1	2
Container No	c1	sk	tc1	33	D2
Mass of container, g	5.60	5.80	5.60	5.50	5.60
Mass of container + Wet soil, g	28.30	27.00	28.60	11.90	13.20
Mass of container + Dry soil, g	20.30	19.30	19.90	10.70	11.68
Mass of water, g	8.00	7.70	8.70	1.20	1.52
Mass of dry soil, g	14.70	13.50	14.30	5.20	6.08
Water content, %	54.42	57.04	60.84	23.08	25.00
No of blows	34	24	16	24.04	
	LL=59			PL=24	

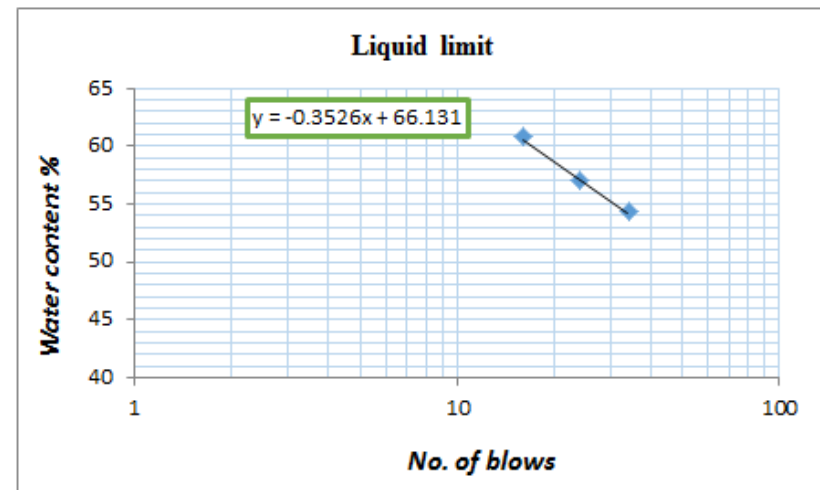


Figure A.2.5 Liquid limit chart for Ifabula 1

Table A-1-5 Grain size analysis for Agri 1

Depth: 2.5 m

Sieve opening	Weight retained (gm)	Percent retained (%)	Cumulative retained %	%age passing
4.75	20.3	4.06	0	100.0
2	46.1	9.22	9.22	90.8
0.85	28.1	5.62	14.84	85.2
0.425	30.2	6.04	20.88	79.1
0.25	6.9	1.38	22.26	77.7
0.15	3.8	0.76	23.02	77.0
0.075	15.2	3.04	26.06	73.9
pan	0	0	26.06	73.9

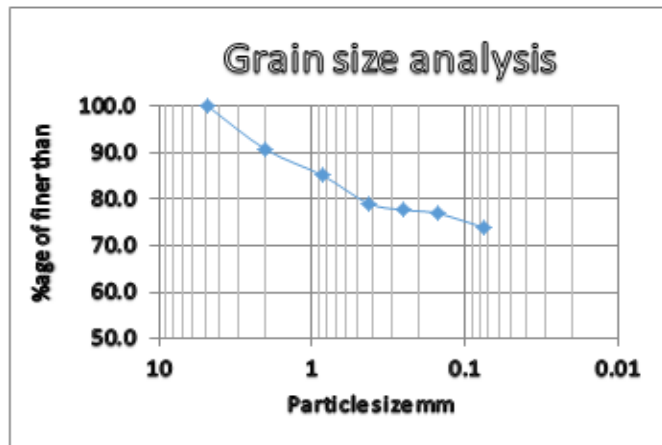


Figure A.1.5 Particle distribution curve for Agri 1

Table A-2-5 Atterberg limit test for Agri 1

Trial No	Liquid limit			Plastic limit	
	1	2	3	1	2
Container No	11	K2	C33	TC2	DC4
Mass of container, gm	5.60	5.70	5.60	5.80	5.70
Mass of container + Wet soil, gm	30.40	29.10	27.40	11.60	12.90
Mass of container + Dry soil, gm	20.30	19.30	18.00	10.20	11.30
Mass of water, gm	10.10	9.80	9.40	1.40	1.60
Mass of dry soil, gm	14.70	13.60	12.40	4.40	5.60
Water content, %	68.71	72.06	75.81	31.82	28.57
No of blows	36	26	16	30.19	
	LL=71			PL=30	

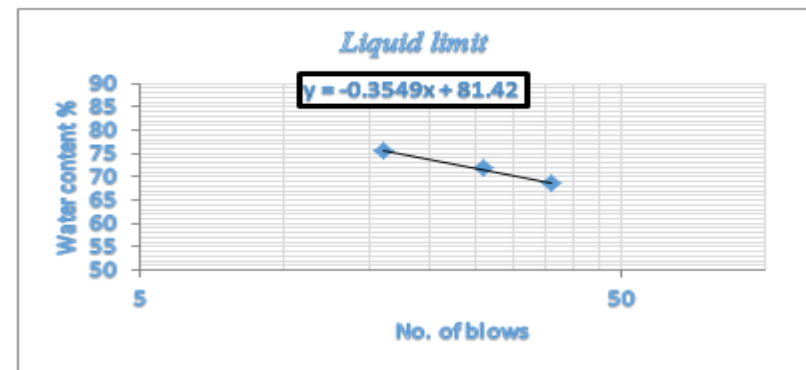


Figure A.2.5 Liquid limit chart for Agri 1

Table A-1-5 Grain size analysis for Frustale1

Depth: 2.5 m

Sieve opening	Weight retained (gm)	Percent retained (%)	Cumulative retained %	%age passing
4.75	1.3	0.26	0	100.0
2	5.4	1.08	1.08	98.9
0.85	10.3	2.06	3.14	96.9
0.425	7.9	1.58	4.72	95.3
0.25	14	2.8	7.52	92.5
0.15	8.2	1.64	9.16	90.8
0.075	9.1	1.82	10.98	89.0
pan	2.6	0.52	11.5	88.5

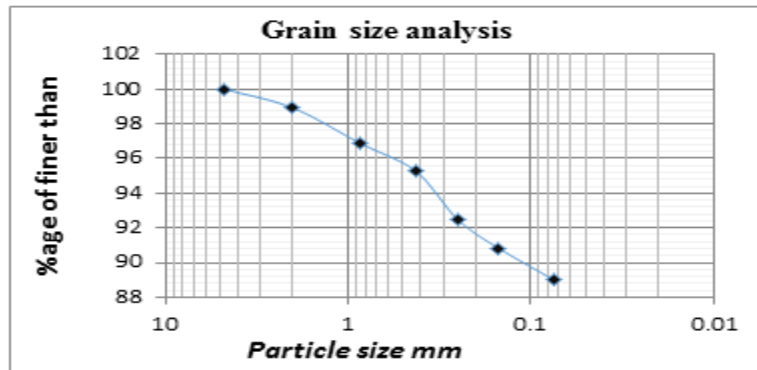


Figure A.1.5 Particle distribution curve for Frustale1

Table A-2-5 Atterberg limit test for Frustale1

Trial No	Liquid limit			Plastic limit	
	1	2	3	1	2
Container No	D2	TC2	K1	C33	TC1
Mass of container, g	5.70	5.40	5.70	5.60	5.50
Mass of container + Wet soil, g	32.60	31.20	25.30	11.30	13.60
Mass of container + Dry soil, g	21.00	19.50	16.10	9.20	10.65
Mass of water, g	11.10	11.00	9.20	2.10	2.95
Mass of dry soil, g	15.30	14.10	10.40	3.60	5.15
Water content, %	72.55	78.01	88.46	58.33	57.28
No of blows	36	29	18	57.81	
	<b>LL=82</b>			<b>PL=58</b>	

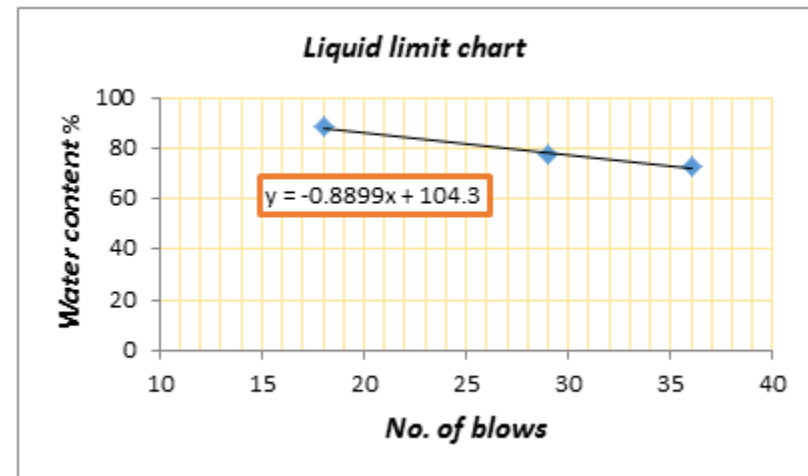


Figure A.2.5 Liquid limit chart for Frustale1

Table A-1-5 Grain size analysis for Ajip 1

Depth: 2 m

Sieve opening	Weight retained (gm)	Percent retained (%)	Cumulative retained %	%age passing
4.75	0	0	0	100.0
2	3.2	0.64	0.64	99.4
0.85	9.1	1.82	2.46	97.5
0.425	12.4	2.48	4.94	95.1
0.25	22.1	4.42	9.36	90.6
0.15	9.6	1.92	11.28	88.7
0.075	40.3	8.06	19.34	80.7
pan	2.4	0.48	19.82	80.2

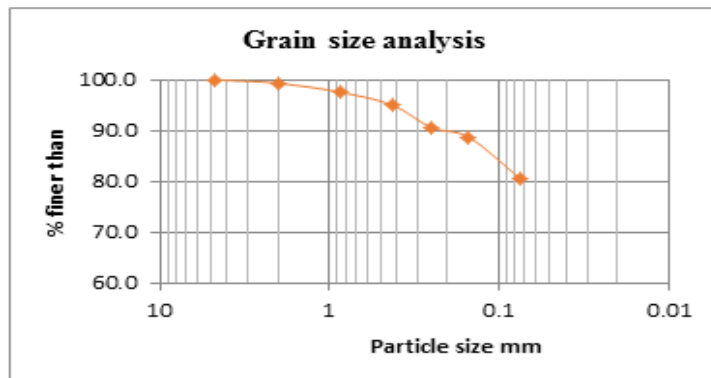


Figure A.1.5 Particle distribution curve for Ajip 1

Table A-2-5 Atterberg limit test for Ajip 1

Trial No	Liquid limit			Plastic limit	
	1	2	3	1	2
Container No	c1	sk	tc1	33	D2
Mass of container, g	5.60	5.80	5.60	5.50	5.60
Mass of container + Wet soil, g	26.30	31.10	29.40	14.10	12.90
Mass of container + Dry soil, g	18.10	20.70	19.30	11.90	11.10
Mass of water, g	8.20	10.40	10.10	2.20	1.80
Mass of dry soil, g	12.50	14.90	13.70	6.40	5.50
Water content, %	65.60	69.80	73.72	34.38	32.73
No of blows	37	22	17	33.55	
	LL=69			PL=33.6	

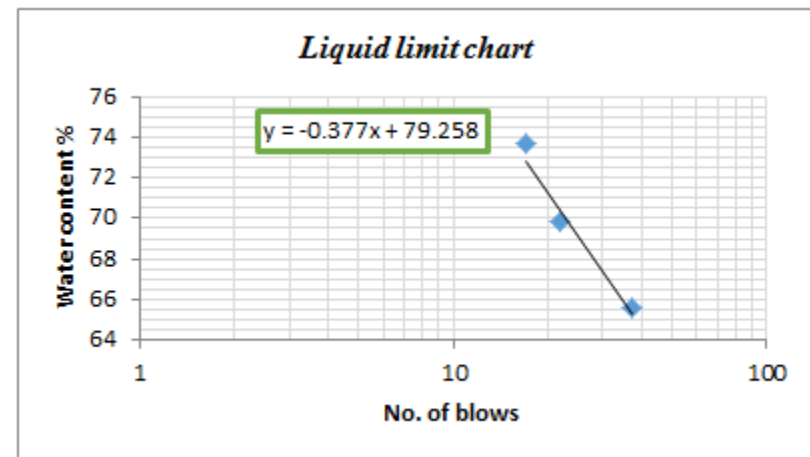


Figure A.2.5 Liquid limit chart for Ajip 1

Table A-1-5 Grain size analysis for Teknik 1

Depth: 1.5 m

Sieve opening	Weight retained (gm)	Percent retained (%)	Cumulative retained %	%age passing
4.75	3.1	0.62	0	100.0
2	9.8	1.96	1.96	98.0
0.85	29.3	5.86	7.82	92.2
0.425	21.9	4.38	12.2	87.8
0.25	3.2	0.64	12.84	87.2
0.15	9.8	1.96	14.8	85.2
0.075	13.6	2.72	17.52	82.5
pan	1.9	0.38	17.9	82.1

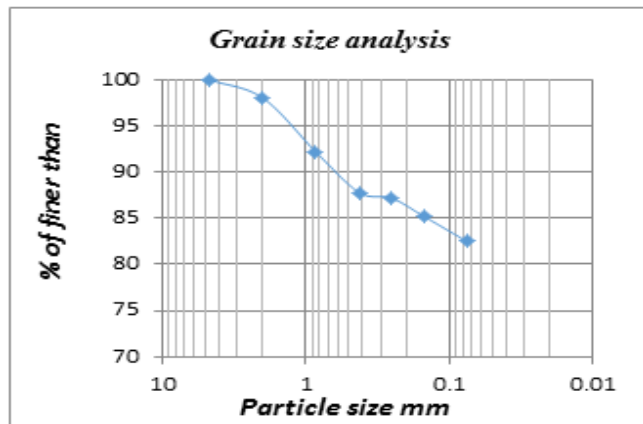


Figure A.1.5 Particle distribution curve for Teknik 1

Table A-2-5 Atterberg limit test for Teknik 1

Trial No	Liquid limit			Plastic limit	
	1	2	3	1	2
Container No	11	C33	K2	DC4	TC2
Mass of container, g	5.60	5.60	5.70	5.70	5.80
Mass of container + Wet soil, g	30.80	26.30	26.70	13.30	16.40
Mass of container + Dry soil, g	21.10	18.10	18.10	11.40	13.80
Mass of water, g	9.70	8.20	8.60	1.90	2.60
Mass of dry soil, g	15.50	12.50	12.40	5.70	8.00
Water content, %	62.58	65.60	69.35	33.33	32.50
No of blows	33	23	17	32.92	
	LL=65			PL=32.9	

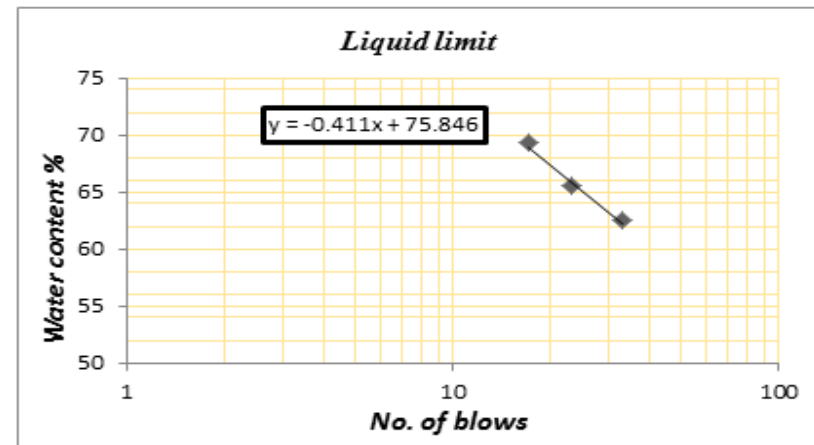


Figure A.2.5 Liquid limit chart for Teknik 1

Table A-1-5 Grain size analysis for Bore 1

Depth: 1 m

Sieve opening	Weight retained (gm)	Percent retained (%)	Cumulative retained %	%age passing
4.75	0	0	0	100.0
2	8.2	1.64	1.64	98.4
0.85	13.6	2.72	4.36	95.6
0.425	21.3	4.26	8.62	91.4
0.25	9.6	1.92	10.54	89.5
0.15	1.6	0.32	10.86	89.1
0.075	23.5	4.7	15.56	84.4
pan	1.4	0.28	15.84	84.2

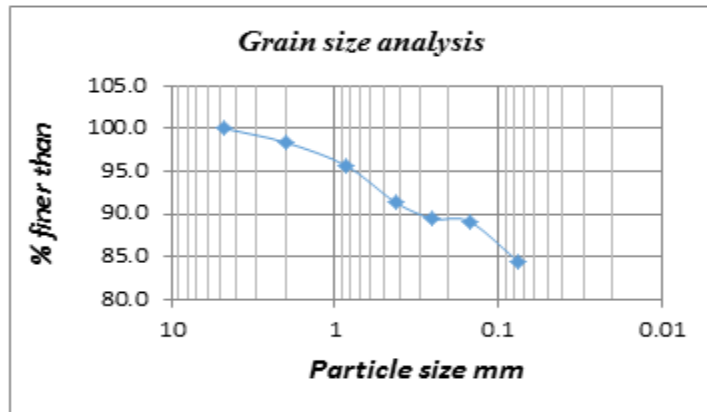


Figure A.1.5 Particle distribution curve for Bore 1

Table A-2-5 Atterberg limit test for Bore 1

Trial No	Liquid limit			Plastic limit	
	1	2	3	1	2
Container No	D2	TC2	K1	C33	TC1
Mass of container, g	5.70	5.40	5.70	5.60	5.50
Mass of container + Wet soil, g	30.20	25.90	29.60	11.90	13.80
Mass of container + Dry soil, g	22.10	18.90	20.90	11.00	12.60
Mass of water, g	8.10	7.00	8.70	0.90	1.20
Mass of dry soil, g	16.40	13.50	15.20	5.40	7.10
Water content, %	49.39	51.85	57.24	16.67	16.90
No of blows	34	24	16	16.78	
	LL=71			PL=16.8	

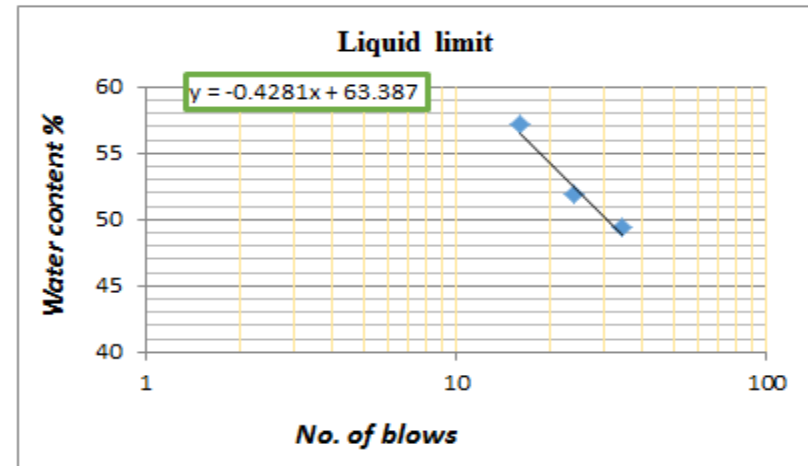


Figure A.2.5 Liquid limit chart for Bore 1



Table A-1-5 Grain size analysis for Jiren 1

Depth: 1.5 m

Sieve opening	Weight retained (gm)	Percent retained (%)	Cumulative retained %	%age passing
4.75	1.9	0.38	0	100.0
2	4.1	0.82	0.82	99.2
0.85	3.9	0.78	1.6	98.4
0.425	10.2	2.04	3.64	96.4
0.25	3.8	0.76	4.4	95.6
0.15	5.6	1.12	5.52	94.5
0.075	8.9	1.78	7.3	92.7
pan	2.3			

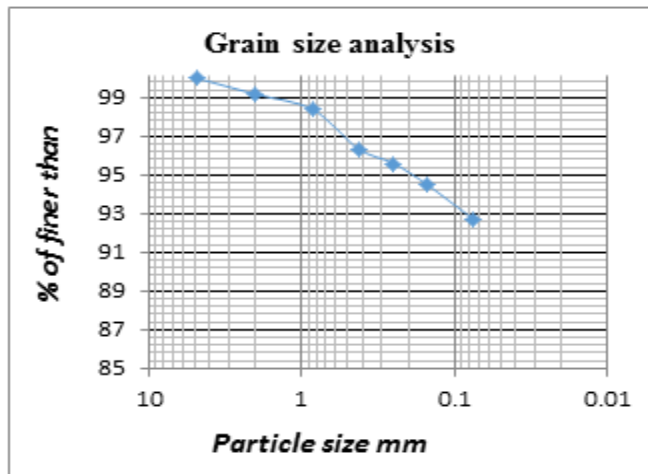


Figure A.1.5 Particle distribution curve for Jiren 1

Table A-2-5 Atterberg limit test for Jiren 1

Trial No	Liquid limit			Plastic limit	
	1	2	3	1	2
Container No	12	G2	C4	TC2	G2
Mass of container, g	5.60	5.60	5.80	5.70	5.60
Mass of container + Wet soil, g	35.10	32.10	26.80	13.60	12.70
Mass of container + Dry soil, g	23.80	21.60	18.20	11.60	10.90
Mass of water, g	11.30	10.50	8.60	2.00	1.80
Mass of dry soil, g	18.20	16.00	12.40	5.90	5.30
Water content, %	62.09	65.63	69.35	33.90	33.96
No of blows	32	24	15	33.93	
	LL=65			PL=33.9	

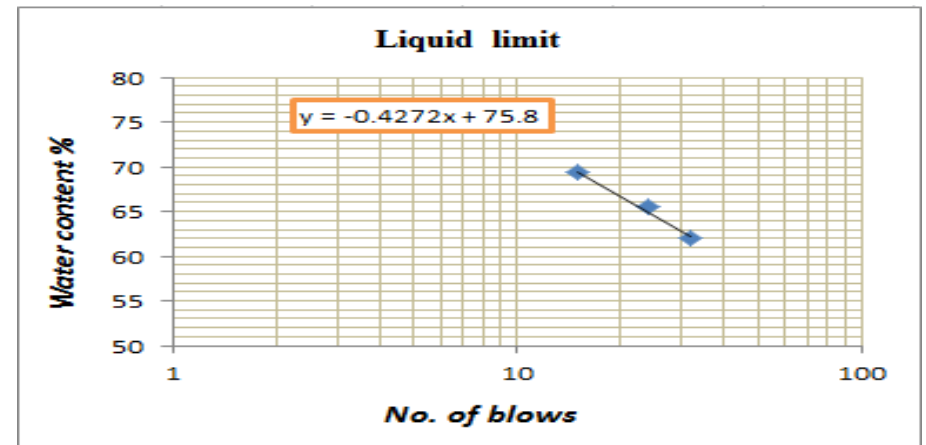


Figure A.2.5 Liquid limit chart for Jiren 1

Table A-1-5 Grain size analysis for B/Bore

Depth: 1 m

Sieve opening	Weight retained (gm)	Percent retained (%)	Cumulative retained %	%age passing
4.75	3.9	0.78	0	100.0
2	32.5	6.5	6.5	93.5
0.85	10.2	2.04	8.54	91.5
0.425	10.9	2.18	10.72	89.3
0.25	3.8	0.76	11.48	88.5
0.15	9.8	1.96	13.44	86.6
0.075	21.2	4.24	17.68	82.3
pan	3.1	0.62	18.3	81.7

Table A-2-5 Atterberg limit test for B/Bore

Trial No	Liquid limit			Plastic limit	
	1	2	3	1	2
Container No	CK	SK	C22	SC2	11
Mass of container, g	5.60	5.70	5.70	5.50	5.40
Mass of container + Wet soil, g	30.25	32.90	29.70	13.30	12.90
Mass of container + Dry soil, g	21.30	22.60	20.10	11.30	11.00
Mass of water, g	8.95	10.30	9.60	2.00	1.90
Mass of dry soil, g	15.70	16.90	14.40	5.80	5.60
Water content, %	57.01	60.95	66.67	34.48	33.93
No of blows	35	22	18	34.21	
	LL=61			PL=34.2	

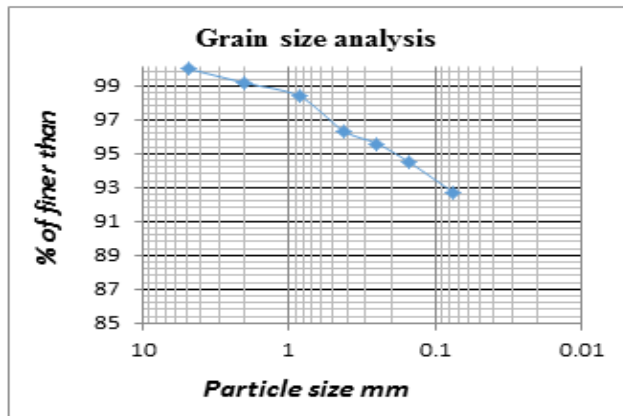


Figure A.1.5 Particle distribution curve for B/Bore

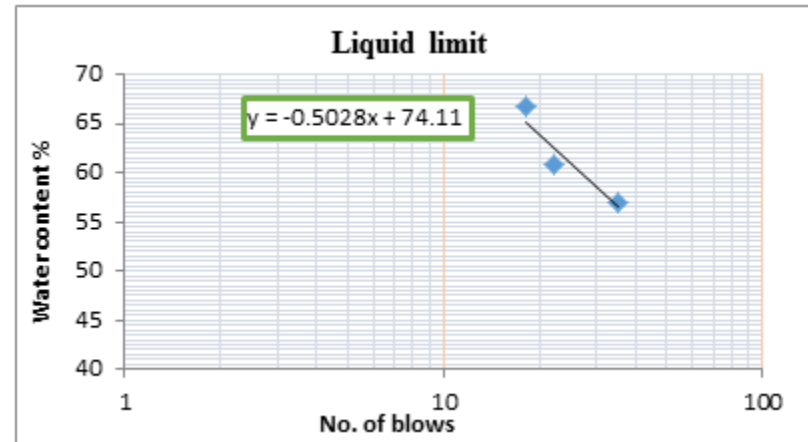


Figure A.2.5 Liquid limit chart for B/Bore

Table A-1-5 Grain size analysis for Mercato 1

Depth: 1.5 m

Opening (mm)	Mass of Retained Soil (g)	Percentage Retained (%)	Cumulative % Retained	%age Passing
4.75	0	0	0	100
2	0	0	0	100
0.85	3.8	0.38	0.38	100
0.425	21	2.1	2.48	99.62
0.25	15.9	1.59	4.07	97.52
0.15	14.5	1.45	5.52	95.93
0.075	16.8	1.68	7.2	94.48
pan	928	92.3		

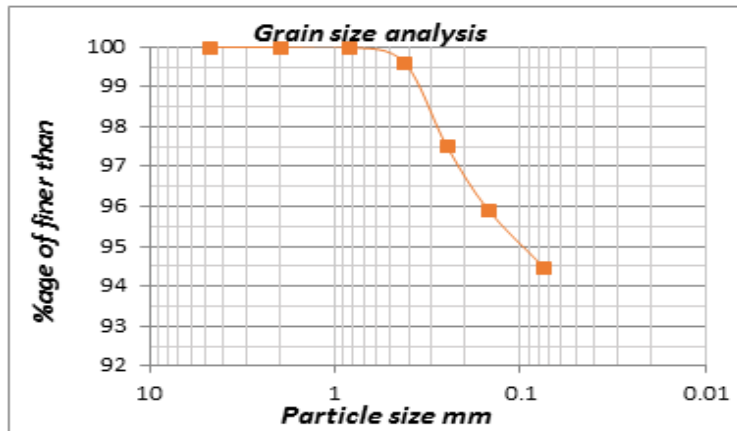


Figure A.1.5 Particle distribution curve for Mercato 1

Table A-2-5 Atterberg limit test for Mercato 1

Trial No	Liquid limit			Plastic limit	
	1	2	3	1	2
Container No	T1	B2	A-21	B	F2
Mass of container, g	5.90	6.30	5.70	5.60	6.30
Mass of container + Wet soil, g	34.5	34.8	25.1	12.3	14.5
	0	0	0	0	0
Mass of container + Dry soil, g	22.1	21.6	15.7	10.6	12.5
	7	3	6	8	3
Mass of water, g	12.3	13.1			
	3	7	9.34	1.62	1.97
Mass of dry soil, g	16.2	15.3	10.0	5.08	6.23
	7	3	6		
Water content, %	75.7	85.9	92.8	31.8	31.6
	8	1	4	9	2
No of blows	33	22	17	31.76	
	LL=81			PL=31.8	

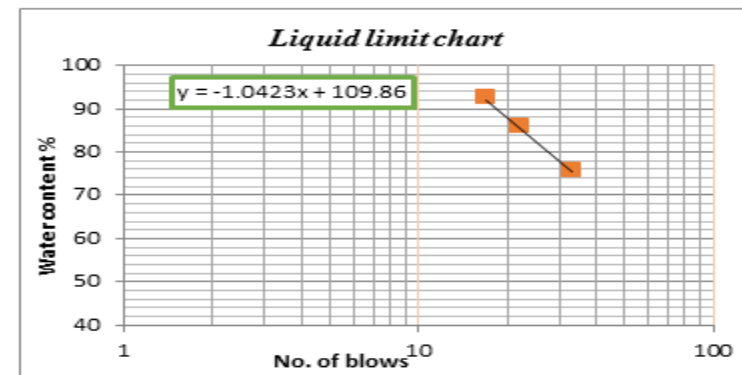
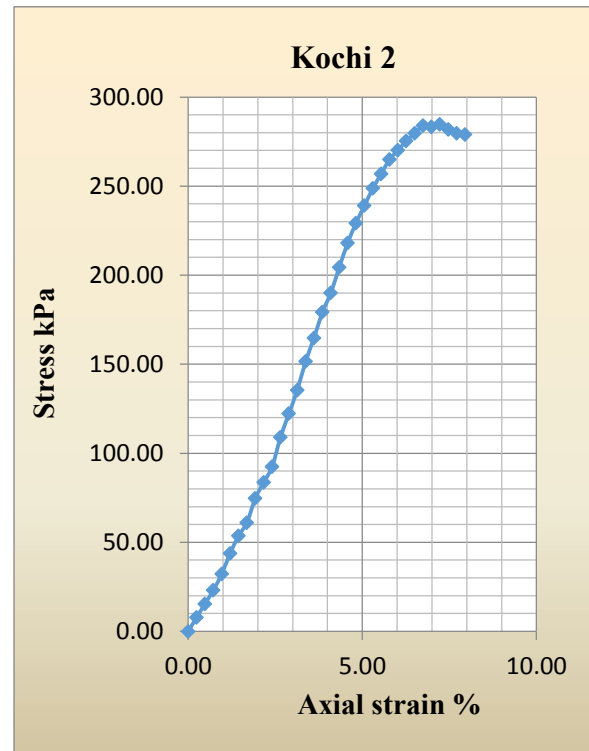
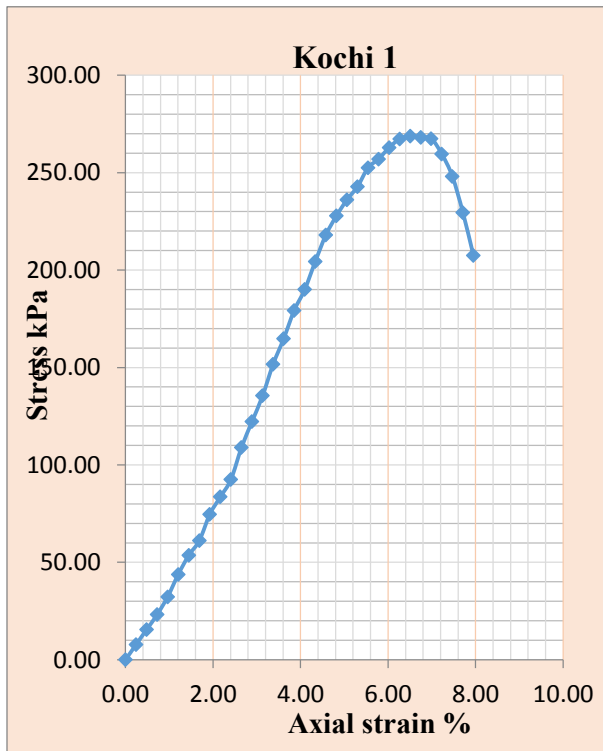
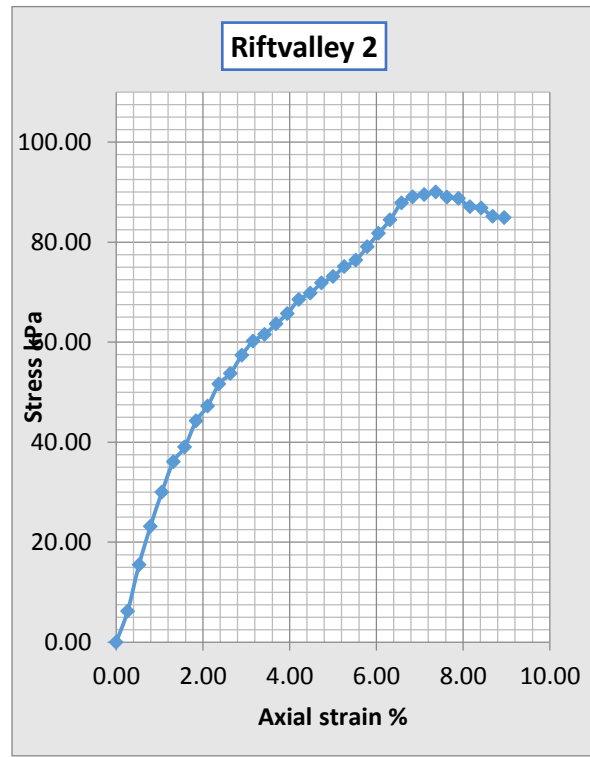
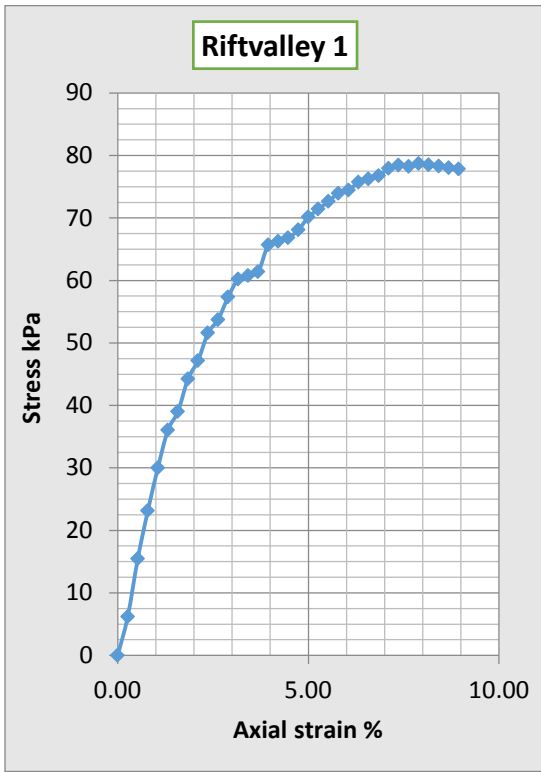
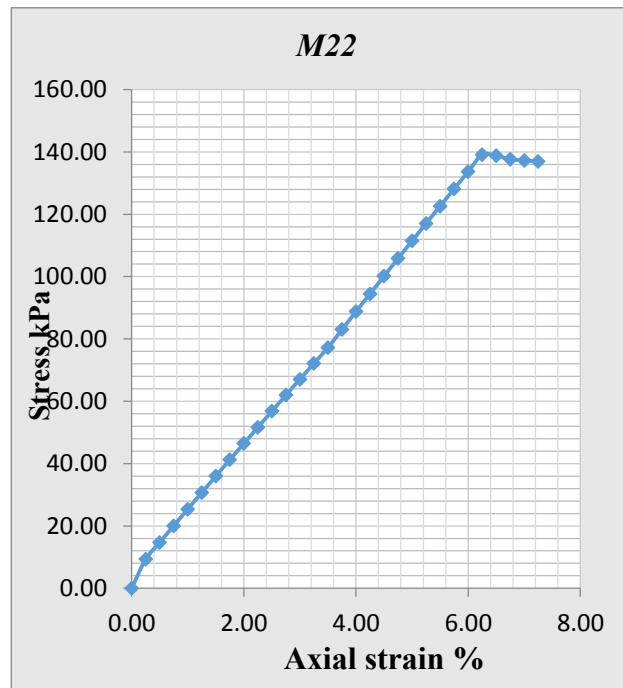
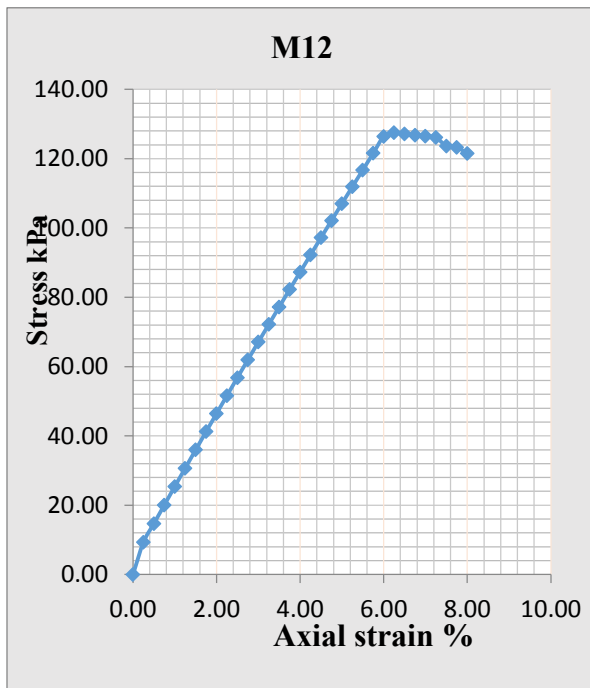
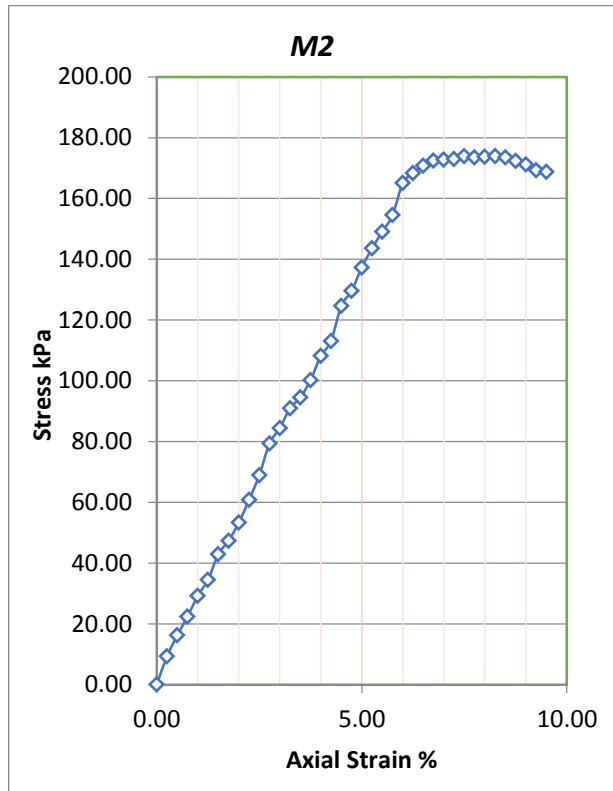
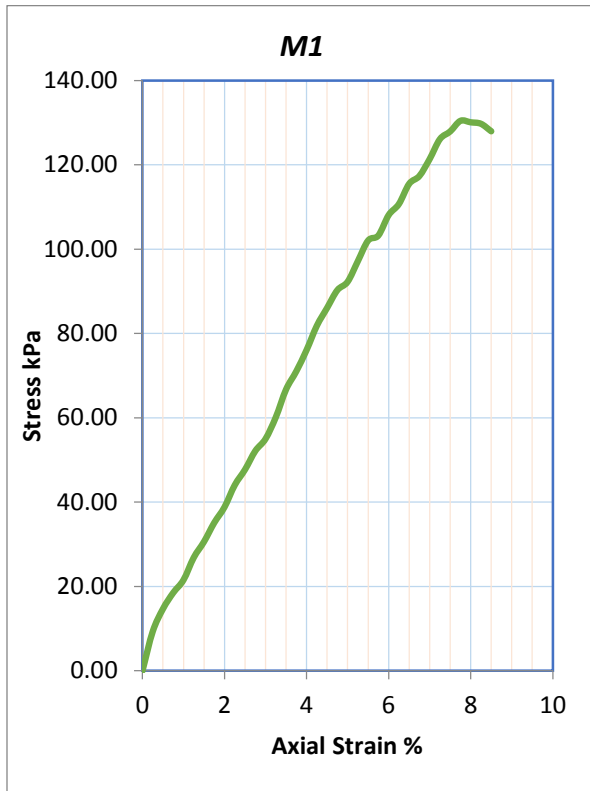
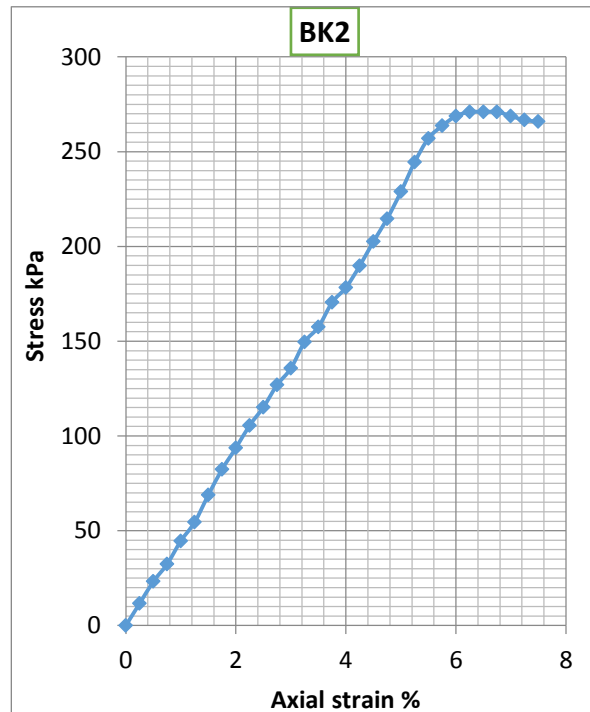
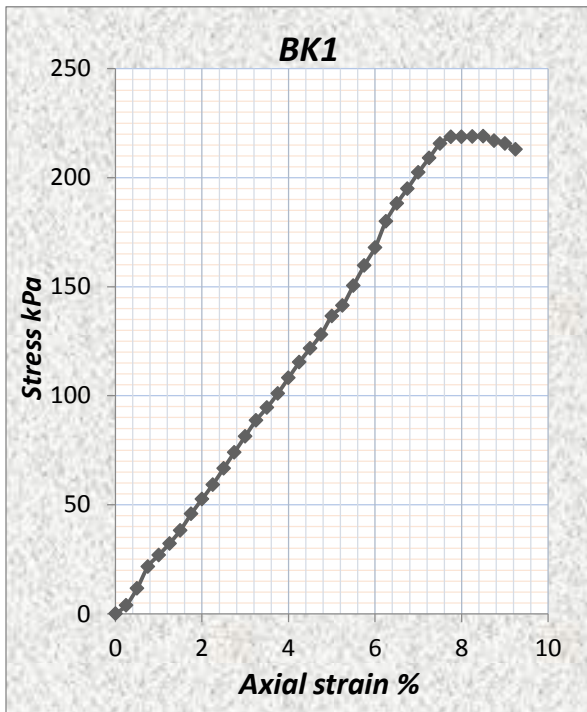
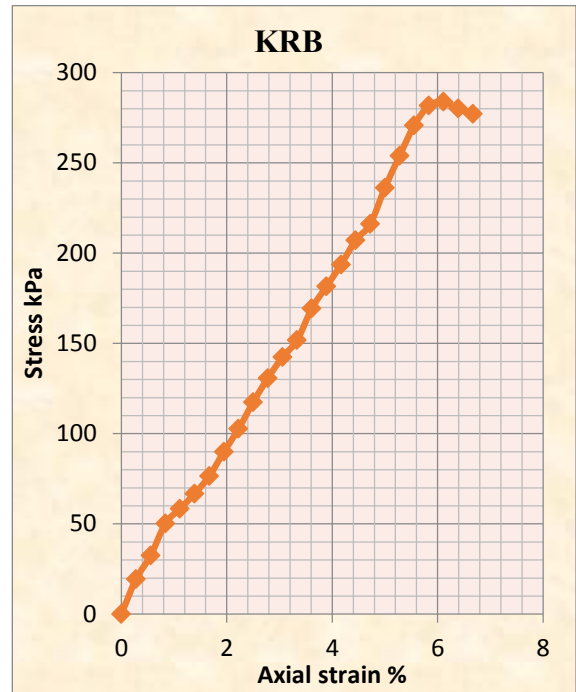
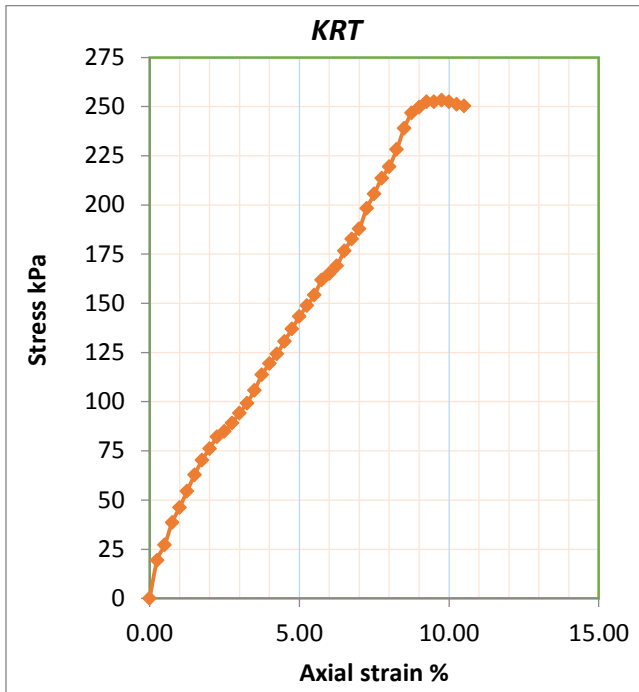


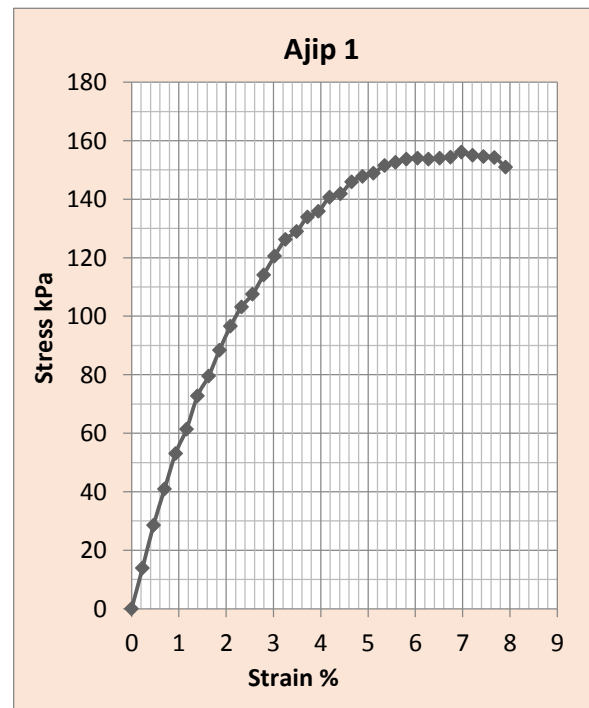
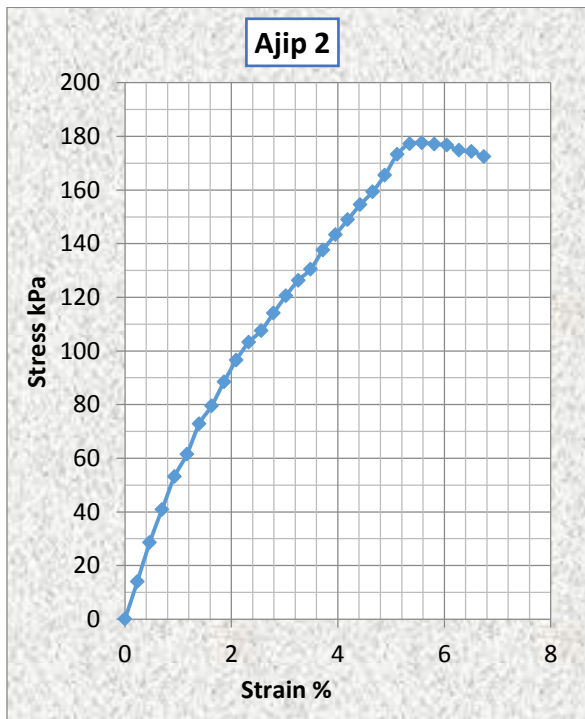
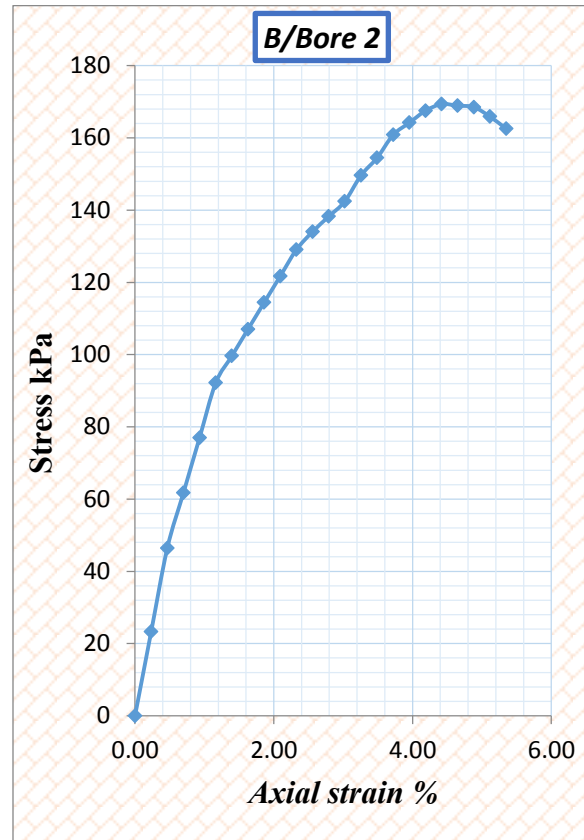
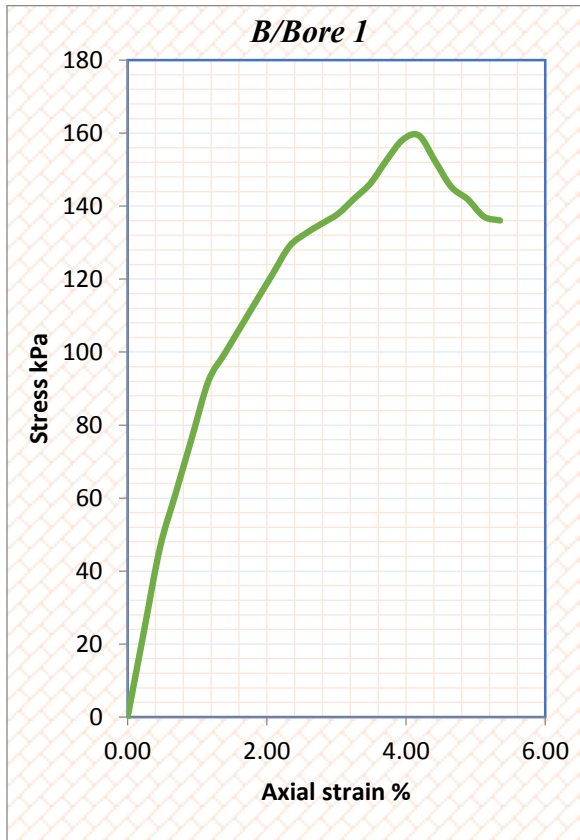
Figure A.2.5 Liquid limit chart for Mercato 1

## APPENDIX B: DETAIL OF UNCONFINED COMPRESSION TEST RESULTS

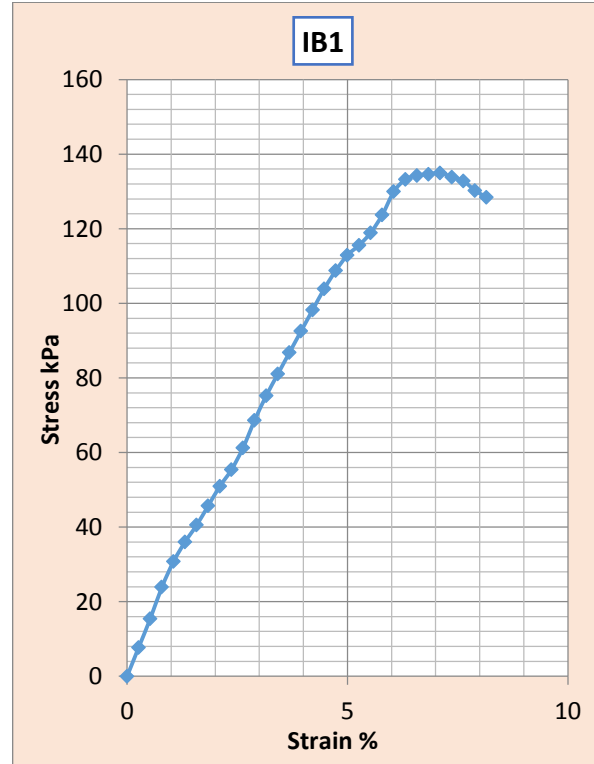
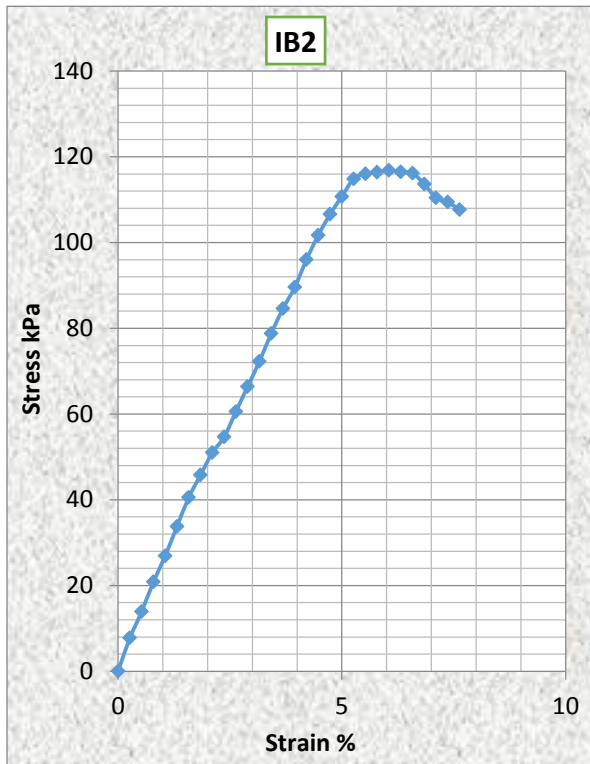
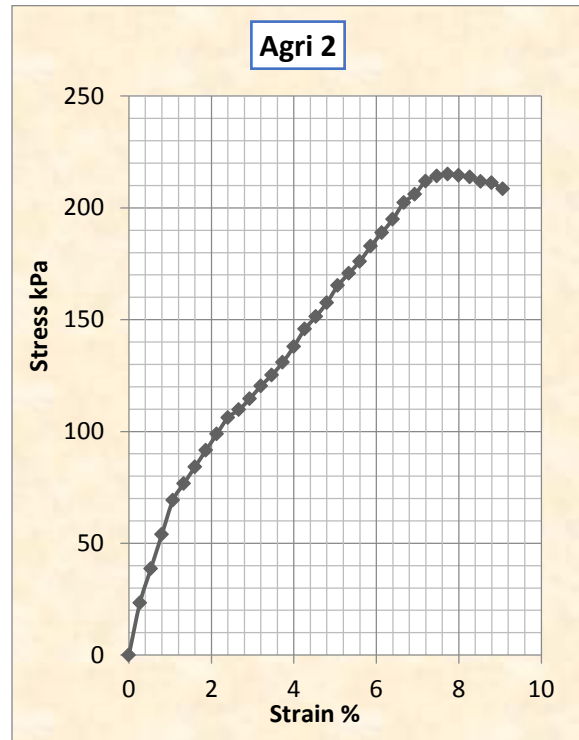
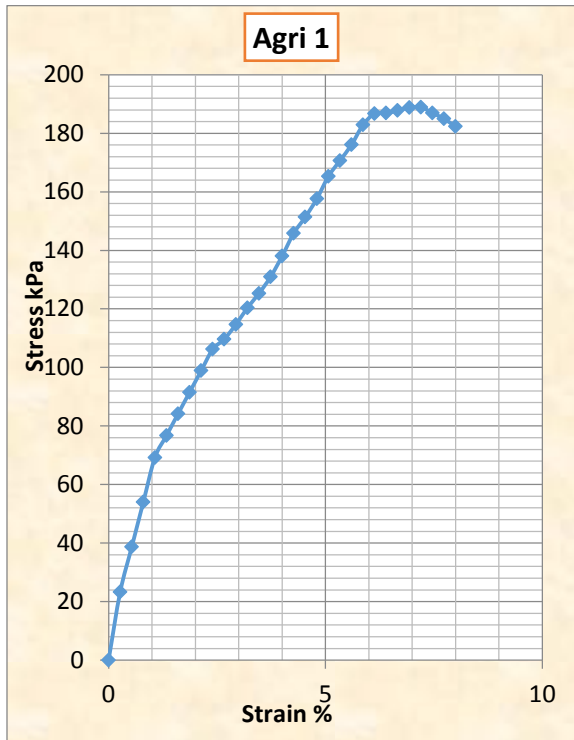


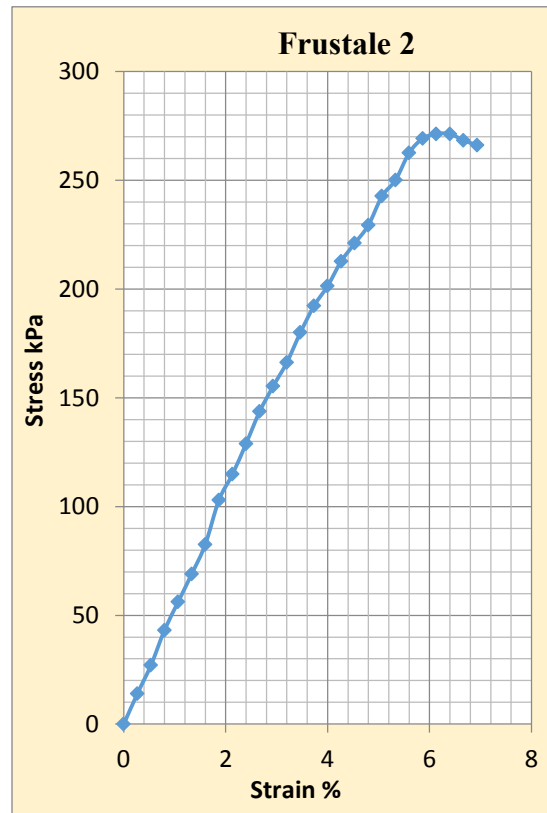
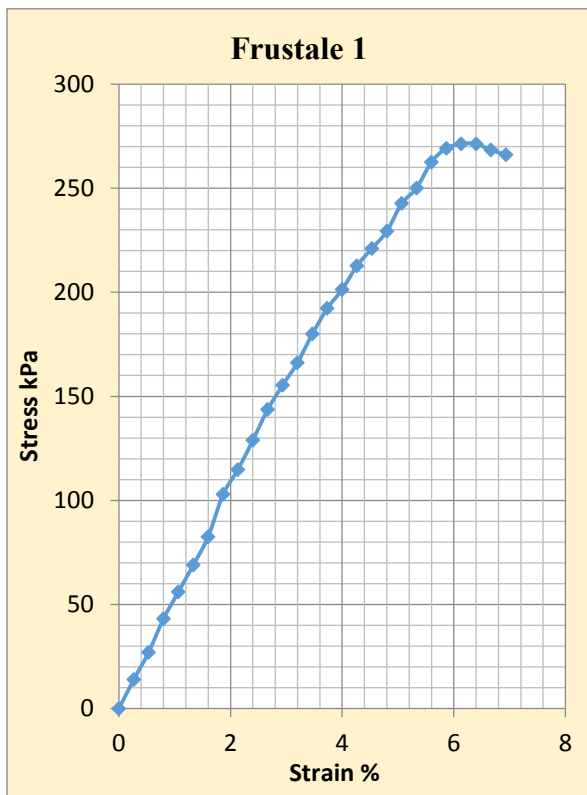
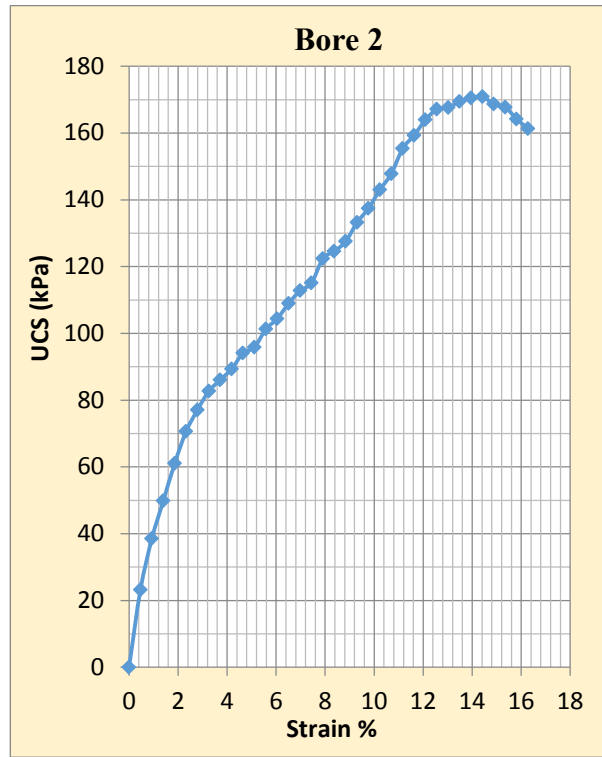
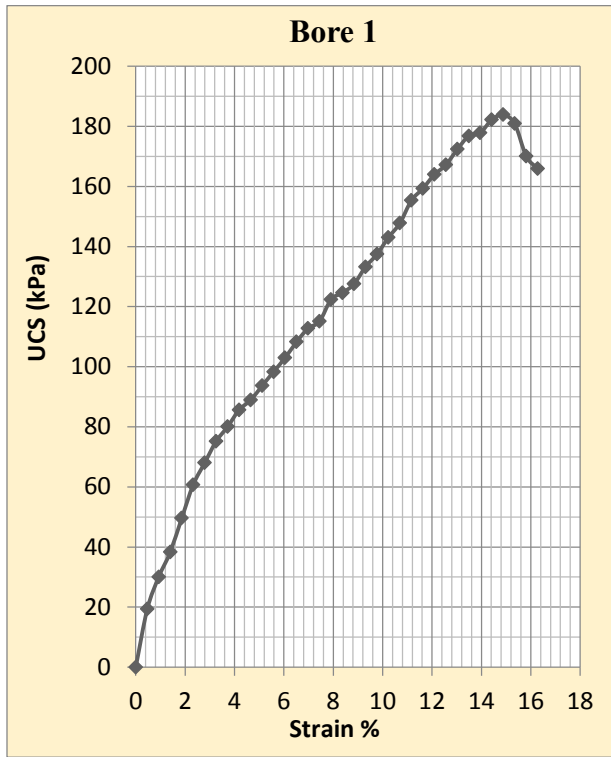


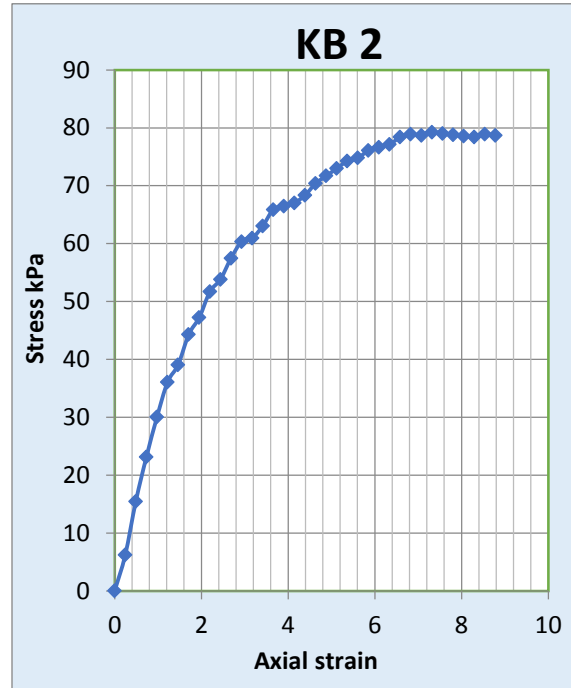
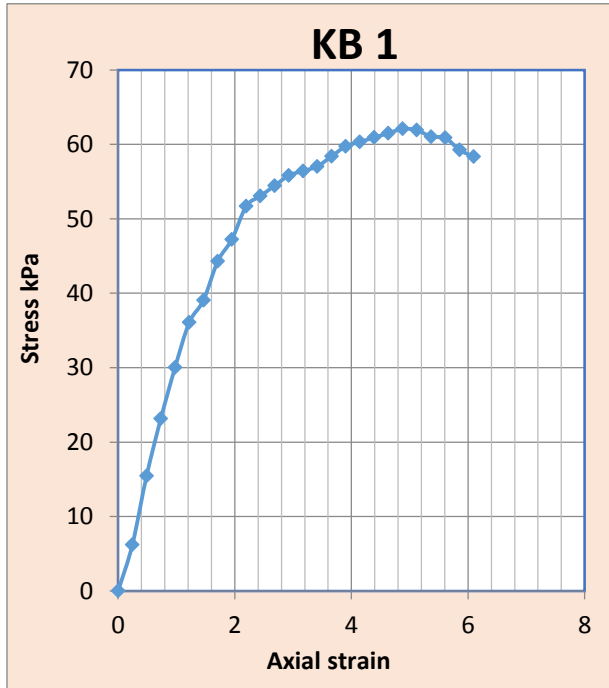
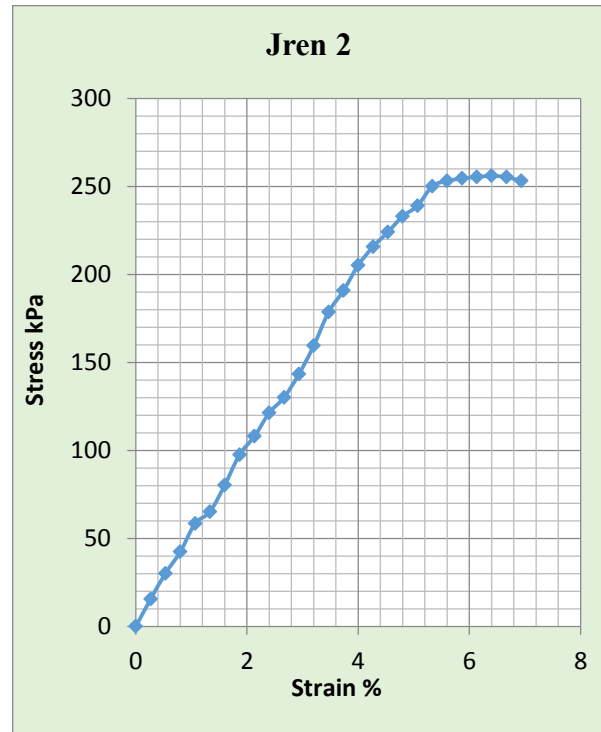
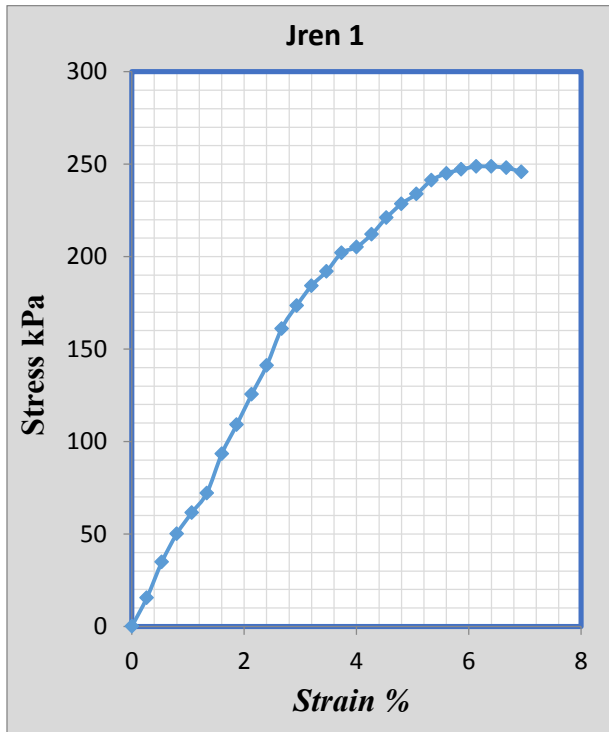


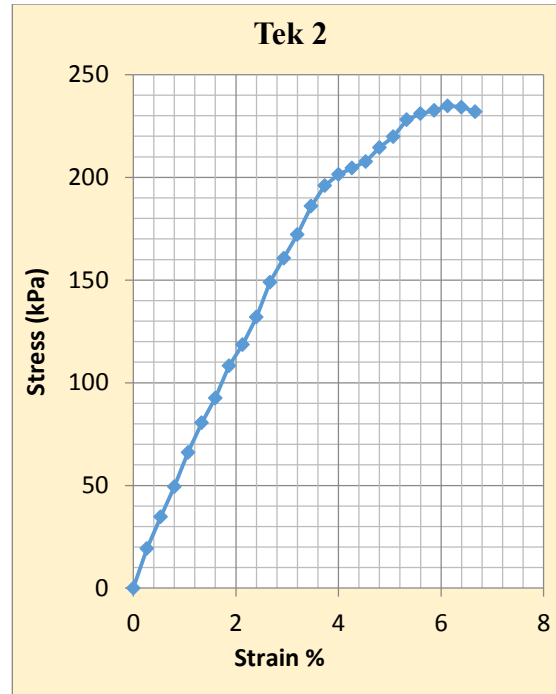
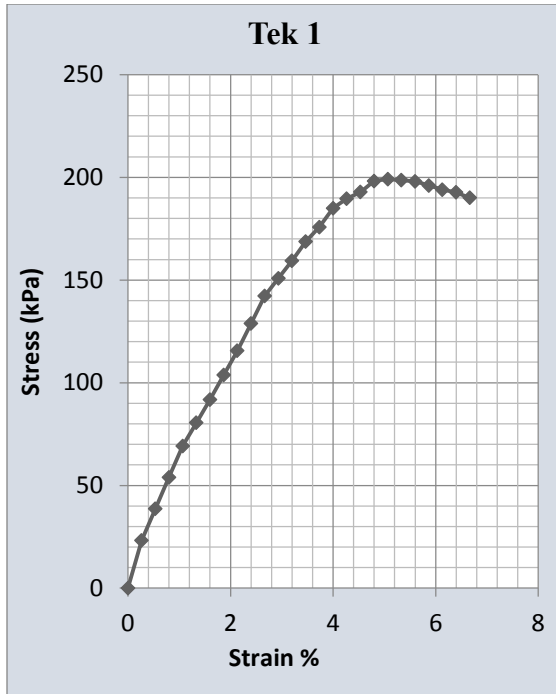












## **APPENDIX C: DETAIL OF DYNAMIC CONE PENETRATION DATA**

Table C 1.1 Penetration Data Report for Ifa bula 1

S.N	No. of blows	Cumulative no. of blows	depth of penetration (mm)	DCPI	Penetration rate
1	0	0	72		
2	1	1	102	30	30
3	1	2	146	44	44
4	1	3	211	65	65
5	1	4	253	42	42
6	1	5	298	45	45
7	1	6	332	34	34
8	1	7	379	47	47
9	1	8	403	24	24
10	1	9	443	40	40
11	1	10	469	26	26
12	1	11	497	28	28
13	1	12	513	16	16
14	1	13	541	28	28
15	1	14	576	35	35
16	1	15	605	29	29
17	1	16	639	34	34
18	1	17	677	38	38
19	1	18	702	25	25
20	1	19	739	37	37
21	1	20	778	39	39

22	1	21	801	23	23
23	1	22	828	27	27
24	1	23	859	31	31
25	1	24	882	23	23

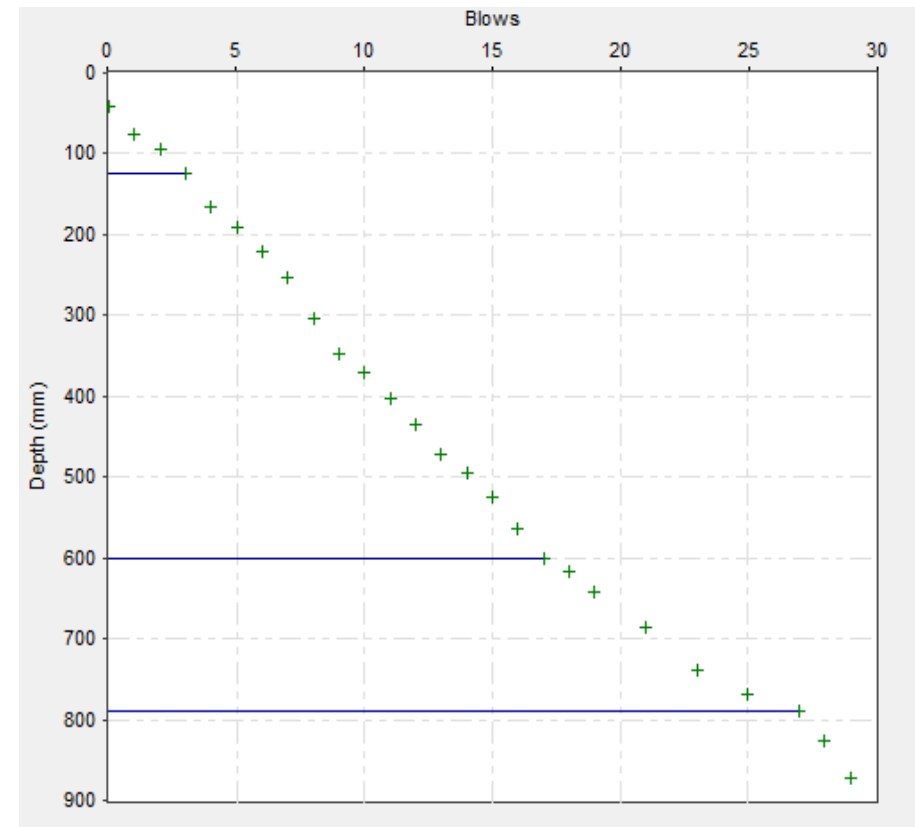


Figure C 1.1 DCP layer boundaries for Ifa bula 1

Table C 1.2 Penetration data report for Frustale 1

S.N	No. of blows	Cumulative no. of blows	depth of penetration (mm)	DCPI	Penetration rate
1	0	0	68		
2	1	1	101	33	33
3	1	2	142	41	41
4	1	3	193	51	51
5	1	4	218	25	25
6	1	5	259	41	41
7	1	6	289	30	30
8	1	7	331	42	42
9	1	8	372	41	41
10	1	9	403	31	31
11	1	10	441	38	38
12	1	11	473	32	32
13	1	12	502	29	29
14	1	13	540	38	38
15	1	14	554	14	14
16	1	15	565	11	11
17	2	17	592	27	13.5
18	2	19	629	37	18.5
19	2	21	651	22	11
20	1	22	697	46	46
21	1	23	731	34	34
22	1	24	769	38	38
23	1	25	806	37	37
24	1	26	842	36	36

25	1	27	869	27	27
----	---	----	-----	----	----

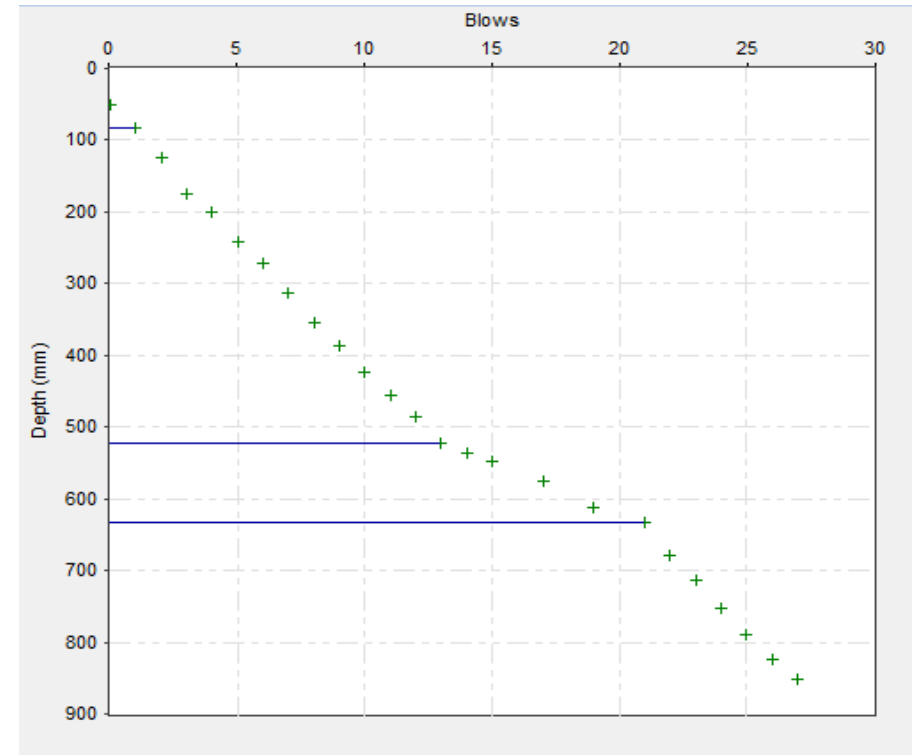


Figure C-1.2 DCP layer boundaries for Frustale 1

Table C 1.3 Penetration data report for Agriculture campus 1

S.N	No. of blows	Cumulative no. of blows	depth of penetration (mm)	DCPI	Penetration rate
1	0	0	58		
2	1	1	93	35	35
3	1	2	112	19	19
4	1	3	142	30	30
5	1	4	183	41	41
6	1	5	209	26	26
7	1	6	238	29	29
8	1	7	271	33	33
9	1	8	321	50	50
10	1	9	364	43	43
11	1	10	387	23	23
12	1	11	419	32	32
13	1	12	451	32	32
14	1	13	489	38	38
15	1	14	511	22	22
16	1	15	541	30	30
17	1	16	582	41	41
18	1	17	618	36	36
19	1	18	652	34	34
20	1	19	681	29	29
21	1	20	711	30	30
22	1	21	756	45	45
23	1	22	786	30	30
24	1	23	807	21	21

25	1	24	844	37	37
26	1	25	889	45	45

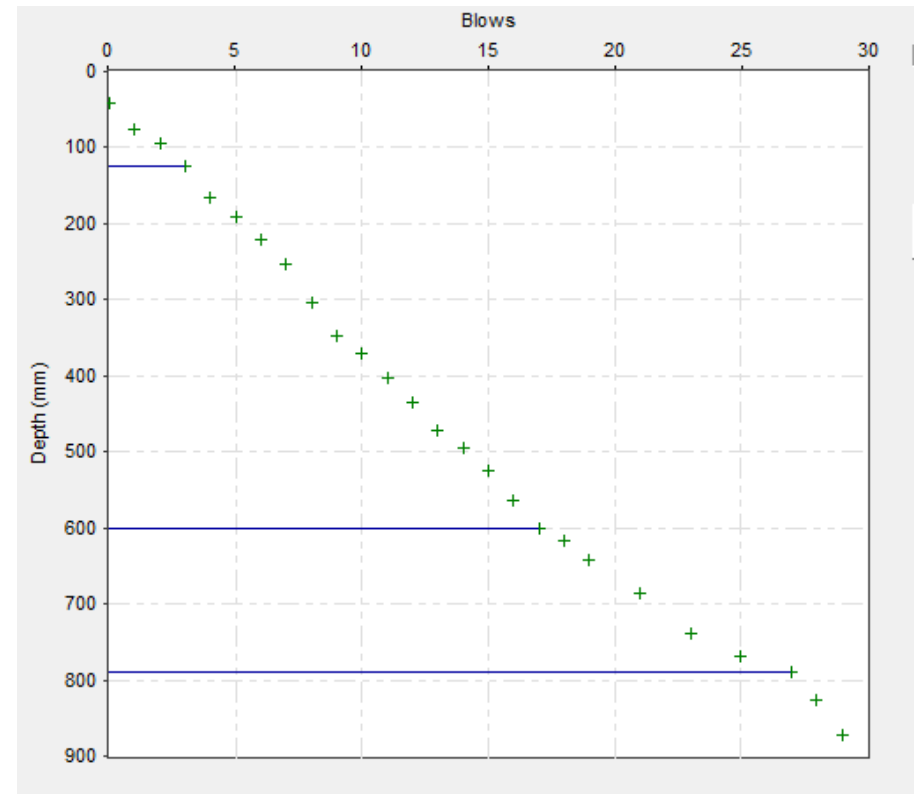


Figure C-1.3 DCP layer boundaries for Agriculture campus 1



Table C 1.4 Penetration data report for Ajip 1

<i>S.N</i>	<i>No. of blows</i>	<i>Cumulative no. of blows</i>	<i>depth of penetration (mm)</i>	<i>DCPI</i>	<i>Penetration rate</i>
1	0	0	40		
2	1	1	78	38	38
3	1	2	102	24	24
4	1	3	134	32	32
5	1	4	172	38	38
6	1	5	202	30	30
7	1	6	250	48	48
8	1	7	284	34	34
9	1	8	309	25	25
10	1	9	332	23	23
11	1	10	356	24	24
12	1	11	389	33	33
13	1	12	412	23	23
14	1	13	443	31	31
15	1	14	471	28	28
16	1	15	487	16	16
17	1	16	518	31	31
18	1	17	538	20	20
19	1	18	572	34	34
20	1	19	598	26	26
21	1	20	631	33	33
22	1	21	673	42	42
23	1	22	699	26	26

24	1	23	733	34	34
25	1	24	756	23	23
26	1	25	778	22	22
27	1	26	796	18	18
28	1	27	822	26	26
29	1	28	856	34	34
30	1	29	878	22	22

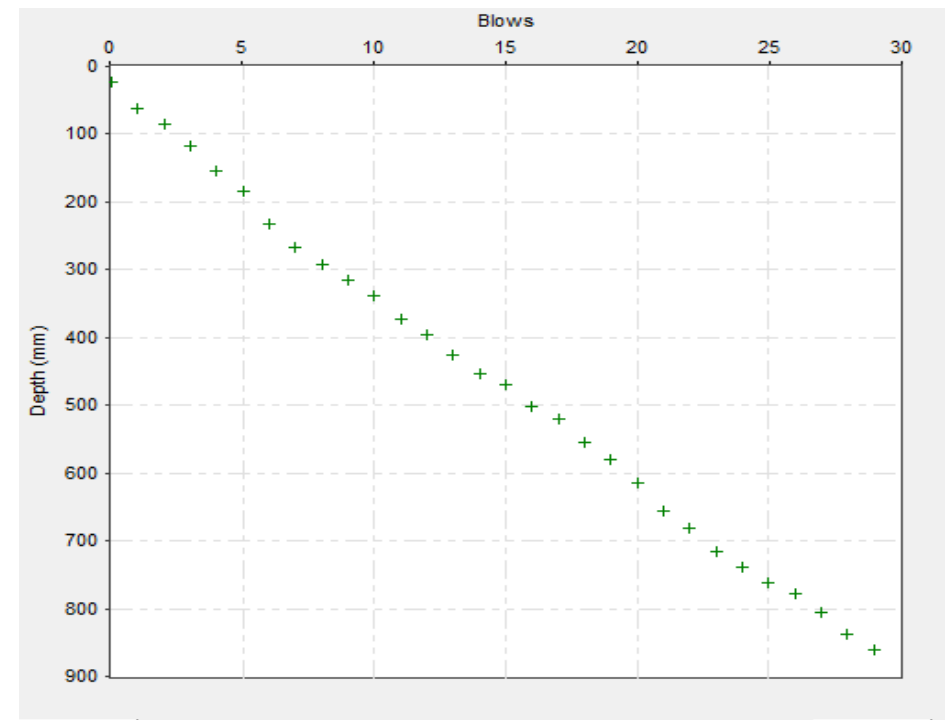


Figure C-1.4 DCP layer boundaries for Ajip 1

Table C-1.5 Penetration data report for Riftvalley 1

<i>S.N</i>	<i>No. of blows</i>	<i>Cumulative no. of blows</i>	<i>depth of penetration (mm)</i>	<i>DCPI</i>	<i>Penetration rate</i>
1	0	0	160		
2	1	1	278	118	118
3	1	2	362	84	84
4	1	3	431	69	69
5	1	4	498	67	67
6	1	5	529	31	31
7	1	6	561	32	32
8	1	7	589	28	28
9	1	8	618	29	29
10	1	9	653	35	35
11	1	10	693	40	40
12	1	11	732	39	39
13	1	12	769	37	37
14	1	13	815	46	46
15	1	14	870	55	55
16	1	15	933	63	63

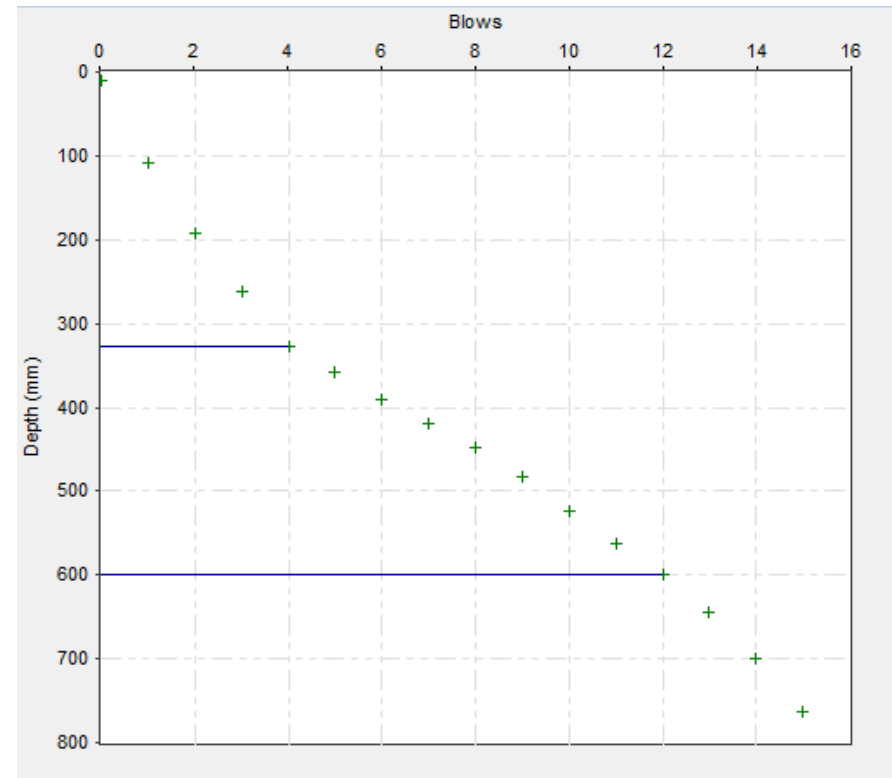


Figure C-1.5 DCP layer boundaries for Riftvalley 1

Table C-1.5 Penetration data report for Kochi 1

S.N	No. of blows	Cumulative no. of blows	depth of penetration (mm)	DCPI	Penetration rate
1	0	0	40		
2	1	1	80	40	40
3	1	2	104	24	24
4	1	3	135	31	31
5	1	4	175	40	40
6	1	5	210	35	35
7	1	6	243	33	33
8	1	7	280	37	37
9	1	8	308	28	28
10	1	9	333	25	25
11	1	10	354	21	21
12	1	11	380	26	26
13	1	12	404	24	24
14	1	13	427	23	23
15	1	14	447	20	20
16	1	15	468	21	21
17	1	16	488	20	20
18	1	17	507	19	19
19	1	18	526	19	19
20	1	19	544	18	18
21	1	20	565	21	21
22	1	21	583	18	18
23	1	22	601	18	18
24	1	23	619	18	18

25	1	24	639	20	20
26	1	25	655	16	16
27	1	26	671	16	16
28	1	27	687	16	16
29	1	28	703	16	16
30	1	29	709	6	6
31	1	30	731	22	22
32	1	31	746	15	15
33	1	32	760	14	14
34	1	33	774	14	14
35	1	34	787	13	13
36	1	35	799	12	12
38	2	37	825	21	21

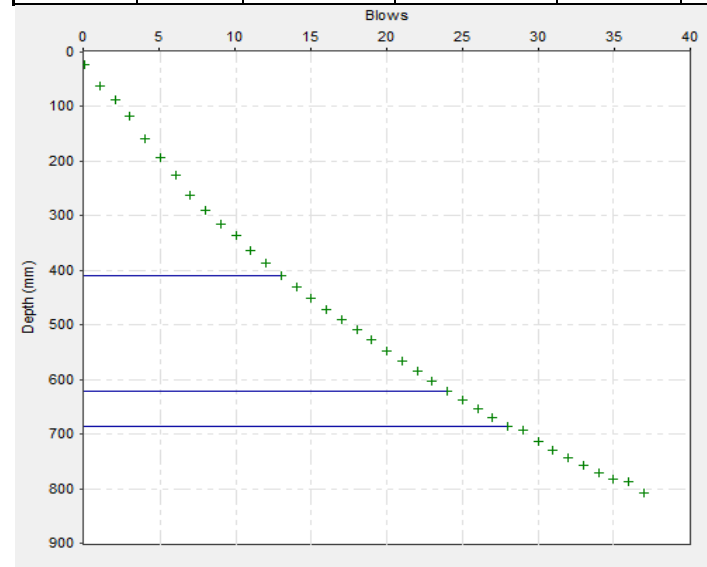


Figure C-1.6 DCP layer boundaries for Kochi 1

Table C-1.5 Penetration data report for Mercato 1

<i>S.N</i>	<i>No. of blows</i>	<i>Cumulative no. of blows</i>	<i>depth of penetration (mm)</i>	<i>DCPI</i>	<i>Penetration rate</i>
1	0	0	60		
2	1	1	141	81	81
3	1	2	163	22	22
4	1	3	187	24	24
5	1	4	218	31	31
6	1	5	234	16	16
7	1	6	263	29	29
8	1	7	280	17	17
9	1	8	291	11	11
10	2	10	302	11	5.5
11	2	12	311	9	4.5
12	2	14	325	14	7
13	2	16	353	28	14
14	2	18	384	31	15.5
15	2	20	394	10	5
16	2	22	402	8	4
17	5	27	419	17	3.4
18	5	32	436	17	3.4
19	5	37	478	42	8.4
20	1	38	501	23	23
21	1	39	524	23	23
22	1	40	548	24	24
23	1	41	574	26	26

24	1	42	600	26	26
25	1	43	620	20	20
26	1	44	642	22	22
27	1	45	663	21	21
28	1	46	683	20	20
29	1	47	704	21	21
30	1	48	724	20	20
31	1	49	745	21	21
32	1	50	764	19	19
33	1	51	781	17	17
34	1	52	798	17	17
35	1	53	808	10	10
36	1	54	841	33	33
37	1	55	861	20	20
38	1	56	881	20	20

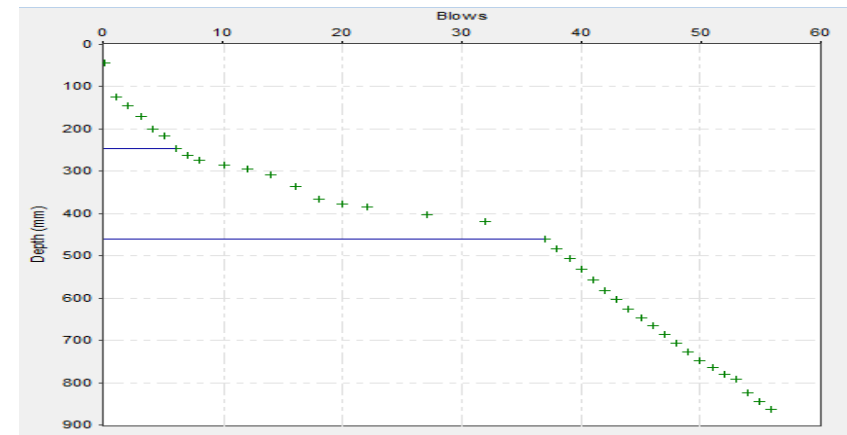


Figure C-1.4 DCP layer boundaries for Mercato 1

Table C-1.5 Penetration data report for Mercato 21

<i>S.N</i>	<i>No. of blows</i>	<i>Cumulative no. of blows</i>	<i>depth of penetration (mm)</i>	<i>DCPI</i>	<i>Penetration rate</i>
1	0	0	80		
2	1	1	250	170	170
3	1	2	360	110	110
4	1	3	440	80	80
5	1	4	515	75	75
6	1	5	575	60	60
7	1	6	640	65	65
8	1	7	700	60	60
9	1	8	755	55	55
10	1	9	801	46	46
11	1	10	842	41	41
12	1	11	876	34	34

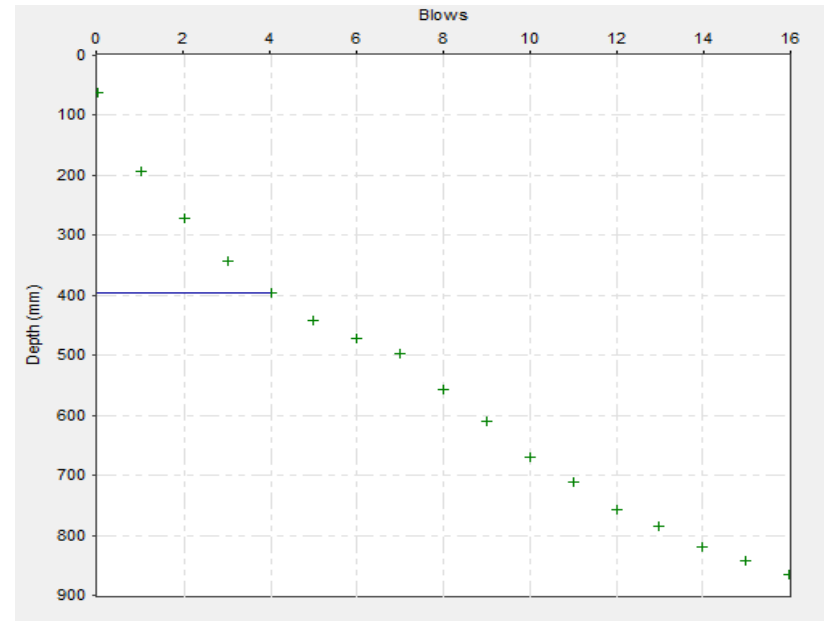


Figure C-1.4 DCP layer boundaries for Mercato 21

Table C-1.5 Penetration data report for Kito red top

<i>S.N</i>	<i>No. of blows</i>	<i>Cumulative no. of blows</i>	<i>depth of penetration (mm)</i>	<i>DCPI</i>	<i>Penetration rate</i>
1	0	0	56		
2	1	1	126	70	70
3	1	2	157	31	31
4	1	3	180	23	23
5	1	4	229	49	49
6	1	5	242	13	13
7	1	6	263	21	21
8	1	7	297	34	34
9	1	8	333	36	36
10	1	9	360	27	27
11	1	10	401	41	41
12	1	11	434	33	33
13	1	12	478	44	44
14	1	13	506	28	28
15	1	14	530	24	24
16	1	15	563	33	33
17	1	16	593	30	30
18	1	17	626	33	33
19	1	18	661	35	35
20	1	19	695	34	34
21	1	20	728	33	33
22	1	21	757	29	29
23	1	22	783	26	26

24	1	23	808	25	25
25	1	24	836	28	28
26	1	25	864	28	28
27	1	26	889	25	25
28	1	27	918	29	29

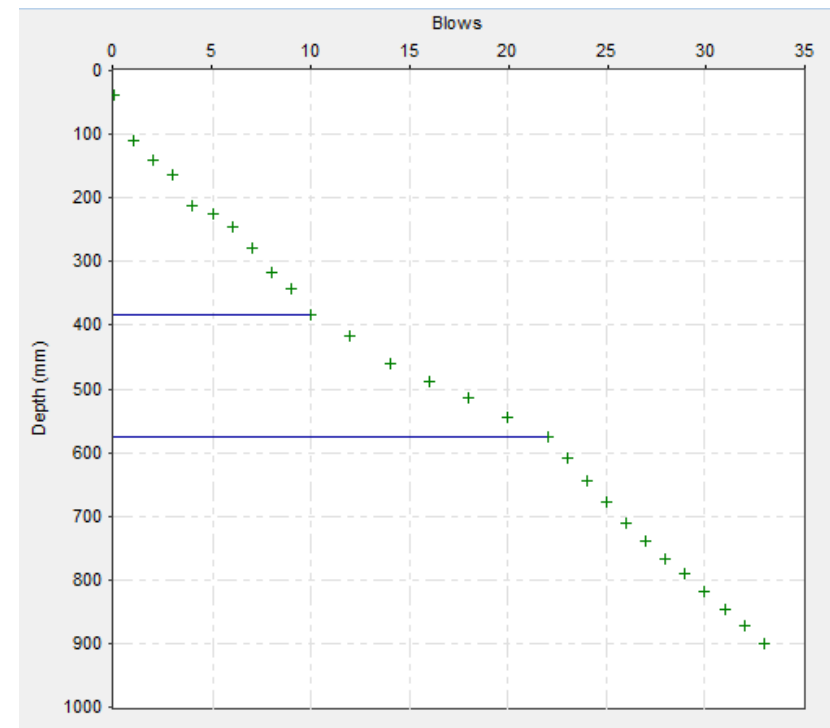


Figure C-1.4 DCP layer boundaries for Kito red top

Table C-1.5 Penetration data report for Kito black 1

<i>S.N</i>	<i>No. of blows</i>	<i>Cumulative no. of blows</i>	<i>depth of penetration (mm)</i>	<i>DCPI</i>	<i>Penetration rate</i>
1	0	0	88		
2	1	1	234	146	146
3	1	2	261	27	27
4	1	3	283	22	22
5	1	4	347	64	64
6	1	5	483	136	136
7	1	6	558	75	75
8	1	7	607	49	49
9	1	8	655	48	48
10	1	9	692	37	37
11	1	10	731	39	39
12	1	11	764	33	33
13	1	12	796	32	32
14	1	13	826	30	30
15	1	14	847	21	21
16	1	15	873	26	26
17	1	16	896	23	23

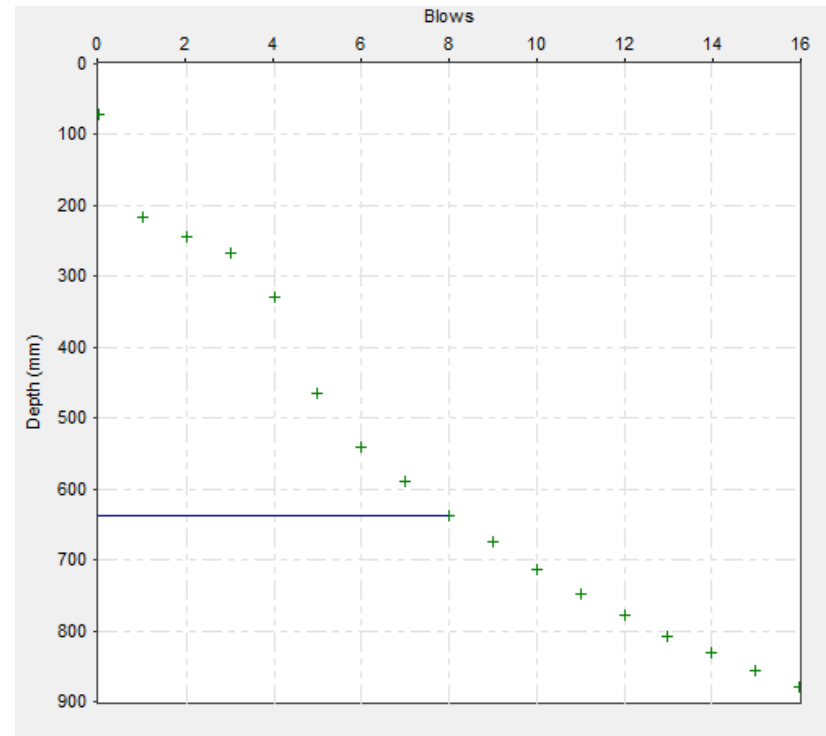


Figure C-1.4 DCP layer boundaries for Kito black 1

Table C-1.5 Penetration data report for Teknik 1

S.N	No. of blows	Cumulative no. of blows	depth of penetration (mm)	DCPI	Penetration rate
1	0	0	0	0	
2	1	1	48	48	48
3	1	2	219	171	171
4	1	3	364	145	145
5	1	4	443	79	79
6	1	5	504	61	61
7	1	6	554	50	50
8	1	7	589	35	35
9	1	8	621	32	32
10	1	9	647	26	26
11	1	10	668	21	21
12	1	11	688	20	20
13	1	12	706	18	18
14	1	13	725	19	19
15	1	14	741	16	16
16	1	15	759	18	18
17	1	16	776	17	17
18	1	17	792	16	16
19	1	18	807	15	15
20	1	19	824	17	17
21	1	20	839	15	15
22	1	21	852	13	13
23	1	22	866	14	14

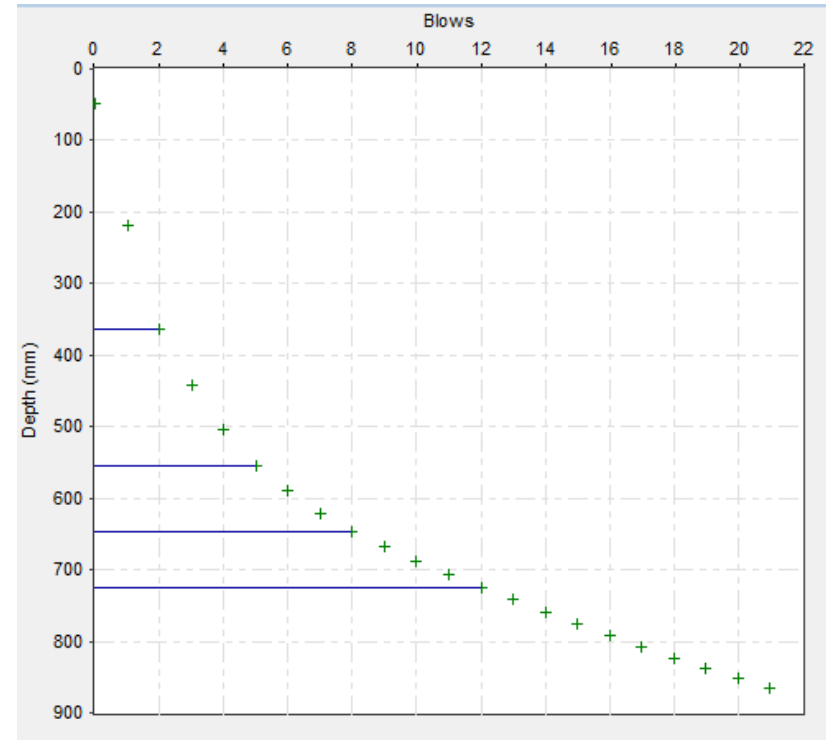


Figure C-1.4 DCP layer boundaries for Teknik 1



Table C-1.5 Penetration data report for B/bore 1

<i>S.N</i>	<i>No. of blows</i>	<i>Cumulative no. of blows</i>	<i>depth of penetration (mm)</i>	<i>DCPI</i>	<i>Penetration rate</i>
1	0	0	84		
2	1	1	121	37	37
3	1	2	168	47	47
4	1	3	198	30	30
5	1	4	232	34	34
6	1	5	256	24	24
7	1	6	287	31	31
8	1	7	321	34	34
9	1	8	365	44	44
10	1	9	389	24	24
11	1	10	419	30	30
12	1	11	445	26	26
13	1	12	465	20	20
14	1	13	489	24	24
15	1	14	521	32	32
16	1	15	558	37	37
17	1	16	576	18	18
18	1	17	597	21	21
19	1	18	621	24	24
20	1	19	649	28	28
21	1	20	681	32	32
22	1	21	702	21	21
23	1	22	740	38	38

24	1	23	778	38	38
25	1	24	804	26	26
26	1	25	833	29	29
27	1	26	853	20	20

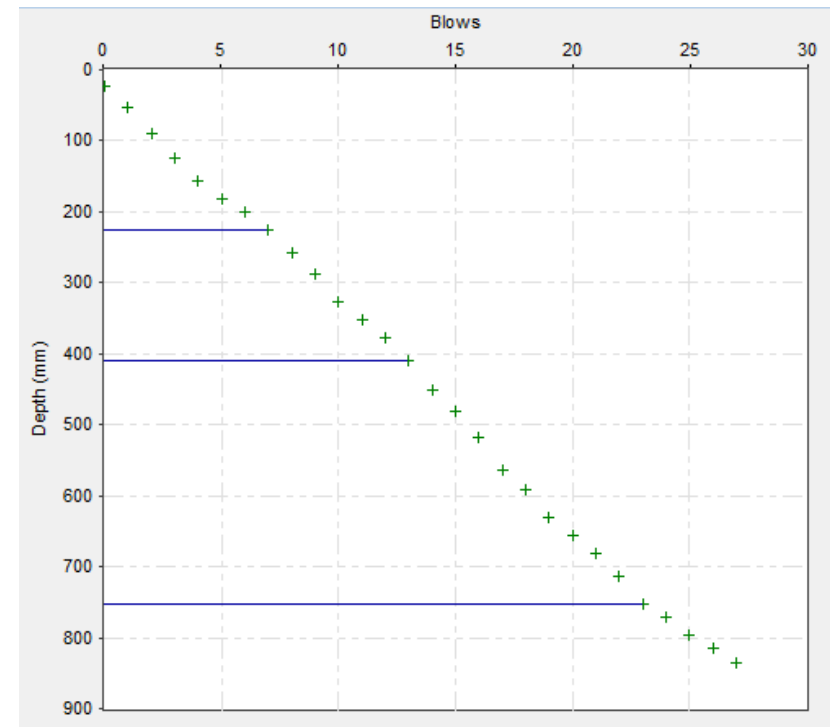


Figure C-1.4 DCP layer boundaries for B/bore 1

Table C-1.5 Penetration data report for Jiren 1

<i>S.N</i>	<i>No. of blows</i>	<i>Cumulative no. of blows</i>	<i>depth of penetration (mm)</i>	<i>DCPI</i>	<i>Penetration rate</i>
1	0	0	48		
2	1	1	87	39	39
3	1	2	116	29	29
4	1	3	154	38	38
5	1	4	174	20	20
6	1	5	189	15	15
7	1	6	217	28	28
8	1	7	258	41	41
9	1	8	297	39	39
10	1	9	331	34	34
11	1	10	373	42	42
12	1	11	426	53	53
13	1	12	475	49	49
14	1	13	501	26	26
15	1	14	520	19	19
16	1	15	531	11	11
17	1	16	553	22	22
18	1	17	560	7	7
19	1	18	586	26	26
20	1	19	612	26	26
21	1	20	648	36	36
22	1	21	669	21	21
23	1	22	699	30	30

24	1	23	721	22	22
25	1	24	740	19	19
26	1	25	755	15	15
27	1	26	771	16	16
28	1	27	793	22	22
29	1	28	804	11	11
30	1	29	813	9	9
31	1	30	837	24	24

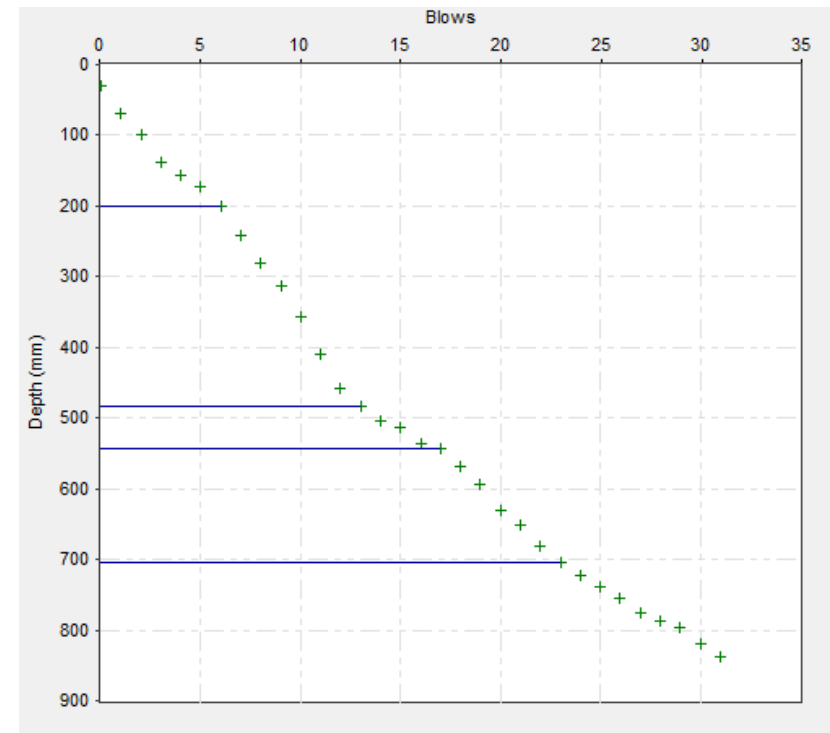


Figure C-1.4 DCP layer boundaries for Jiren 1

Table C-1.5 Penetration data report for Bore

<i>S.N</i>	<i>No. of blows</i>	<i>Cumulative no. of blows</i>	<i>depth of penetration (mm)</i>	<i>DCPI</i>	<i>Penetration rate</i>
1	0	0	0	0	
2	1	1	37	37	37
3	1	2	84	47	47
4	1	3	114	30	30
5	1	4	148	34	34
6	1	5	172	24	24
7	1	6	203	31	31
8	1	7	237	34	34
9	1	8	281	44	44
10	1	9	305	24	24
11	1	10	335	30	30
12	1	11	361	26	26
13	1	12	381	20	20
14	1	13	405	24	24
15	1	14	437	32	32
16	1	15	474	37	37
17	1	16	492	18	18
18	1	17	513	21	21
19	1	18	537	24	24
20	1	19	565	28	28
21	1	20	597	32	32
22	1	21	618	21	21
23	1	22	656	38	38

24	1	23	694	38	38
25	1	24	720	26	26
26	1	25	749	29	29
27	1	26	769	20	20

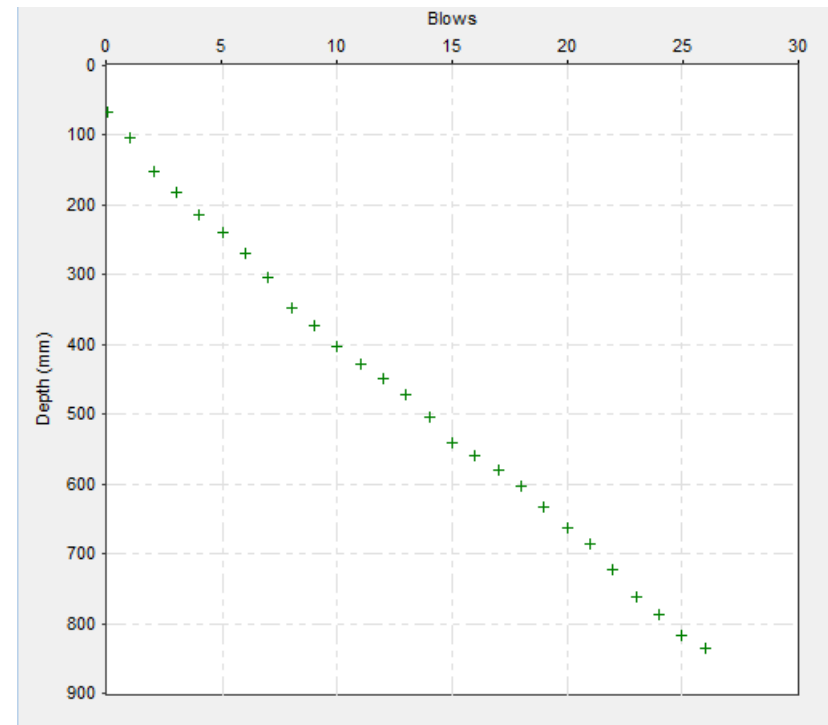


Figure C-1.4 DCP layer boundaries for Bore 1

Table C-1.5 Penetration data report for Bosa kito 1

<i>S.N</i>	<i>No. of blows</i>	<i>Cumulative no. of blows</i>	<i>depth of penetration (mm)</i>	<i>DCPI</i>	<i>Penetration rate</i>
1	0	0	0		
2	1	1	187	187	187
3	1	2	250	63	63
4	1	3	312	62	62
5	1	4	390	78	78
6	1	5	434	44	44
7	1	6	481	47	47
8	1	7	517	36	36
9	1	8	568	51	51
10	1	9	629	61	61
11	1	10	974	345	345
12	1	11	714	-260	-260
13	1	12	752	38	38
14	1	13	791	39	39
15	1	14	829	38	38
16	1	15	864	35	35
17	2	17	901	37	18.5
18	2	19	923	22	11
19	2	21	961	38	19
20	2	23	982	21	10.5

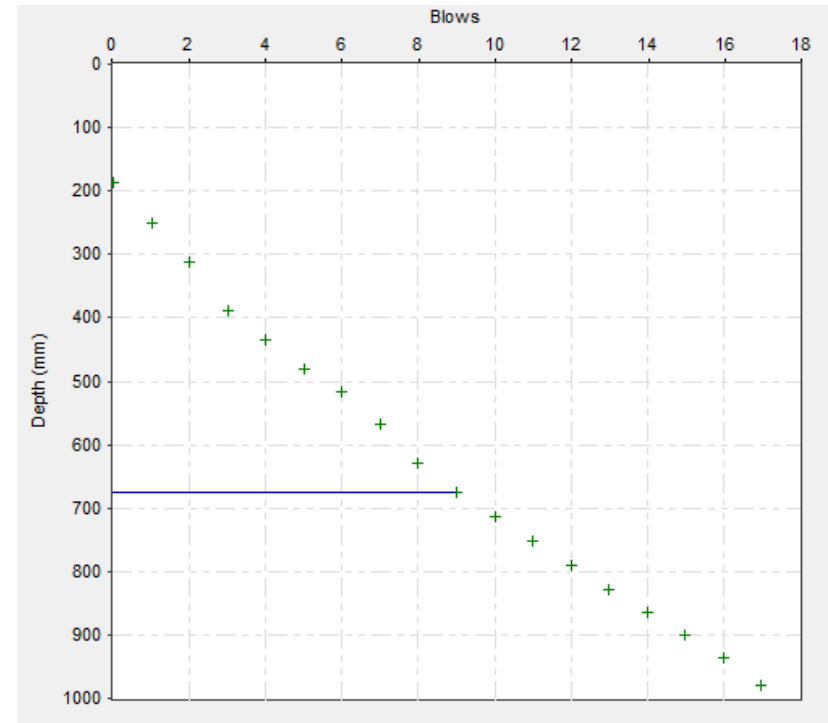


Figure C-1.4 DCP layer boundaries for Bosa kito 1

## **APPENDIX D: DETAIL OF CBR DATA FOR SELECTED SAMPLES**

Sample Location: Rift valley 1

Table D-1-1 CBR penetration data for Rift valley 1 after four days soaking

Penetration (mm) / Load	Load (kN)			Standard Stress (Mpa)
	65 Blows	30 Blows	10 Blows	
0	0	0	0	
0.625	0.118	0.12	0.124	
1.25	0.149	0.13	0.136	
1.875	0.169	0.14	0.144	
2.5	0.186	0.15	0.15	6.92
3.75	0.198	0.17	0.162	88
5	0.212	0.18	0.171	10.3
7.5	0.235	0.19	0.183	13.11
10	0.26	0.21	0.197	15.87
12.5	0.291	0.23	0.213	17.94
<b>CBR @ 2.54 mm</b>	1.4	1.2	1.1	
<b>CBR @ 5.08 mm</b>	1.1	0.9	0.9	

Summary of CBR data

No of blows	10	30	65
MDD(g/cm <sup>3</sup> )	1.27	1.31	1.36
CBR (%)	1.1	1.2	1.4

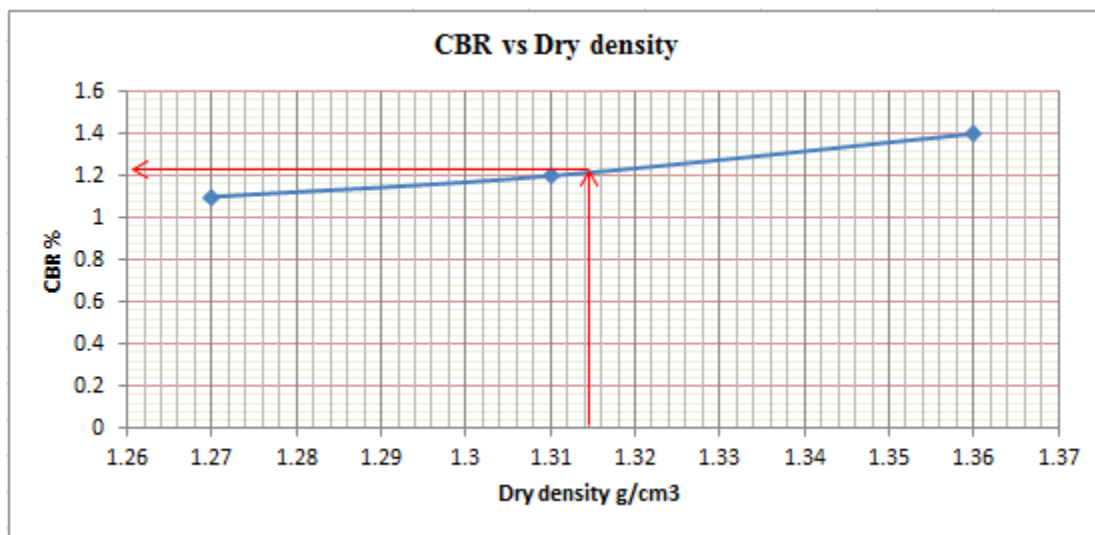


Figure D.1.1 CBR vs Dry density curve

Sample Location: Kochi 1

Table D-1-2 CBR penetration data for Kochi 1 after four days soaking

Penetration (mm)	Load (kN)			Standard Stress (Mpa)
	65 Blows	30 Blows	10 Blows	
0	0	0	0	
0.625	0.367	0.415	0.304	
1.25	0.62	0.641	0.448	
1.875	0.792	0.793	0.563	
2.5	0.916	0.896	0.653	6.92
3.75	1.073	1.037	0.782	88
5	1.178	1.145	0.876	10.3
7.5	1.336	1.307	1.024	13.11
10	1.47	1.443	1.136	15.87
12.5	1.594	1.56	1.24	17.94
<b>CBR @ 2.54 mm</b>	6.9	6.8	4.9	
<b>CBR @ 5.08 mm</b>	5.9	5.7	4.4	

Summary of CBR data

No of blows	10	30	65
MDD(g/cm <sup>3</sup> )	1.25	1.3	1.32
CBR (%)	6.9	6.8	4.9

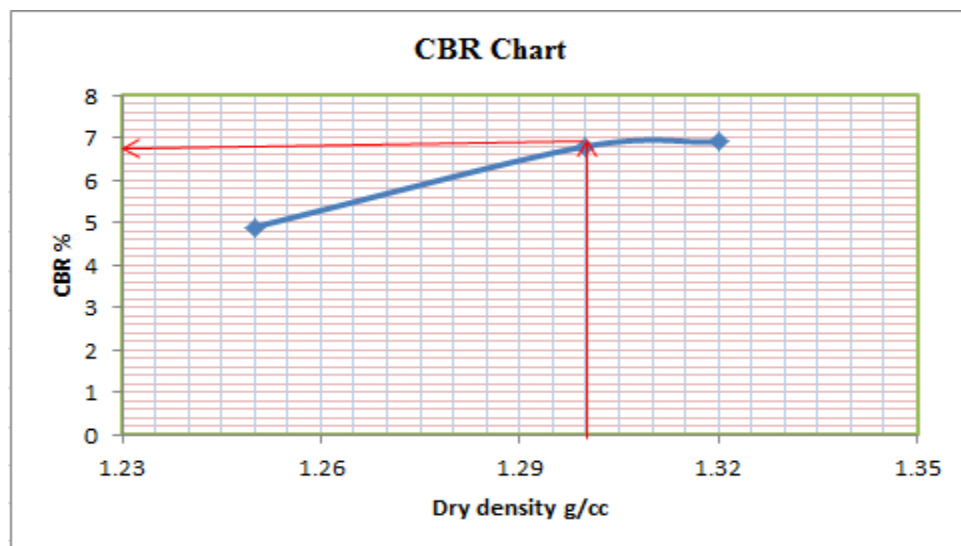


Figure D.1.2 CBR vs Dry density curve

Sample Location: Mercato 1

Table D-1-3 CBR penetration data for Mercato 1 after four days soaking

Penetration (mm)	Load (kN)			Standard Stress (Mpa)
	65 Blows	30 Blows	10 Blows	
<b>0</b>	0	0	0	
<b>0.625</b>	0.29	0.245	0.213	
<b>1.25</b>	0.39	0.382	0.289	
<b>1.875</b>	0.473	0.441	0.352	
<b>2.5</b>	0.559	0.49	0.443	6.92
<b>3.75</b>	0.731	0.635	0.493	88
<b>5</b>	0.781	0.736	0.597	10.3
<b>7.5</b>	0.963	0.803	0.639	13.11
<b>10</b>				15.87
<b>12.5</b>				17.94
<b>CBR @ 2.54 mm</b>	4.23	3.71	3.36	
<b>CBR @ 5.08 mm</b>	3.91	3.68	2.99	

Summary of CBR data

No of blows	10	30	65
MDD(g/cm <sup>3</sup> )	1.23	1.28	1.39
CBR (%)	3.4	3.7	4.2

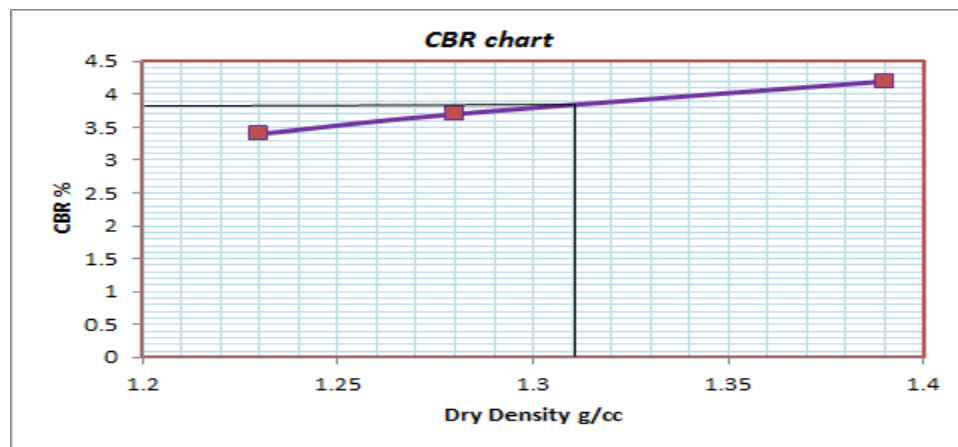


Figure D.1.3 CBR vs Dry density curve



Sample Location: Mercato 2-1

Table D-1-4 CBR penetration data for Mercato 2-1 after four days soaking

Penetration (mm)	Load (kN)			Standard Stress (Mpa)
	65 Blows	30 Blows	10 Blows	
0	0	0	0	
0.625	0.34	0.293	0.273	
1.25	0.474	0.426	0.375	
1.875	0.588	0.498	0.441	
2.5	0.673	0.578	0.487	6.92
3.75	0.813	0.71	0.555	88
5	0.912	0.792	0.607	10.3
7.5	1.084	0.891	0.684	13.11
10				15.87
12.5				17.94
<b>CBR @ 2.54 mm</b>	5.10	4.38	3.69	
<b>CBR @ 5.08 mm</b>	4.56	3.96	3.04	

Summary of CBR data

No of blows	10	30	65
MDD(g/cm <sup>3</sup> )	1.24	1.36	1.39
CBR (%)	3.69	4.38	5.1

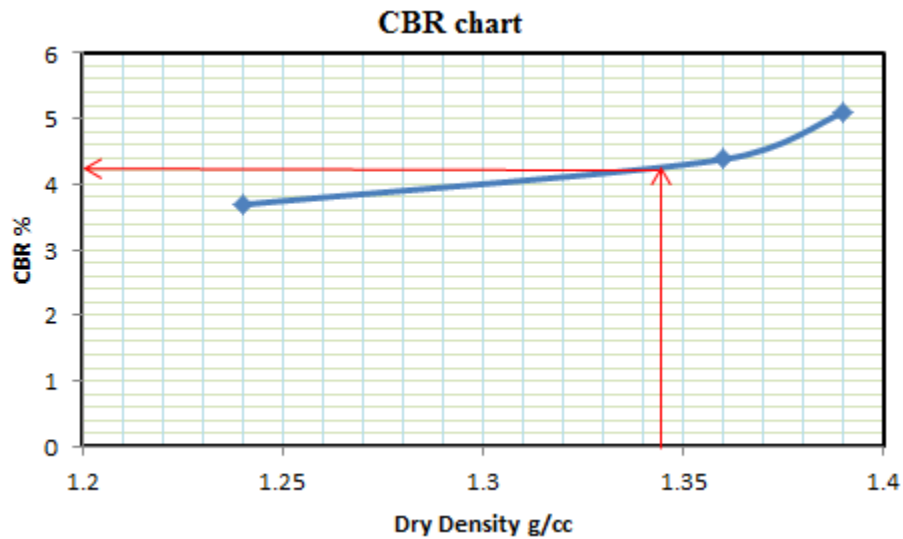


Figure D.1.4 CBR vs Dry density curve

Sample Location: Kito red 1

Table D-1-5 CBR penetration data for Kito red 1 after four days soaking

Penetration (mm)	Load (kN)			Standard Stress (Mpa)
	65 Blows	30 Blows	10 Blows	
0	0	0	0	
0.625	0.68	0.269	0.47	
1.25	1.01	0.749	0.67	
1.875	1.228	1.103	0.82	
2.5	1.362	1.316	0.92	6.92
3.75	1.552	1.483	1.06	88
5	1.675	1.594	1.15	10.3
7.5	1.904	1.8	1.31	13.11
10				15.87
12.5				17.94
<b>CBR @ 2.54 mm</b>	10.4	10.3	7	
<b>CBR @ 5.08 mm</b>	8.4	8.1	5.8	

**Summary of CBR data**

No of blows	10	30	65
MDD(g/cm <sup>3</sup> )	1.26	1.3	1.34
CBR (%)	7	10.3	10.4

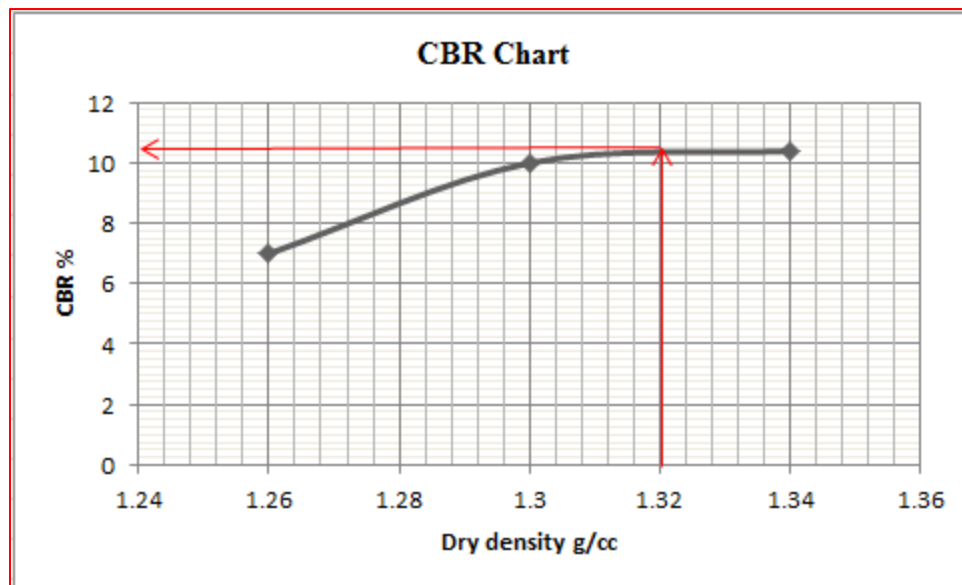


Figure D.1.5 CBR vs Dry density curve

Sample Location: Kito black 1

Table D-1-6 CBR penetration data for Kito black 1 after four days soaking

Penetration (mm)	Load (kN)			Standard Stress (Mpa)
	65 Blows	30 Blows	10 Blows	
0	0	0	0	
0.625	0.059	0.106	0.137	
1.25	0.082	0.146	0.198	
1.875	0.105	0.187	0.258	
2.5	0.134	0.242	0.36	6.92
3.75	0.166	0.29	0.419	88
5	0.208	0.357	0.519	10.3
7.5	0.293	0.483	0.701	13.11
10	0.379	0.597	0.867	15.87
12.5	0.462	0.701	1.025	17.94
<b>CBR @ 2.54 mm</b>	1.02	1.83	2.73	
<b>CBR @ 5.08 mm</b>	1.00	1.80	2.60	

Summary of CBR data

No of blows	10	30	65
MDD(g/cm <sup>3</sup> )	1.31	1.33	1.35
CBR (%)	1.02	1.83	2.73

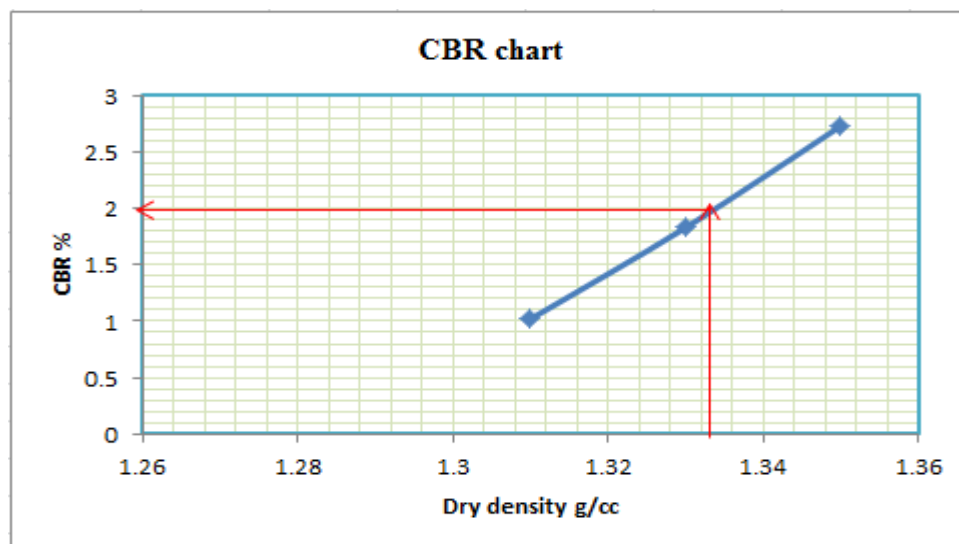


Figure D.1.6 CBR vs Dry density curve

Sample Location: Ifabula 1

Table D-1-7 CBR penetration data for Ifabula 1 after four days soaking

Penetration (mm)	Load for blows (kN)			Standard Stress (Mpa)
	10 blows	30 blows	65 blows	
0	0	0	0	
0.64	0.07	0.11	0.24	
1.27	0.13	0.12	0.28	
1.91	0.21	0.21	0.33	
2.54	0.33	0.45	0.52	6.92
3.81	0.42	0.52	0.56	88
5.08	0.52	0.53	0.61	10.3
7.61	0.59	0.54	0.64	13.11
CBR @2.54mm	2.5	3.4	3.9	
CBR @5.08mm	2.6	2.65	3.05	

Summary of CBR data

No of blows	10	30	65
MDD(g/cm <sup>3</sup> )	1.32	1.39	1.45
CBR (%)	2.6	3.4	3.9

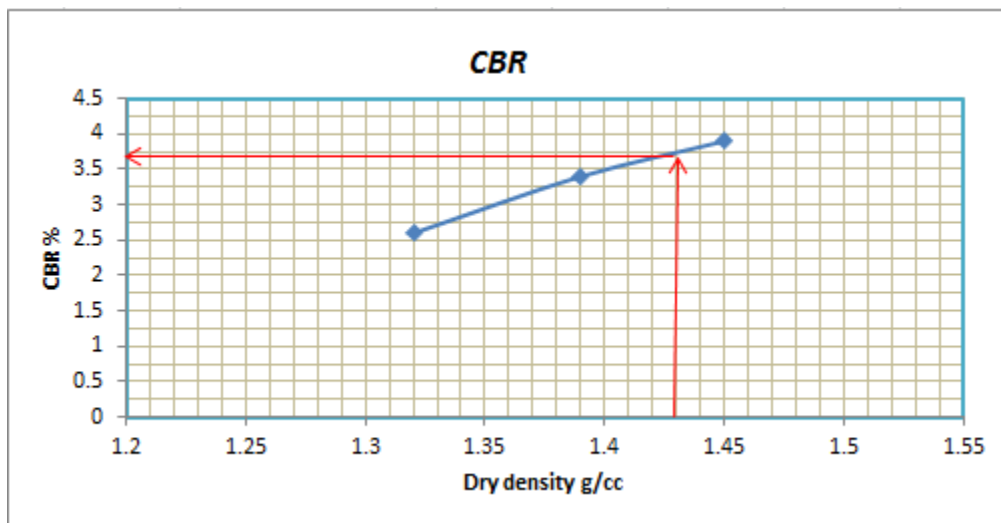


Figure D.1.7 CBR vs Dry density curve

Sample Location: Agri 2

Table D-1-8 CBR penetration data for Agri 1 after four days soaking

Penetration (mm)	Load for blows (kN)			Standard Stress (Mpa)
	10	30	65	
0	0	0	0	
0.64	0.06	0.12	0.17	
1.27	0.09	0.12	0.28	
1.91	0.11	0.23	0.36	
2.54	0.36	0.47	0.51	6.92
3.81	0.43	0.51	0.64	8.8
5.08	0.54	0.69	0.71	10.3
7.61	0.61	0.73	0.78	13.11
CBR @ 2.54mm	2.73	3.56	3.86	
CBR @ 5.08 mm	2.7	3.45	3.55	

Summary of CBR data

No of blows	10	30	65
MDD (g/cm <sup>3</sup> )	1.26	1.33	1.38
CBR (%)	2.73	3.56	3.86

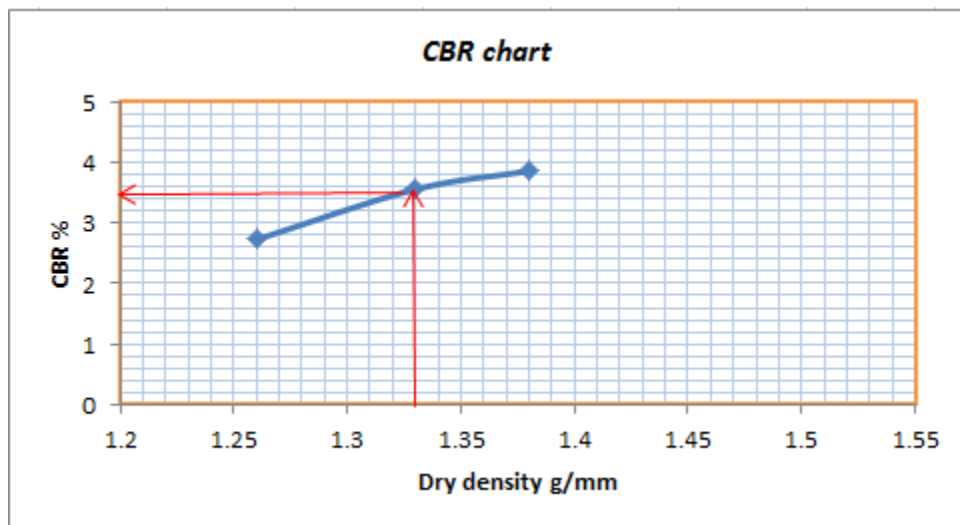


Figure D.1.8 CBR vs Dry density curve

Sample Location: Frustale 1

Table D-1-9 CBR penetration data for Ifabula 1 after four days soaking

Penetration (mm)	Load for r blows (kN)			Standard Stress (Mpa)
	10	30	65	
0	0	0	0	
0.64	0.32	0.41	0.46	
1.27	0.6	0.69	0.61	
1.91	0.84	0.95	1.02	
2.54	0.96	1.11	1.27	6.92
3.81	1.12	1.36	1.56	88
5.08	1.29	1.49	1.71	10.3
7.61	1.38	1.62	1.89	13.11
CBR @ 2.54mm	7.27	8.41	9.62	
CBR @ 5.08 mm	6.45	7.45	8.55	

Summary of CBR data

No of blows	10	30	65
MDD(g/cm3)	1.12	1.29	1.42
CBR (%)	7.27	8.41	9.62

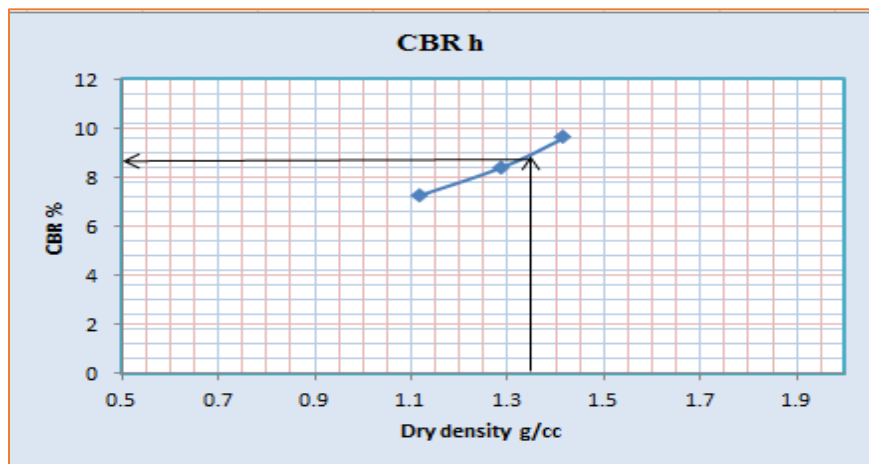


Figure D.1.9 CBR vs Dry density curve

Sample Location: Ajip 1

Table D-1-10 CBR penetration data for Ajip 1 after four days soaking

Penetration (mm)	Load for blows (kN)			Standard Stress (Mpa)
	10	30	65	
0	0	0	0	
0.64	0.15	0.18	0.19	
1.27	0.29	0.37	0.33	
1.91	0.41	0.41	0.47	
2.54	0.53	0.58	0.66	6.92
3.81	0.62	0.68	0.84	88
5.08	0.75	0.79	0.95	10.3
7.61	0.84	0.85	1.09	13.11
<b>CBR @ 2.54mm</b>	4.02	4.39	5.00	
<b>CBR @ 5.08 mm</b>	3.75	3.95	4.75	

Summary of CBR data

No of blows	10	30	65
MDD(g/cm <sup>3</sup> )	1.28	1.3	1.38
CBR (%)	4.02	4.39	5

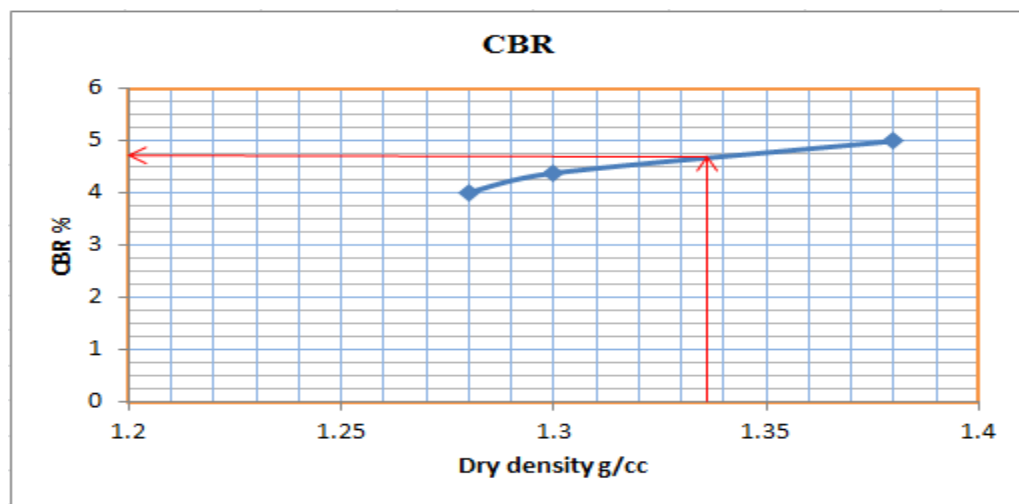


Figure D.1.10 CBR vs Dry density curve

Sample Location: Teknik sefer 1

Table D-1-11 CBR penetration data for Teknik sefer 1 after four days soaking

Penetration (mm)	Load for blows (kN)			Standard Stress (Mpa)
	10	30	65	
0	0	0	0	
0.64	0.15	0.2	0.31	
1.27	0.22	0.26	0.35	
1.91	0.3	0.39	0.47	
2.54	0.43	0.52	0.65	6.92
3.81	0.49	0.64	0.79	88
5.08	0.58	0.75	0.91	10.3
7.61	0.69	0.91	1.09	13.11
CBR @ 2.54mm	3.23	3.90	4.88	
CBR @ 5.08 mm	2.90	3.75	4.55	

Summary of CBR data

No of blows	10	30	65
MDD(g/cm <sup>3</sup> )	1.29	1.34	1.47
CBR (%)	3.23	3.90	4.88

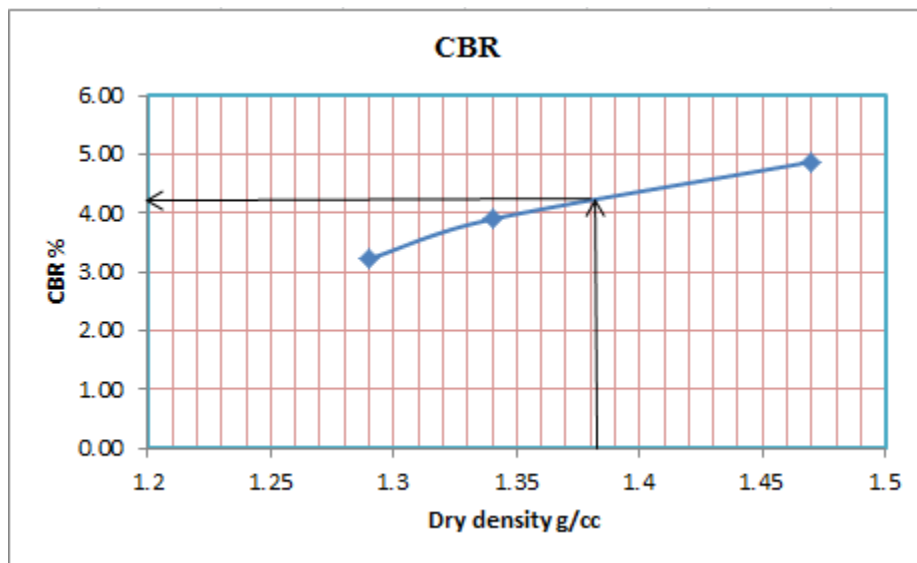


Figure D.1.11 CBR vs Dry density curve



Sample Location: Bore

Table D-1-12 CBR penetration data for Bore 1 after four days soaking

Penetration (mm)	Load for blows (kN)			Standard Stress (Mpa)
	10	30	65	
0	0	0	0	
0.64	0.13	0.16	0.19	
1.27	0.21	0.27	0.35	
1.91	0.27	0.39	0.5	
2.54	0.34	0.48	0.71	6.92
3.81	0.39	0.63	0.89	88
5.08	0.46	0.73	1.06	10.3
7.61	0.51	0.81	1.29	13.11
<b>CBR @ 2.54mm</b>	2.58	3.64	5.38	
<b>CBR @ 5.08 mm</b>	2.3	3.65	5.3	

Summary of CBR data

No of blows	10	30	65
<b>MDD (g/cm<sup>3</sup>)</b>	1.26	1.38	1.45
<b>CBR (%)</b>	2.58	3.64	5.38

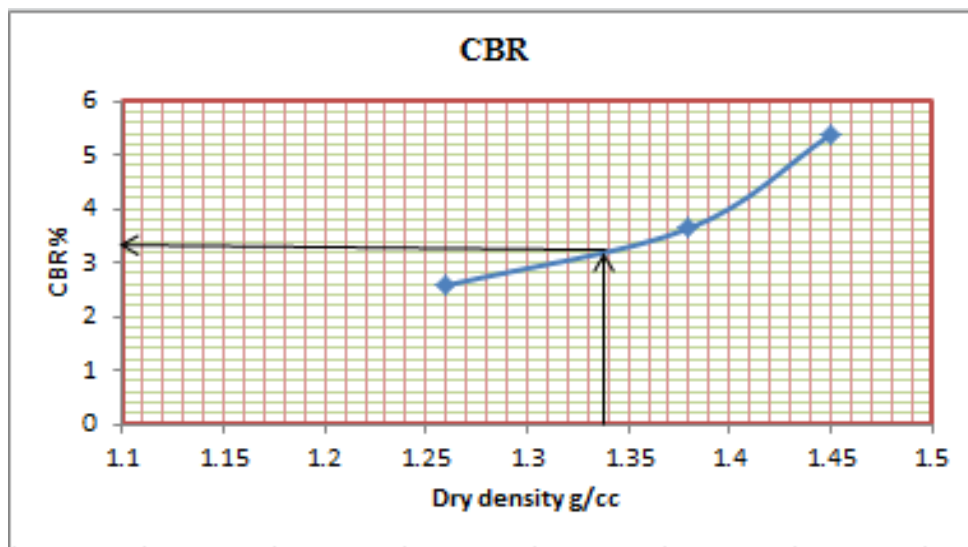


Figure D.1.12 CBR vs Dry density curve

Sample Location: Jiren

Table D-1-13 CBR penetration data for Jiren 1 after four days soaking

Penetration (mm)	Load for blows (kN)			Standard Stress (Mpa)
	10	30	65	
0	0	0	0	
0.64	0.13	0.15	0.18	
1.27	0.27	0.31	0.54	
1.91	0.39	0.63	0.99	
2.54	0.59	0.99	1.43	6.92
3.81	0.7	1.54	1.89	88
5.08	0.86	1.88	2.24	10.3
7.61	0.95	1.98	2.53	13.11
CBR @ 2.54mm	4.47	7.50	10.83	
CBR @ 5.08 mm	4.3	9.4	11.2	

Summary of CBR data

<i>No of blows</i>	<i>10</i>	<i>30</i>	<i>65</i>
<i>MDD (g/cm<sup>3</sup>)</i>	1.29	1.38	1.47
<i>CBR (%)</i>	4.47	7.5	10.83

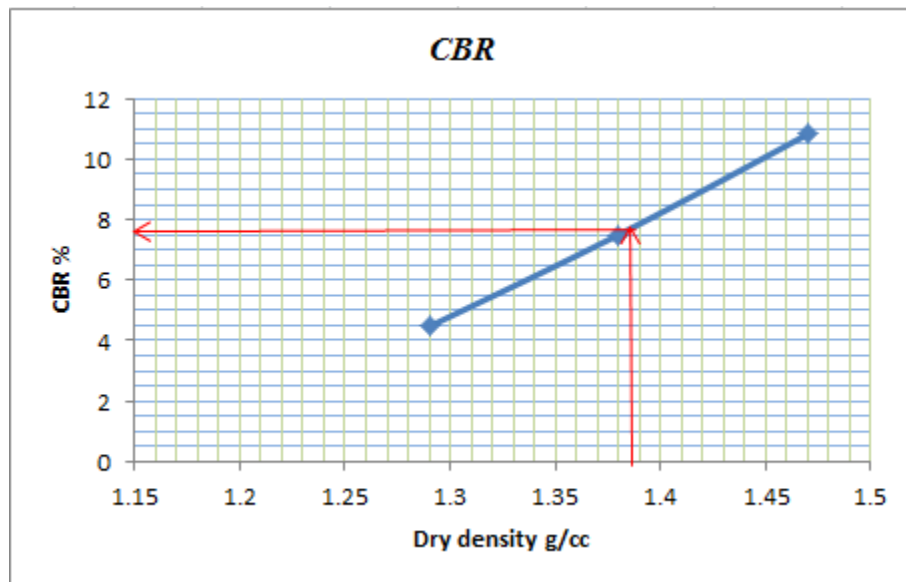


Figure D.1.13 CBR vs Dry density curve

Sample Location: Bacho Bore

Table D-1-14 CBR penetration data for Bacho Bore 1 after four days soaking

Penetration (mm)	Load for blows (kN)			Standard Stress (Mpa)
	10	30	65	
0	0	0	0	
0.64	0.14	0.16	0.18	
1.27	0.22	0.27	0.29	
1.91	0.35	0.36	0.43	
2.54	0.56	0.57	0.64	6.92
3.81	0.69	0.76	0.83	88
5.08	0.83	0.78	0.96	10.3
7.61	0.97	0.98	1.21	13.11
<b>CBR @ 2.54mm</b>	4.24	4.32	4.85	
<b>CBR @ 5.08 mm</b>	4.15	3.9	4.8	

Summary of CBR data

No of blows	10	30	65
<b>MDD(g/cm<sup>3</sup>)</b>	1.32	1.39	1.46
<b>CBR (%)</b>	4.24	4.32	4.85

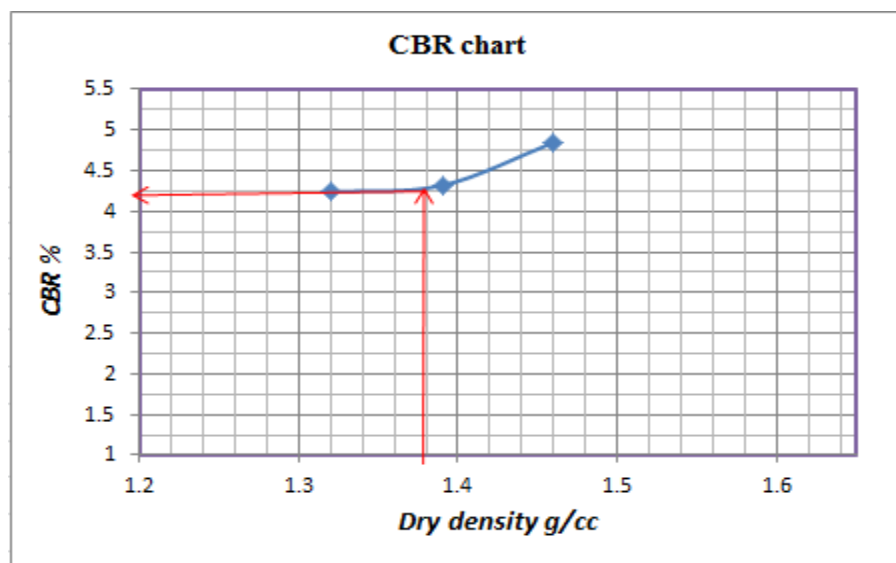


Figure D.1.14 CBR vs Dry density curve

## **APPENDIX E: REGRESSION OUT PUTS**

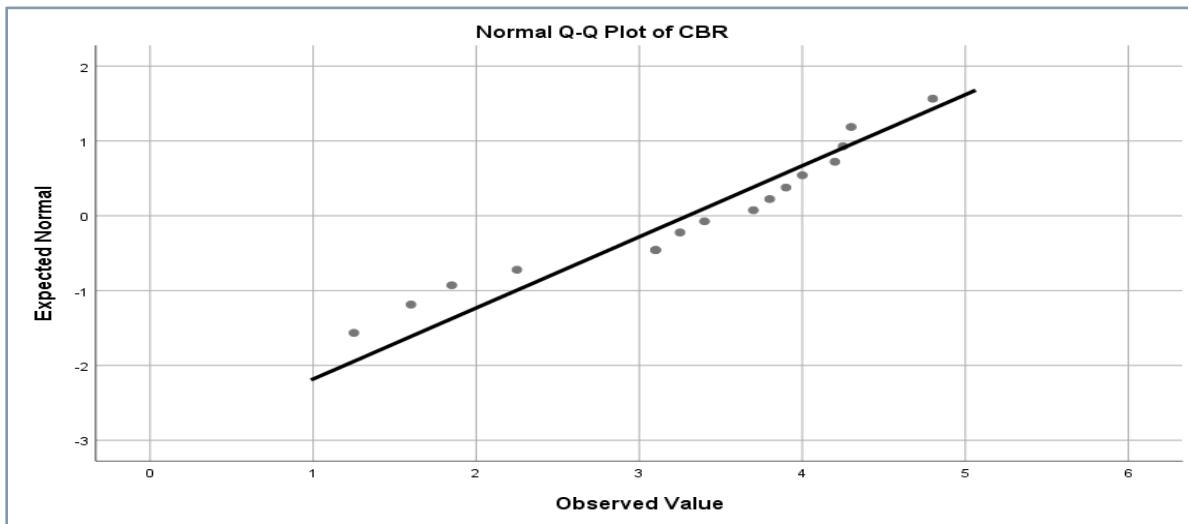
**E1. Normality test data using Shapiro-Wilk and Univariate analysis using normal Q-Q plot**

**A. Category-1 data**

**1.CBR**

**Tests of Normality**

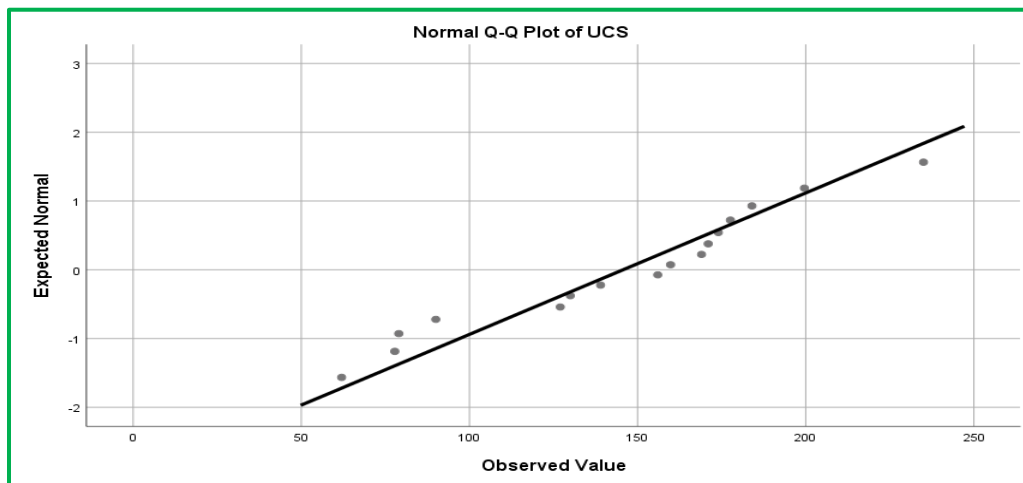
	Kolmogorov-Smirnov <sup>a</sup>			Shapiro-Wilk		
	Statistic	df	Sig.	Statistic	df	Sig.
CBR	0.176	16	.200*	0.923	16	0.187



**2. UCS**

**Tests of Normality**

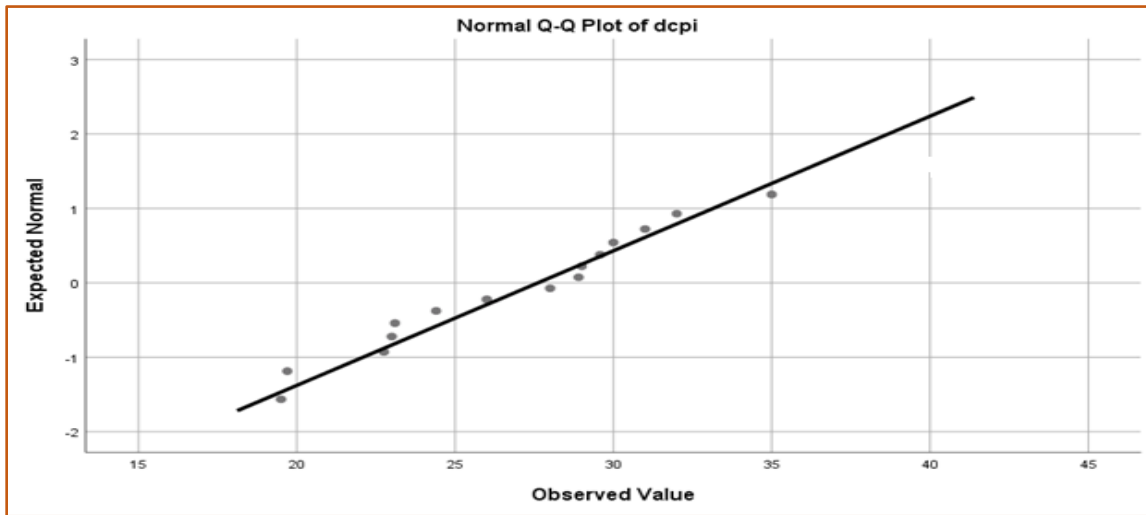
	Kolmogorov-Smirnov <sup>a</sup>			Shapiro-Wilk		
	Statistic	df	Sig.	Statistic	df	Sig.
UCS	0.147	16	.200*	0.952	16	0.528



### 3. DCPI

**Tests of Normality**

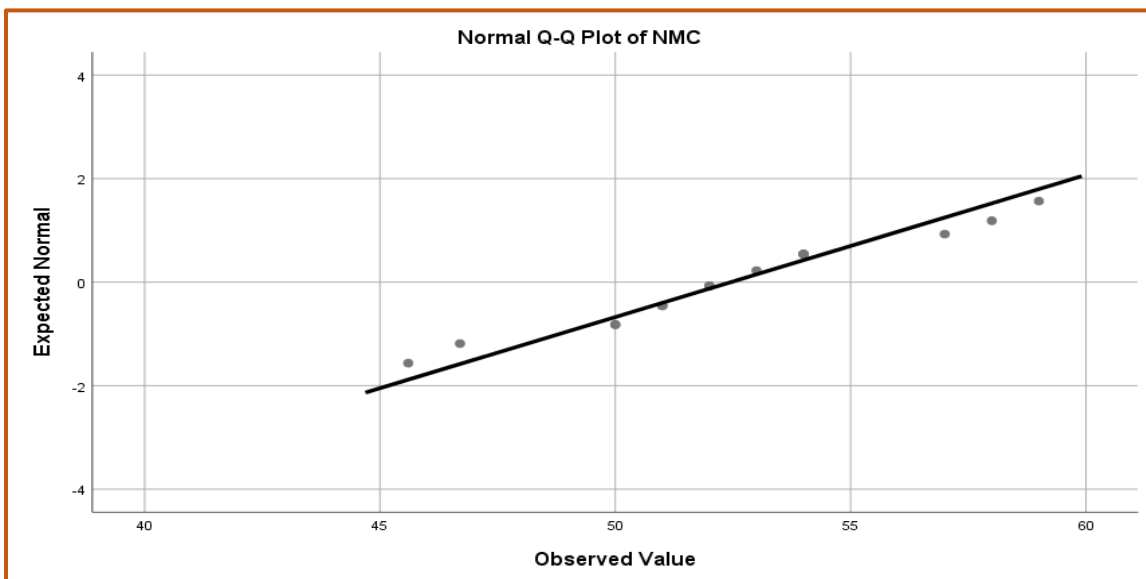
	Kolmogorov-Smirnov <sup>a</sup>			Shapiro-Wilk		
	Statistic	df	Sig.	Statistic	df	Sig.
DCPI	0.106	16	.200*	0.961	16	0.687



### 4. NMC

**Tests of Normality**

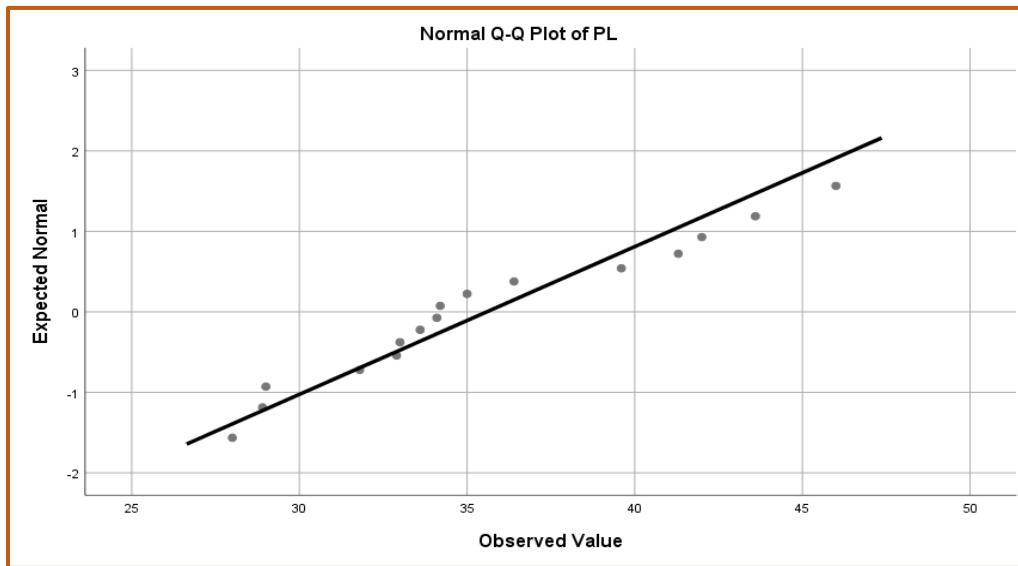
	Kolmogorov-Smirnov <sup>a</sup>			Shapiro-Wilk		
	Statistic	df	Sig.	Statistic	df	Sig.
NMC	0.148	16	.200*	0.962	16	0.706



5. PL

Tests of Normality

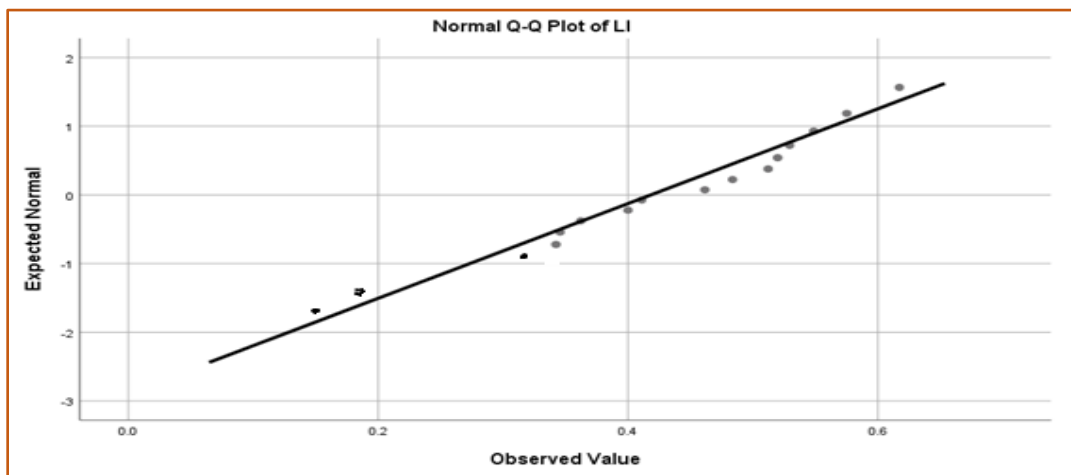
	Kolmogorov-Smirnov <sup>a</sup>			Shapiro-Wilk		
	Statistic	df	Sig.	Statistic	df	Sig.
PL	0.168	16	.200*	0.939	16	0.335



6. LI

Tests of Normality

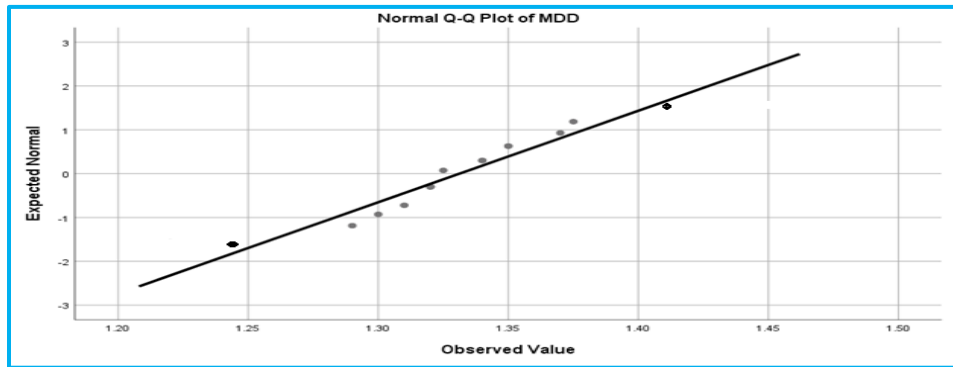
	Kolmogorov-Smirnov <sup>a</sup>			Shapiro-Wilk		
	Statistic	df	Sig.	Statistic	df	Sig.
LI	0.167	16	.200*	0.918	16	0.159



7. MDD

Tests of Normality

	Kolmogorov-Smirnov <sup>a</sup>			Shapiro-Wilk		
	Statistic	df	Sig.	Statistic	df	Sig.
MDD	0.16	16	.200*	0.913	16	0.13

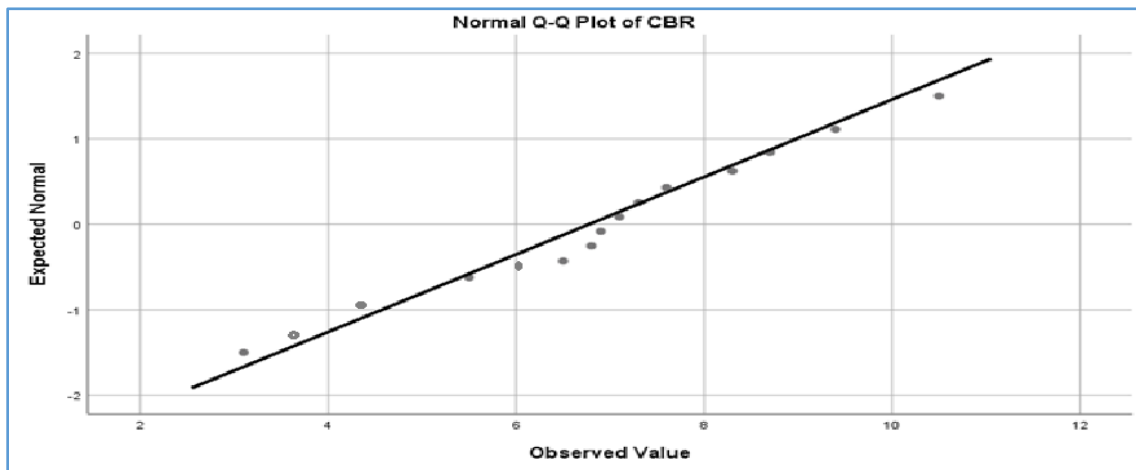


B. Category-2

1. CBR

Case Processing Summary

	Cases					
	Valid		Missing		Total	
	N	Percent	N	Percent	N	Percent
CBR	14	100.00%	0	0.00%	14	100.00%



Tests of Normality

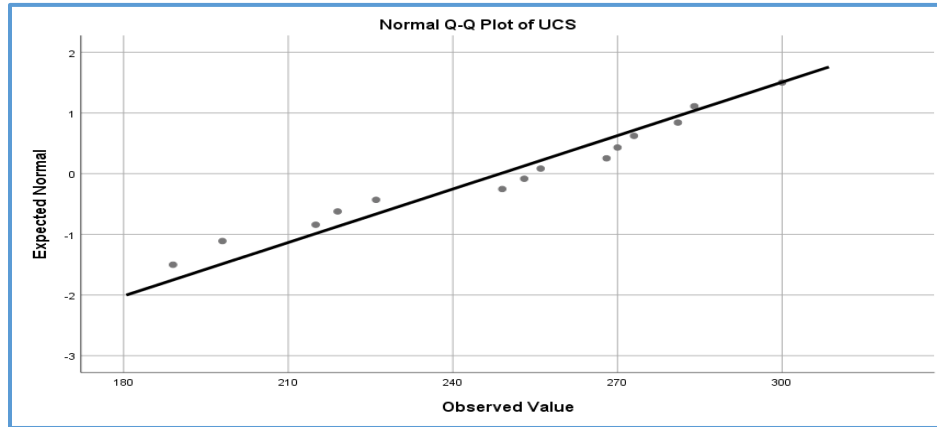
	Kolmogorov-Smirnov <sup>a</sup>			Shapiro-Wilk		
	Statistic	df	Sig.	Statistic	df	Sig.
CBR	0.164	14	.200*	0.951	14	0.569



2. UCS

Tests of Normality

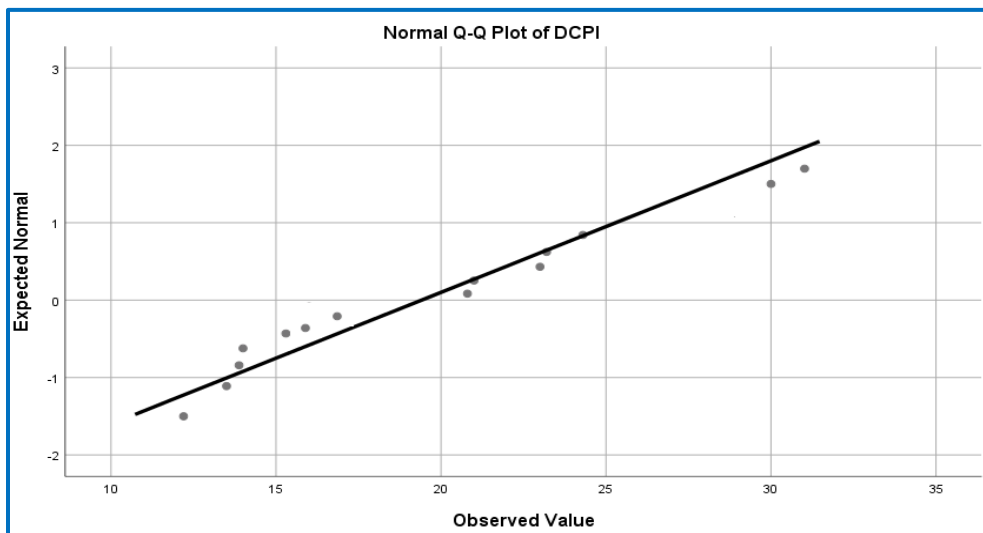
	Kolmogorov-Smirnov <sup>a</sup>			Shapiro-Wilk		
	Statistic	df	Sig.	Statistic	df	Sig.
UCS	0.147	14	.200*	0.95	14	0.564



3. DCPI

Tests of Normality

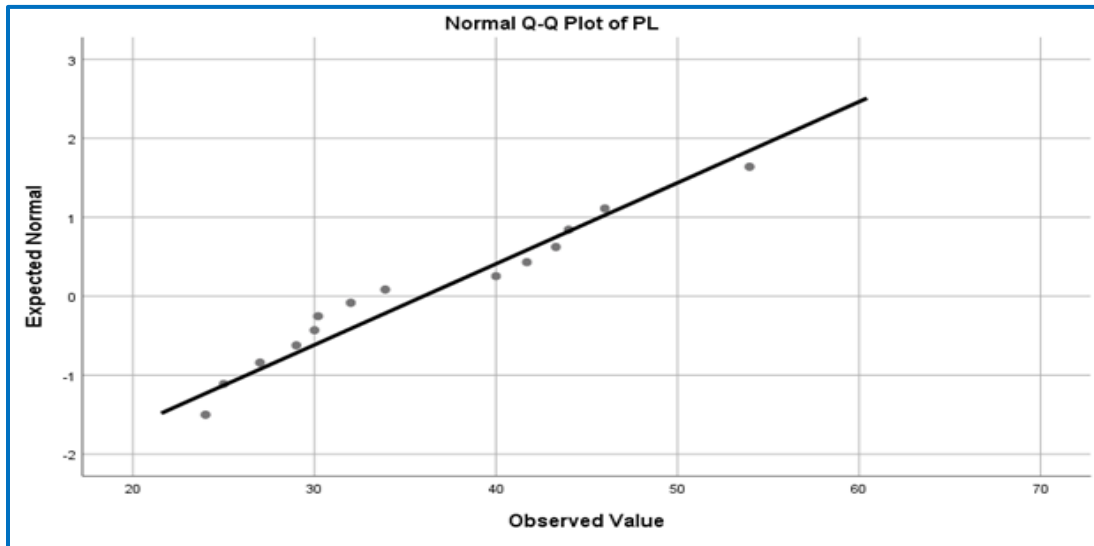
	Kolmogorov-Smirnov <sup>a</sup>			Shapiro-Wilk		
	Statistic	df	Sig.	Statistic	df	Sig.
DCPI	.219	14	.067	.905	14	.135



4. PL

Tests of Normality

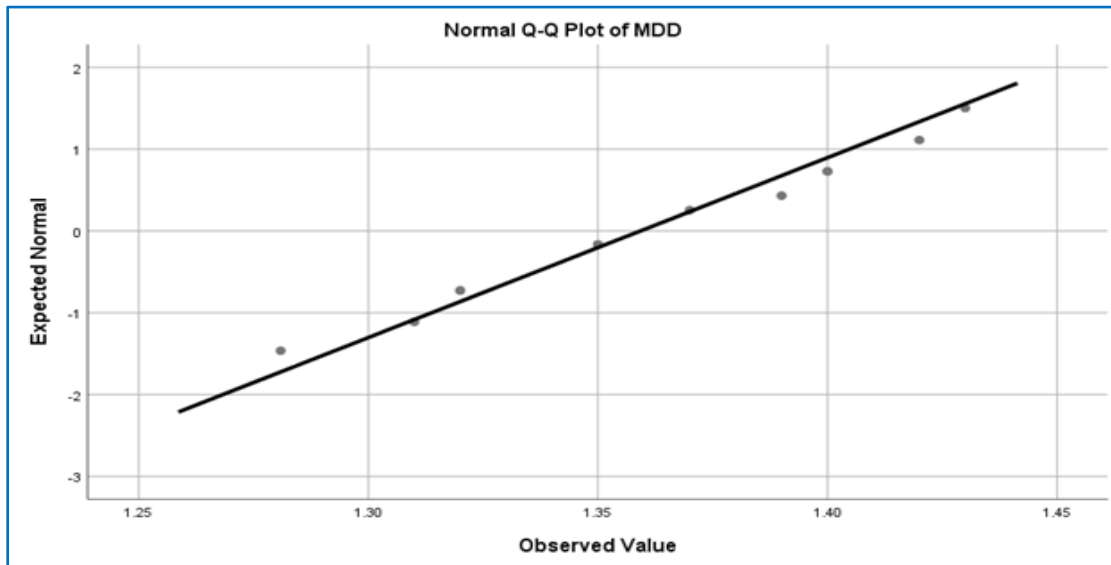
	Kolmogorov-Smirnov <sup>a</sup>			Shapiro-Wilk		
	Statistic	df	Sig.	Statistic	df	Sig.
PL	0.16	14	.200*	0.925	14	0.256



5. MDD

Tests of Normality

	Kolmogorov-Smirnov <sup>a</sup>			Shapiro-Wilk		
	Statistic	df	Sig.	Statistic	df	Sig.
MDD	0.152	14	.200*	0.964	14	0.79



### E2.1 Interdependence check using Chi square test method (A. Category-1 Black clay soils)

#### 1. DCPI, NMC, FDD, Compaction characteristics and Atterberg limits

**Chi-Square Tests**

DCPI and LI	Value	df	Asymptotic Significance (2-sided)
Pearson Chi-Square	240.000 <sup>a</sup>	225	0.235
Likelihood Ratio	88.723	225	1
Linear-by-Linear Association	4.552	1	0.033
N of Valid Cases	16		

**Chi-Square Tests**

DCPI and MDD	Value	df	Asymptotic Significance (2-sided)
Pearson Chi-Square	160.000 <sup>a</sup>	150	0.273
Likelihood Ratio	72.087	150	1
Linear-by-Linear Association	0	1	0.991
N of Valid Cases	16		

**Chi-Square Tests**

PL and MDD	Value	df	Asymptotic Significance (2-sided)
Pearson Chi-Square	240.000 <sup>a</sup>	225	0.235
Likelihood Ratio	88.723	225	1
Linear-by-Linear Association	8.279	1	0.004
N of Valid Cases	16		

### E.2.2 Interdependence check using Chi square test method (A. Category-2 Red clay soils)

#### 1. DCPI, NMC, FDD, Compaction characteristics and Atterberg limits

**Chi-Square Tests**

DCPI and MDD	Value	df	Asymptotic Significance (2-sided)
Pearson Chi-Square	112.000 <sup>a</sup>	104	0.279
Likelihood Ratio	57.258	104	1
Linear-by-Linear Association	5.312	1	0.021
N of Valid Cases	14		

**Chi-Square Tests**

DCPI and LI	Value	df	Asymptotic Significance (2-sided)
Pearson Chi-Square	182.000 <sup>a</sup>	169	0.234
Likelihood Ratio	73.894	169	1
Linear-by-Linear Association	5.044	1	0.025
N of Valid Cases	14		

**Chi-Square Tests**

DCPI and FDD	Value	df	Asymptotic Significance (2-sided)
Pearson Chi-Square	182.000 <sup>a</sup>	169	0.234
Likelihood Ratio	73.894	169	1
Linear-by-Linear Association	1.838	1	0.175
N of Valid Cases	14		

**Chi-Square Tests**

NMC and $\gamma_d$	Value	df	Asymptotic Significance (2-sided)
Pearson Chi-Square	154.000 <sup>a</sup>	143	0.25
Likelihood Ratio	68.348	143	1
Linear-by-Linear Association	3.783	1	0.052
N of Valid Cases	14		

**Chi-Square Tests**

MDD and PL	Value	df	Asymptotic Significance (2-sided)
Pearson Chi-Square	112.000 <sup>a</sup>	104	0.279
Likelihood Ratio	57.258	104	1
Linear-by-Linear Association	2.021	1	0.155
N of Valid Cases	14		

**E3. MULTIPLE REGRESSION OF CATEGORY -1 (BLACK SOIL)**

**A. UCS (Unconfined Compressive Strength) multiple linear regression for Category-1**

**Variables Entered/Removed<sup>a</sup>**

Model	Variables Entered	Variables Removed	Method
1	LI, $\gamma_d$ , NMC <sup>b</sup>	.	Enter

**Model Summary<sup>b</sup>**

Model	R	R Square	Adjusted R Square	Std. Error of the Estimate	Change Statistics		
					R Square Change	F Change	df1
1	.871 <sup>a</sup>	0.758	0.718	21.7951	0.839	20.884	3

**ANOVA<sup>a</sup>**

Model		Sum of Squares	df	Mean Square	F	Sig.
1	Regression	29761.22	3	9920.406	20.884	.000 <sup>b</sup>
	Residual	5700.293	12	475.024		
	Total	35461.51	15			

**Coefficients<sup>a</sup>**

Model		Unstandardized Coefficients		Standardized Coefficients	t	Sig.
		B	Std. Error	Beta		
1	(Constant)	957.465	212.021		4.516	0.001
	NMC	-11.831	1.961	-0.886	-6.034	0
	$\gamma_d$	-29.389	13.54	-0.309	-2.17	0.051
	LI	258.058	40.36	0.77	6.394	0

**B. CBR (Californian Bearing Ratio) multiple regression for category-1**

**Variables Entered/Removed<sup>a</sup>**

Model	Variables Entered	Variables Removed	Method
1	MDD, DCPI, OMC <sup>b</sup>		Enter

**Model Summary<sup>b</sup>**

Model	R	R Square	Adjusted R Square	Std. Error of the Estimate	Change Statistics		
					R Square Change	F Change	df1
1	.921 <sup>a</sup>	0.848	0.801	0.45912	0.848	22.27	3

**ANOVA<sup>a</sup>**

Model		Sum of Squares	df	Mean Square	F	Sig.
1	Regression	14.083	3	4.694	22.27	.000 <sup>b</sup>
	Residual	2.53	12	0.211		
	Total	16.612	15			

**Coefficients<sup>a</sup>**

Model		Unstandardized Coefficients		Standardized Coefficients	t	Sig.
		B	Std. Error	Beta		
1	(Constant)	12.897	4.471		2.885	0.014
	OMC	-0.034	0.031	-0.151	-1.087	0.029
	DCPI	-0.074	0.01	-0.863	-7.268	0
	MDD	-4.647	2.946	-0.212	-1.577	0.014

**E2. MULTIPLE REGRESSION OF CATEGORY -2 (RED SOIL)**

**A. UCS (Unconfined Compressive Strength) multiple linear regression for Category-2**

**Variables Entered/Removed<sup>a</sup>**

Model	Variables Entered	Variables Removed	Method
1	LI, $\gamma_d$ , DCP <sup>b</sup>	.	Enter

**Model Summary**

Model	R	R Square	Adjusted R Square	Std. Error of the Estimate	Change Statistics		
					R Square Change	F Change	df1
1	.0863 <sup>a</sup>	0.745	0.691	18.6964	0.913	35.17	3

**ANOVA<sup>a</sup>**

Model		Sum of Squares	df	Mean Square	F	Sig.
1	Regression	36881.74	3	12293.91	35.17	.000 <sup>b</sup>
	Residual	3495.551	10	349.555		
	Total	40377.29	13			

Model		Unstandardized Coefficients		Standardized Coefficients	t	Sig.
		B	Std. Error	Beta		
1	(Constant)	506.387	91.82		5.515	0
	DCP	-6.202	0.939	-0.809	-6.605	0
	$\gamma_d$	-11.131	7.003	-0.161	-1.59	0.014
	LI	-37.311	15.971	-0.28	-2.336	0.042

**B. CBR (Californian Bearing Ratio) multiple regression for category-2**

**Variables Entered/Removed<sup>a</sup>**

Model	Variables Entered	Variables Removed	Method
1	MDD, PL, OMC <sup>b</sup>	.	Enter

**Model Summary**

Model	R	R Square	Adjusted R Square	Std. Error of the Estimate	Change Statistics		
					R Square Change	F Change	df1
1	.876 <sup>a</sup>	0.768	0.698	1.2124	0.768	11.013	3

**ANOVA<sup>a</sup>**

Model		Sum of Squares	df	Mean Square	F	Sig.
1	Regression	48.564	3	16.188	11.013	.002 <sup>b</sup>
	Residual	14.699	10	1.47		
	Total	63.264	13			

**Coefficients<sup>a</sup>**

Model		Unstandardized Coefficients		Standardized Coefficients	t	Sig.
		B	Std. Error	Beta		
1	(Constant)	-43.167	38.576		-1.119	0.289
	OMC	0.442	0.23	0.937	1.925	0.048
	PL	0.122	0.038	0.537	3.197	0.01
	MDD	23.146	23.287	0.477	0.994	0.034